Technical Report
TR-22-08
December 2022

Glacial erosion in the Öregrund archipelago

Potential for headward erosion towards Forsmark in future glaciations?

Adrian M Hall
Maarten Krabbendam
Mikis van Boeckel

SVENSK KÄRNBRÄNSLEHANTERING AB

SWEDISH NUCLEAR FUEL
AND WASTE MANAGEMENT CO

Box 3091, SE-169 03 Solna
Phone +46 8 459 84 00
skb.se

SVENSK KÄRNBRÄNSLEHANTERING

ISSN 1404-0344
SKB TR-22-08
ID 1983747

December 2022

Glacial erosion in the Öregrund archipelago

Potential for headward erosion towards Forsmark in future glaciations?

Adrian M Hall[1,2], Maarten Krabbendam[3], Mikis van Boeckel[4]

1 Department of Physical Geography, Stockholm University
2 Institute of Geography, University of Edinburgh
3 British Geological Survey
4 Earth Surface and Seabed Division, Norges Geologiske Undersøkelse (NGU)

Keywords: Glacial erosion, Headward erosion, Fractures, Trenches, Öregrund.

Preface

The following report describes a study on past and future glacial erosion in rock trenches in the Uppland county, including the spent nuclear fuel repository site at Forsmark. It includes an assessment of how long it potentially would take for areas away from Forsmark, characterized by greater historical glacial erosion, to reach the Forsmark site by headward erosion during future glacial cycles. The study is a complement to the comprehensive study on denudation and glacial erosion in Forsmark and Uppland reported in TR-19-07.

The study was initiated by Jens-Ove Näslund (SKB) and it was jointly designed by Jens-Ove Näslund, Adrian Hall (Stockholm University) and Maarten Krabbendam (British Geological Survey). Adrian Hall coordinated the scientific work within the study. Mikis van Boeckel (Stockholm University) produced many of the figures in the report. All authors contributed to the final revision of the report.

The results will be used, together with other scientific information, for constructing future scenarios of climate and climate-related processes in SKB's work on assessing long-term safety of nuclear waste repositories in Sweden. The safety assessments performed for the planned repository for spent nuclear fuel in Forsmark, Sweden, cover a total time span of one million years. Since this time span covers the timescales relevant for glacial cycles, the effect of future glacial erosion needs to be analysed in the safety assessments.

The report was scientifically reviewed by Ingmar Borgström, Dept. of physical geography, Stockholm university and Mark Johnson, Dept. of Earth sciences, Gothenburg university.

Stockholm, December 2022

Jens-Ove Näslund

Coordinator Climate Research Programme SKB

Abstract

Glacial erosion in the Öregrund archipelago has led to the formation of rock trenches, valleys and basins, now submerged between the low-lying islands. The depths of these topographic depressions are 10–50 m, greater than in areas to the West and South. This study explores the likely reasons for enhanced glacial erosion in the Öregrund archipelago and the potential for future extension of topographic depressions ENE towards Forsmark.

The present basement topography of Uppland is inherited from the sub-Cambrian basement unconformity. Previous work has reconstructed its form in summit envelope surfaces as a smooth, block faulted surface. The elevations of the floors of bedrock depressions represent depths of glacial erosion below the re-exposed unconformity surface found on neighbouring, upstanding basement fault blocks. In the Öregrund archipelago, the presence of Proterozoic sandstones and Ordovician limestones in down-faulted positions indicates that most glacial erosion was a result of erosion in these relatively soft and closely fractured sedimentary rocks. In the basement gneisses, glacial erosion was generally low across the fault block tops and mainly focussed along the regional deformation zones and faults.

Previous analyses of fracture lengths and spacings at Forsmark and in its surroundings indicate that fractures in the gneissic basement conform to general power-law relationships. Major regional brittle deformation zones have lengths of 10s of km, spacings of 20 to 40 km but widths which do not normally exceed ~100 m but which vary along strike. Together with regional faults, these major fracture zones control the locations of long rock trenches which delineate the edges of exhumed fault blocks. Many individual trenches across scales remain segmented by rock thresholds. Comparisons of fracture and trench network topologies show relatively poor connectivity of trench networks, with many isolated trenches developed on short fractures on fault block tops. Previous studies show that *in situ* joint-bound rock block sizes in fracture zones are < 0.1–0.5 m. As in other crystalline rocks, *in situ* joint-bound rock-block size can be regarded as the dominant control on patterns and rates of glacial erosion in lowland gneissic terrain beneath the Fennoscandian Ice Sheet.

The faulted surface of the sub-Cambrian unconformity provides a reference surface for estimating depths of denudation, including glacial erosion. The onset of deep glacial erosion around the Baltic Sea basin was at 1.2 Ma. Assuming a similar timing for the Öregrund archipelago, rates of glacial erosion for past 100 ka glacial cycles can be derived. Minimum rates of erosion in sedimentary cover were 3–4 m/100 ka. Average erosion rates in basement were lower at 1.8–2.0 m/100 ka. Terrestrial cosmogenic nuclide inventories at Forsmark indicate erosion rates for rock surfaces on gneiss bedrock hills of 1.6–3.5 m/100 ka, similar to estimates of average erosion based on geomorphological criteria. Except for the rim of the Åland Deep, rates of trench deepening were 0.8–4.2 m/100 ka and rates of trench widening were 13–71 m/100 ka. Thalweg steepening remains largely confined to incision of the western rim of the Åland Deep; in the eastern Öregrund archipelago, headward erosion operated at 0.4–1.2 km/100 ka.

Erosion in past glacial cycles at Forsmark involved downwearing of fault-block tops, backwearing of fault-block edges and incision of trenches and basins along fracture zones (involving both deepening and widening of the trenches); the pattern of erosion in future glacial cycles will likely be similar. Rates of downwearing of rock surfaces during future glaciations are estimated to < 1 m/100 ka based on modelling of cosmogenic nuclides and of future climate/glacial periods. In the past, fault scarps on block edges elsewhere in Uppland have retreated at 42–125 m/100 ka; future backwearing is unlikely to extend far behind existing fault block edges over the next 100 ka. The Singö, Eckarfjärden and Forsmark deformation zones carry relatively shallow and segmented trenches at Forsmark when compared to their continuations in the Öregrund archipelago. Block removal by future glacial erosion is likely to excavate rock trenches within the main deformation zones at Forsmark. The limited widening of trenches beyond underlying fracture zones during the Pleistocene indicates that future trench erosion will remain largely confined within the deformation zones that delineate the Forsmark tectonic lens. Future trench development can be expected to extend to depths of 10–50 m and widths of < 1 km over the next 1 Ma under assumptions of a similar future total duration of glacial conditions. Thus, headward erosion of rock trenches from the Öregrund archipelago would require around 1 Ma to reach Forsmark. Recent modelling suggests, however, that glacial cycles over the coming several 100 ka will be short. Hence, the timescales for headward erosion under this scenario would extend beyond 1 Ma.

Sammanfattning

Glacial erosion har i Öregrundsarkipelagen lett till bildandet av sprickdalar (klippdalar) och bergsänkor, vilka idag är täckta av hav mellan de låglänta öarna. Djupet hos dessa topografiska sänkor är 10–50 m, vilket är större än i områdena västerut och söderut, inklusive vid Forsmarksplatsen. Denna studie undersöker de sannolika orsakerna till den högre graden av glacial erosion i Öregrundsarkipelagen samt potentialen för framtida tillväxt av de topografiska sänkorna i riktning mot Forsmarksplatsen.

Topografin hos dagens berggrundsyta i Uppland är nära besläktad med ytan hos den Sub-Kambriska inkonformiteten. Tidigare studier har rekonstruerat denna äldre yta till att beskriva en ursprunglig jämn bergrundsyta, påverkad av förkastade bergblock. Rekonstruktionen gjordes genom att använda maxhöjder inom och mellan bergblock som ankarpunkter. Höjdskillnaden från den rekonstruerade äldre ytan, vars rester idag återfinns i de högsta delarna av terrängen, ner till bottnen av dagens topografiska sänkor representerar storleken hos, framförallt, den glacial erosion som skett av den kristallina berggrunden. I Öregrundsarkipelagen återfinns proterozoisk sandsten och ordovicisk kalksten i nedförkastade lägen i låga topografiska lägen. Dessa sedimentära bergrundsrester indikerar att det mesta av den glaciala erosionen här har utgjorts av erosion av de relativt mjuka och sprickiga sedimentära bergarterna och inte erosion av kristallint berg. Över de högsta delarna av den kristallina berggrunden har den glaciala erosionen generellt varit låg och i huvudsak fokuserad längs regionala deformationszoner och förkastningar.

Tidigare studier har visat att större regionala deformationszoner har längder på tiotals km och ligger åtskilda runt 20 till 40 km medan de har en bredd som normalt inte överskrider ~100 m (dock varierande i stryknings-riktningen). De större regionala deformationszonerna kontrollerar, tillsammans med regionala förkastningar, läget hos längre sprickdalar vilka i sin tur avgränsar kanterna på de exhumerade förkastningsblocken. Analys av sprick- och sprickdalstopologier visar på en relativt låg konnektivitet hos sprickdalsnätverken, med många isolerade sprickdalar utbildade längs relativt korta sprickor i höga lägen på förkastningsblocken.

Den förkastade ytan hos den Sub-Kambriska inkonformiteten utgör en referensyta för uppskattningar av denudationen av den kristallina berggrunden, inklusive glacial erosion. Starten för kraftig glacial erosion i Östersjösänkan skedde för runt 1.2 miljoner år sedan. Om man antar att erosionen i Öregrundsarkipelagen startade vid samma tidpunkt kan den glaciala erosionshastigheten under de senaste glaciala cyklerna beräknas. Ett minimimått på erosionen i sedimentära täckbergarter var 3–4 m per 100 000 år. Den genomsnittliga erosionshastigheten i det underliggande kristallina berget var lägre, runt 1,8–2.0 m per 100 000 år. Analys av kosmogena nuklider från berggrunden i Forsmark indikerar en erosionshastighet på 1,6–3,5 m per 100 000 år för kristallina bergkullar, dvs en erosionshastighet liknande den som erhålls från den geomorfologiska analysen. Med undantag av kanten av Ålandsdjupet så var hastigheten med vilken sprickdalarna fördjupades 0,8–4,2 m per 100 000 år, medan bredden ökade med 13–71 m per 100 000 år. En ökning av lutningen hos dalar (längs deras lägsta punkter) skedde i huvudsak i anslutning till bildandet den västra kanten av Ålandsdjupet. I Öregrundsarkipelagen längre österut skedde den bakåtgripande erosionen i sprickdalarna med en hastighet på 0,4–1,2 km per 100 000 år.

Under tidigare glaciala cykler utgjordes erosionen i Forsmark av i) nednötning av förkastningsblockens höjdpunkter, ii) erosion av blockens sidor samt iii) fördjupning och breddning av sprickdalar och sänkor längs sprickzoner. Det är sannolikt att mönstret hos den glaciala erosionen kommer vara detsamma under kommande glaciala cykler. Hastigheten hos nednötningen av den kristallina berggrunden under framtida nedisningar har, generellt sett, uppskattas till < 1 m per 100 000 år, baserat på modellering av kosmogena nuklider och tider för framtida glaciala perioder. Historiskt har förkastningsbranter längs blocksidor på andra platser i Uppland retirerat med en hastighet på 42–125 m per 100 000 år. Det betyder att det är osannolikt att branternas reträtt under de kommande 100 000 åren kommer att sträcka sig långt förbi de existerande kanterna hos förkastningsblocken.

Singö-, Eckarfjärden- och Forsmarkdeformationszonerna hyser relativt grunda och segmenterade sprickdalar i Forsmark i jämförelse med deras förlängningar i Öregrundarkipelagen. Vid framtida glacial erosion kommer plockning av block sannolikt att bilda sprickdalar längs de större deformationszonerna i Forsmark. Den begränsade breddningen av sprickdalar utanför de underliggande sprickzonerna under Pleistocen indikerar dock att framtida erosion av sprickdalar i huvudsak kommer att ske inom deformationszonerna som avgränsar den tektoniska linsen i Forsmark. Framtida bildning av sprickdalar under de kommande en miljon åren kan förväntas sträcka sig till djup om 10–50 m och med en bredd som understiger 1 km, under antagandet om liknande total tid av glaciala förhållanden som de senaste en miljon åren. På detta sätt skulle det krävas en tid på omkring en miljon år för att området med kraftigare glacial erosion i Öregrundsarkipelagen skulle kunna nå Forsmark genom bakåtgripande erosion. Simuleringar av framtida klimat indikerar dock att de kommande 100 000-tals åren skulle kunna få begränsade glaciala perioder, vilket skulle öka tiden för den bakåtgripande erosionen till mer än en miljon år att nå Forsmark.

Contents

1 Introduction

The term *headward erosion* refers to the extension of river channels in the upstream direction, so that a valley or ravine becomes longer (Schumm 1993). This process involves upstream migration of knickpoints on the long profile of a river or stream (Bishop et al. 2005). In glacial systems, headward erosion is recognised in the retreat of cirque backwalls (Oskin and Burbank 2005), at the heads of glacial troughs (Brocklehurst and Whipple 2002, Alley et al. 2019), in overdeepenings (Patton et al. 2016b), in tunnel valleys (Hooke and Jennings 2006) and, potentially, in rock-cut meltwater channels (Tirén et al. 2001). Several of these examples may be recognised as examples of *backwearing* of steep rock slopes within wider terrain that is lowered by *downwearing* and *incised* by linear erosion along glacial and meltwater valleys. Backwearing and headward erosion have a horizontal direction and rate, and headward erosion can be seen as a special case of backwearing along the long axis of a valley or trench. Downwearing and incision have a vertical direction and rate: downwearing is used herein as the general vertical erosion of a larger surface, whereas incision is used for the localised focussed downward erosion of a *rock trench* – a long, narrow, linear and steep-sided valley typical of selectively eroded fracture zones in glaciated basement terrain.

The volumes of fault-bounded rock basins in the Öregrund archipelago are greater than at Forsmark, 15 km to the NW. This difference suggests greater depths of erosion in the past at Öregrund. The impacts of weathering and fluvial and coastal erosion on basement rocks during the Holocene have been small and were likely so earlier in the Pleistocene. Below sea level these impacts were zero. Hence, excavation of rock trenches, broader valleys and basins mainly represents erosion by the Fennoscandian Ice Sheet during successive Pleistocene glaciations. Depths and rates of erosion beneath ice sheets relate to several controls, mainly geology, preglacial weathering, topography, ice sheet dynamics and time. In Uppland, the basement remained buried beneath Proterozoic and Early Palaeozoic sedimentary rock cover and so was protected from Mesozoic and Cenozoic weathering (Hall et al. 2019a). Topography and ice-sheet dynamics were similar at the regional scale. Hence, the reasons for the contrasts in erosion depths between Öregrund and Forsmark likely relate to geology and time.

The main geological controls on glacial erosion in Uppland have been identified previously as (i) the contrasts in hardness and fracture spacings between Proterozoic to lower Palaeozoic sedimentary cover rocks and the gneissic basement and (ii) the heterogeneous fracture spacing in the basement across scales (Hall et al. 2019b), in common with geological controls on subglacial erosion elsewhere (Krabbendam and Glasser 2011, Hooyer et al. 2012). Basement at Öregrund and Forsmark was likely re-exposed by glacial erosion during the Pleistocene, but the precise timing of re-exposure is presently unknown.

The main influence of time was through the gradual adaptation of the ice sheet bed to glacier flow in response to cumulative glacial erosion through multiple Pleistocene glaciations. In Uppland, this adaptation was through modification of the smooth, low relief surface of the sub-Cambrian basement unconformity which was exhumed by glacial erosion during the Pleistocene (Hall and van Boeckel 2020). Part of this adaptation was through the progressive deepening and backwearing of major rock trenches and basins, leading to a roughening of the ice-sheet bed. These topographic depressions may be (i) deepened and widened in future glaciations and (ii) extend headward towards Forsmark. Potentially, future headward erosion may influence shallow groundwater flow and the near-surface bedrock stress regime at Forsmark, factors which are important in safety assessments for long-term storage of nuclear waste in deep repositories.

This report considers the following main questions:

- Why are average depths of glacial erosion in the rock trenches and rock basins around Öregrund greater than around Forsmark?
- To what extent do basement fracture patterns control the positions and dimensions of these topographic depressions?
- What are the glacial processes that have eroded these bedrock depressions beneath the Fennoscandian Ice Sheet?
- What part, if any, of this erosion in the Öregrund archipelago was a result of headward erosion beneath the Fennoscandian Ice Sheet?
- What were the rates of glacial downwearing, backwearing and incision in the past, including any headward erosion? What are likely future erosion rates of headward erosion in the direction of Forsmark?

2 Regional Setting

2.1 Outline geological history

The Fennoscandian craton stabilised in east central Sweden after the Svecokarelian orogeny at ~1.9 Ga. During the time interval between 1.85 and 1.8 Ga, ductile deformation continued under lower grade metamorphic conditions within the ductile high-strain belts. The bedrock first entered the brittle regime between 1.8 and 1.7 Ga (Söderlund et al. 2009); brittle fractures started to develop from that time onwards. The dominant rock type at Forsmark is medium-grained metagranite with subordinate pegmatitic granite or pegmatite, fine- to medium-grained metagranitoid and amphibolite and other minor mafic to intermediate rocks. Gneissic fabrics are variably developed: some rocks are virtually undeformed; others show strong fabrics. Apart from amphibolite, which contains little or no quartz, the dominant and subordinate rock types have high quartz content (c. 20–50 %) (SKB 2013) (Figure 2-1).

Deep erosion had reduced the craton surface on the Baltica palaeocontinent to hilly and low relief by 1.5 Ga before burial by kilometre-thick Jotnian sediments consisting mainly of quartz sandstones and subordinate mudstones (Gorbatschev 1962). From the final stages of the Sveconorwegian Orogeny at ~960 Ma onwards, much of Scandinavia was subjected to long-term uplift and erosion that led eventually to removal of Jotnian and Sveconorwegian foreland-basin cover rocks from Uppland (Hall et al. 2019a). (U-Th)/He data from surface samples at Forsmark indicate cooling below 70 °C between 750 and 530 Ma (Page et al. 2007); most sedimentary cover was lost by the end of this interval. By the late Neoproterozoic, basement was re-exposed across large areas of Baltica and the palaeocontinent had been eroded close to base level (Hall et al. 2019b). Parts of Baltica that now lie in Sweden were flooded in the Early Cambrian (~515 Ma) in the first of numerous marine transgressive-regressive cycles that continued into the Late Ordovician (Wickström and Stephens 2020). Geological evidence for the remarkable extent and low relief of the sub-Cambrian unconformity surface comes from strike sections around outliers and from the stratigraphic architecture of the overlying sedimentary cover, which reveal remarkable continuity of unit thickness and facies over distances of > 500 km between the Bothnian Sea and southern Sweden (Nielsen and Schovsbo 2015). The sub-Cambrian unconformity surface is termed U2 in the classification of major unconformities on Baltica of Hall et al. (2021). Burial of the basement of Uppland from the Early Cambrian onwards is indicated by Early Cambrian sandstone dykes in basement fractures around its eastern periphery, widespread asphaltite fracture coatings derived from Middle Cambrian and younger Alum Shales and the presence of small outliers of Early to Middle Ordovician limestone offshore that overlie a gently inclined basement surface on the seabed off Forsmark (Hall et al. 2019a and references therein).

At the time of the Caledonian orogeny, Uppland formed part of a foreland basin, and the unconformity and its Early Palaeozoic cover were buried to kilometre depth (Larson and Tullborg 1998). The sub-Cambrian unconformity and its sedimentary cover in Uppland was disrupted by minor faulting with vertical displacement of a few tens of metres likely during the Permian Period (Sandström et al. 2006a). Sedimentary cover covering the sub-Cambrian unconformity was thinned by erosion from the Permian onwards but the basement likely remained buried in parts of Uppland into the Pleistocene before re-exposure by Fennoscandian Ice Sheet erosion (Hall and van Boeckel 2020). Removal of the sedimentary cover (both Caledonian foreland deposits and the Cambro-Ordovician strata) has exposed mosaics of inclined, flat-topped rock blocks on the present basement surface (Beckholmen and Tirén 2010a, Grigull et al. 2019). These flat-topped rock blocks are 10–20 km across and their top surfaces show very gentle dips. Some topographic lineaments between rock blocks are likely products of differential weathering and erosion since exhumation. Where rock-block tops are at different elevations, the height difference is attributed to Phanerozoic faulting beneath sedimentary cover (Beckholmen and Tirén 2010a, Grigull et al. 2019). These rock blocks may be termed *fault blocks* and were originally bounded by *fault scarps*. Backwearing from the original fault plane has occurred since exhumation.

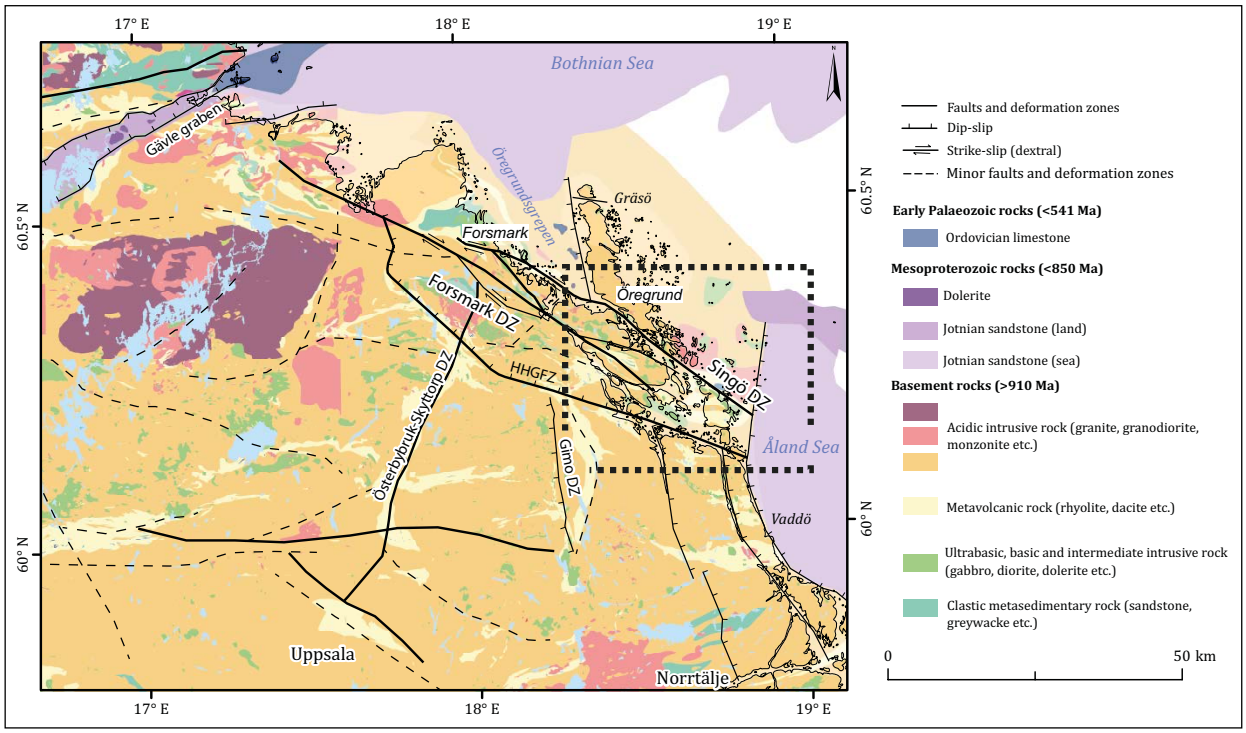

Figure 2-1. *Geology of Uppland and part of Stockholm County from Hall et al. (2019a, Figure 2.1). The Öregrund archipelago lies within the dashed white line. Main deformation zones (DZ) indicated. HHGRZ Hargshamn-Herrång Fracture Zone.*

2.2 Fracture patterns

2.2.1 Fracture development

Evidence of the timing of brittle deformation, fracture opening, groundwater circulation and fracture mineralisation are provided by cross-cutting relationships and by dated fracture coatings. Four main generations (G1–G4) of fracture minerals have been recognised in eastern Sweden (Sandström et al. 2008, 2009, Sandström and Tullborg 2009).

The main regional phase of fracture formation extended through the Svecokarelian orogeny from the initial period of ductile deformation and after the onset of brittle deformation. Regionally significant structures include the Forsmark Deformation Zone (FDZ) and the Singö Deformation Zone (SDZ) (Figure 2-1), with trace lengths greater than 50 km at the present surface (Beckholmen and Tirén 2010b). A deformation zone is a general term referring to an essentially 2D structure along which there is a concentration of brittle, ductile or combined brittle and ductile deformation (Glamheden et al. 2007). The regional deformation zones are elongate and vertical or steeply dipping with WNW−ESE or NW−SE strike (Stephens 2010). A set of abutting, slightly younger shear zones, with trace lengths of 20–40 km, developed in response to polyphase deformation in the ductile and brittle-ductile field late in the orogeny. Examples include the NNE-SSW and N-S striking Österbybruk-Skyttorp (ÖSDZ) (Malehmir et al. 2011) and the Gimo deformation zones (GDZ) (Grigull et al. 2019). At Forsmark, gently dipping fracture zones 1.2–4 km in length intersect the present land surface and occur in 6–185 m thick zones at depths of up to 950 m (Carlsten et al. 2004). Generation 1 (G1) coatings of epidote, chlorite, and quartz which indicate formation under high temperatures at depths of several kilometres (Saintot et al. 2011). Many shorter brittle fractures in the gneisses, including those in fault zones and fracture corridors, also have coatings of G1 minerals. The presence of younger generations of mineral coatings indicate that Svecokarelian fractures were reactivated repeatedly during the Palaeoproterozoic and later.

During the early Mesoproterozoic, tectonic activity shifted to active margins in southern and south-western Sweden during the Gothian (1.66–1.52 Ga) and Hallandian (1.47–1.38 Ga) orogenic phases (Bingen et al. 2008, Stephens et al. 2015). Weak extension in east-central Sweden was associated with minor intrusion of rapakivi granite suites around 1.5 Ga (Sundblad et al. 1993), fault graben formation and deposition of clastic sediments. Jotnian sedimentary units at Gävle are partially bound by faults which strike WSW-ENE for several tens of kilometres under the Bothnian Sea (Flodén 1977). The Jotnian sequence in the Bothnian Sea basin is displaced by long fault lines trending NNE and NNW (Beckholmen and Tirén 2010b).

During the Sveconorwegian orogeny (1.1 to 0.9 Ga), WNW-ESE and NW-SE faults developed or were reactivated at Forsmark (Sandström et al. 2010). Earlier fractures were reactivated, including the SDZ (Stephens et al. 2007, 2015, Saintot et al. 2011). New and reactivated fracture surfaces active at this time have Generation 2 (G2) mineral coatings include adularia, prehnite, laumontite, chlorite, and calcite (Sandström et al. 2010).

The sub-Cambrian unconformity provides a datum for recognising patterns of Phanerozoic faulting across southern Sweden (Johansson et al. 1999, Beckholmen and Tirén 2010a). In Uppland, U2 was broken by minor faulting into fault blocks (Figure 2-2). The main fault blocks have areas of up to 600 km^2 and are broken by shorter fractures into individual fault blocks with surface areas of 10–200 km^2 (Beckholmen and Tirén 2010a). Fault trace lengths on major fault blocks are mainly 20–70 km (Grigull et al. 2019). Phanerozoic faults carry Generation 3 (G3) coatings which are dominated by quartz, calcite and pyrite, with minor corrensite, adularia, analcime, and asphaltite (Krall et al. 2015, Drake et al. 2017). G3 minerals were precipitated as layered coatings at temperatures of ~ 60–190 °C between ~ 460 and 277 Ma (Drake et al. 2018).

The youngest, Generation 4 (G4) group of fracture coatings minerals formed at temperatures below 50 °C in the late Palaeozoic and after. Clay minerals, chlorite/corrensite and thin coatings of calcite dominate, together with small amounts of pyrite and goethite. G4 coatings are often found in hydraulically conductive structures, many of which are reactivated fractures containing G1–G3 minerals (Sandström et al. 2008, Tullborg et al. 2008, Sandström and Tullborg 2009).

During the Quaternary, the Forsmark region was repeatedly covered by ice sheets. During the last glacial maximum, the ice sheet over Forsmark reached a thickness of around 3 km (SKB 2020). The advance and retreat of these ice sheets over the landscape may have reactivated and opened existing gently dipping fractures at depth (Moon et al. 2020). Near-surface subhorizontal fractures at Forsmark were reactivated or formed as joints in the current stress regime (Claesson Liljedahl et al. 2011). Existing fractures opened and new fractures formed in the shallow subsurface in response to hydraulic jacking by subglacial water at overpressure (Krabbendam et al. 2021).

2.2.2 Fracture terminology

A fracture is any separation that divides rock into two or more pieces and includes joints (without displacement across the fracture) and faults (with displacement across the fracture). Fracture patterns may be described in terms of zonation, orientation (dip and strike), dimensions, spacing and topology.

- *Fracture zones* are localised regions where fracture spacing is much lower than in the adjacent host rock. Fracture zones define approximately tabular regions where width is much less than length and height. Fracture zones which flank faults or deformation zones are in geological literature often referred to as *damage zones* (Kim et al. 2004, Henriksen and Braathen 2006, Peacock et al. 2017). (Note that this term is used in a different sense at Forsmark to refer to parts of a rock mass damaged during man-made excavations). Fracture and damage zones commonly exhibit abrupt changes in fracture intensity (the amount of fractures in a given rock mass) at the edges (walls) of the tabular zone, with more diffuse changes being termed *fracture swarms* (Sanderson and Peacock 2019).
- Fractures in hard igneous and metamorphic rocks typically have dominant *orientations*, grouped as *fracture sets* (Ericsson and Ronge 1988). At Forsmark, there are 2 to 4 main sub-vertical fracture sets and 1 sub-horizontal set (La Pointe et al. 2005). A *master joint* is a long, persistent joint plane, generally within a dominant joint set. *Fracture aperture* is the gap between the fracture faces on either side of an individual fracture.

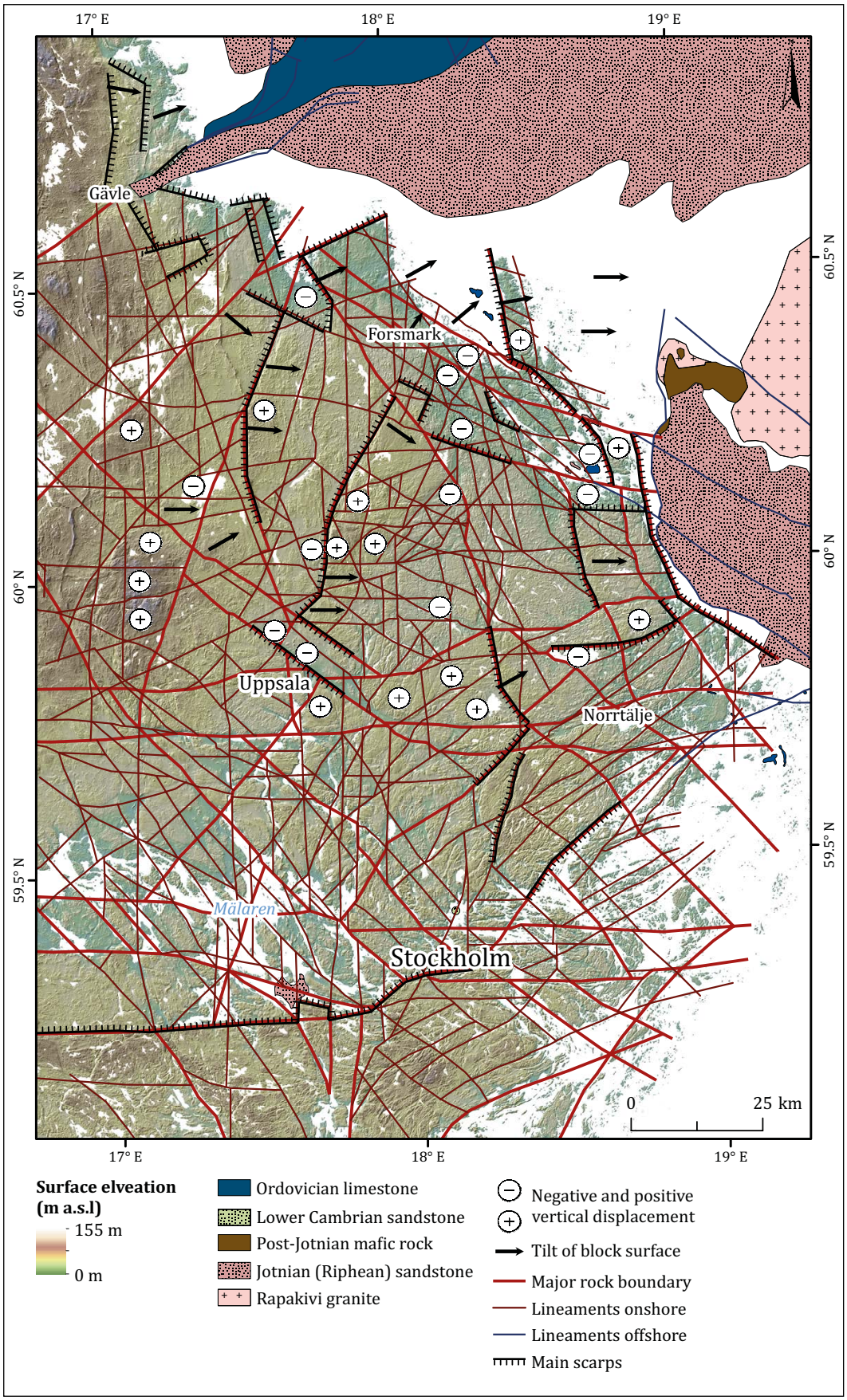

Figure 2-2. *Rock block map of Uppland and surrounding areas (data from Beckholmen and Tirén 2010a), with main fault scarps and positive and negative movements added on the basis of relative topographic position (Hall et al. 2019a, Figure 2-21). Elevations in metres above sea level.*

- Fracture zones occur as parts of different fracture sets. At Forsmark, fracture zones have been classified according to their *dimensions* (Table 2-1). Fracture trace lengths typically follow power laws (Reeves et al. 2012). General models of fracture trace lengths apply across scales to fractures mapped at outcrop of sub-metre length and to fractures inferred from lineaments at Forsmark and in its surroundings with lengths of tens of kilometres (La Pointe et al. 2005). Short fractures often terminate against (*abut*) long fractures (Sanderson et al. 2019).

Table 2-1. Terminology and general dimensions of brittle structures described at Forsmark. (Modified after Table 2-1 in Stephens et al. (2007).

Terminology	Length	Width
Regional deformation zone	> 10 km	> 100 m
Local major deformation zone	1–10 km	5–100 m
Local minor deformation zone	10 m–1 km	0.1–5 m
Fracture	< 10 m	< 0.1 m

- Individual fracture spacings may be clustered, regular or random. Closely-spaced fractures along a single vertical fracture set form *fracture corridors* (Sanderson and Peacock 2019). Fracture spacings along lines, planes or in 3D are termed *fracture intensities.* Fracture spacings commonly follow log-normal distributions in basement rocks in Sweden (Munier 1993).
- *Fracture network topology* is used to characterize fracture networks independently of network geometry (Sanderson and Nixon 2018). Topological networks have *nodes*, linked by branches, which bound regions, to form connected components. In fracture network topologies, an individual fracture is a *branch*. Fracture terminations are *I-nodes*, abutting or splay nodes are *Y-nodes*, and crossing fractures are *X-nodes* (Sanderson and Nixon 2015). (Note that 'Y-nodes' will commonly be represented by T-junctions). The proportions of these node types provide a basis for characterizing the topology and connectivity of a fracture network.

The heterogeneous orientations, spacings and lengths of individual fractures render fresh gneissic bedrock mechanically anisotropic. This heterogeneity makes the gneiss susceptible to differential denudation, by various weathering and erosion processes. For this study, we focus on regional fracture zones where typical fracture spacings are low, fracture apertures are high, fracture intensities are high and *in situ* joint-bound rock block sizes are small (Wang et al. 1991). Due to these properties, regional fracture zones represent major lines of weakness in the basement gneisses in Uppland. Fracture zones have been exploited by glacial erosion during the Pleistocene and have high potential for erosion beneath the Fennoscandian Ice Sheet in future glacial cycles.

2.3 Erosion and burial history of the Öregrund archipelago

The present coast of Uppland occupies a hinge zone along the edge of the exposed basement to the SW and the sedimentary basins of the Bothnian and Åland Seas to the NE (Winterhalter et al. 1981). Seismic surveys in the 1980's and 1990's identified the positions of sedimentary outliers in the Öregrund (Söderberg and Hagenfeldt 1995) and Stockholm archipelagos (Hagenfeldt and Söderberg 1994). Studies of the lithology of clasts of sedimentary rocks found as glacial erratics on the seabed in down-ice positions on the seabed and along the coast allowed the rocks to be assigned to broad age categories (Hagenfeldt 1995).

The basement around the Bothnian basin was first eroded close to its present erosional level at ~1.5 Ga (Hall et al. 2021). The oldest basement unconformity, the sub-Jotnian unconformity (U1) is buried by Jotnian sandstones in the Gävle and Åland basins (Paulamäki and Kuivamäki 2006). The edge of Jotnian sedimentary cover extends southwards in the Öregrundsgrepen towards Forsmark and Öregrund (Figure 2-1). The western edge of the Jotnian sandstone in the Åland sedimentary basin reaches to within a few km of the present coast from Singö southwards (Winterhalter et al. 1981). Small outliers of Proterozoic sandstone occur within the Öregrund archipelago; the northern outlier in the Öregrundsleden is interpreted as Jotnian sandstone and the southern outlier found on the seabed NW of Herräng is of Riphean (likely Neoproterozoic) age (Söderberg and Hagenfeldt 1995).

Cambrian outliers are not recognised from the Öregrund archipelago (Söderberg and Hagenfeldt 1995), likely due to non-deposition and erosion in the 'Hawke Bay Event' during the late Early Cambrian (Nielsen and Schovsbo 2015). Cambrian sandstone dykes occur widely, however, in neighbouring areas of the Stockholm archipelago (Martinsson 1974), on Åland (Bergman 1982) and in SW Finland (Kohonen and Rämö 2005) and in half-grabens at Närke (Thorslund and Jaanusson 1960). Widespread asphaltite fracture coatings indicate a former cover of bituminous middle to late Cambrian Alum Shale in Uppland (Sandström et al. 2006b). Outliers of Ordovician limestone are found in the Öregrundsgrepen and the Öregrund archipelago (Söderberg and Hagenfeldt 1995) and more widely in the Bothnian and Åland basins (Paulamäki and Kuivamäki 2006). These limestones originally covered much of Finland and Sweden, related to the marine transgression in the middle and late Ordovician that extended across eastern Sweden and adjacent parts of the Baltic basin and western Finland (Paulamäki and Kuivamäki 2006).

The discoveries of sedimentary rocks on the seabed have allowed models to be developed of the erosion and burial history in the Öregrund archipelago and its surroundings (Amantov et al. 1995, Söderberg and Hagenfeldt 1995). The main events may be summarised as follows:

- Erosion of the sub-Jotnian unconformity (U1), cut in basement.
- Deposition of Jotnian sandstones in the Mesoproterozoic.
- Erosion of an unconformity in Jotnian sandstone and basement, equivalent to U1b in the scheme of Hall et al. (2020).
- Deposition of Riphean feldspathic sandstones in the Neoproterozoic, likely in the Tonian (Hagenfeldt 1995).
- Erosion of the sub-Cambrian unconformity (U2) across basement and Proterozoic sedimentary rocks.
- Deposition of Early Cambrian sandstone, followed, after an hiatus, by renewed deposition of Late Cambrian Alum Shale and Ordovician limestone.

The Mesoproterozoic-Early Palaeozoic event sequence in the Öregrund archipelago, including ages of the events, is summarised in Figure 2-3.

In southernmost Sweden, Palaeozoic cover rocks were progressively removed by erosion from the Permian onwards, re-exposing the basement to chemical weathering and erosion, and reburied in the Late Cretaceous (Lidmar-Bergström et al. 2017). Around present-day outliers of Palaeozoic rocks, however, re-exposure of the basement was geologically recent and a response to Pleistocene glacial erosion (Hall and van Boeckel 2020). In east-central Sweden, Palaeozoic sedimentary cover is today confined to the southern margin of the Bothnian Sea basin (Figure 2-2). A geologically recent exhumation of the sub-Cambrian unconformity further south is indicated by the preservation of its planar, block-faulted morphology in northern Uppland (Rudberg 1970). In southern Uppland and in Stockholm County the greater relative relief of the present basement surface suggests earlier re-exposure to weathering and erosion consistent with preservation of shallow weathering in parts of Stockholm City (Elvhage and Lidmar-Bergstrom 1987). In quarries and boreholes in Uppland, including at Forsmark, no weathered basement has been reported (Hall et al. 2019a). Hence, the Mesoproterozoic and Ordovician sedimentary cover protected the basement from weathering in the Öregrund archipelago until the Pleistocene.

The erosion and burial history since 1.5 Ga is important in the study of Pleistocene glacial erosion. Firstly, proximity of U1 and the present basement surface in the Öregrund archipelago and around the edge of the Bothnian basin in E Sweden and W Finland indicates that total denudation of basement since 1.5 Ga has been very limited (Hall et al. 2021). The general morphology of the sub-Cambrian unconformity is preserved in parts of the present basement surface (Lidmar-Bergström et al. 2017), allowing its use as a reference surface for estimating depths of denudation, including glacial erosion. Secondly, erosion in the Late Cenozoic has been restricted mainly to the removal of the former sedimentary cover, with an important, geologically recent phase of erosion beneath the Fennoscandian Ice Sheet (Hall and van Boeckel 2020). Thirdly, the re-exposed unconformity surface was in hard basement gneisses, without significant saprolite cover, unlike in southernmost Sweden.

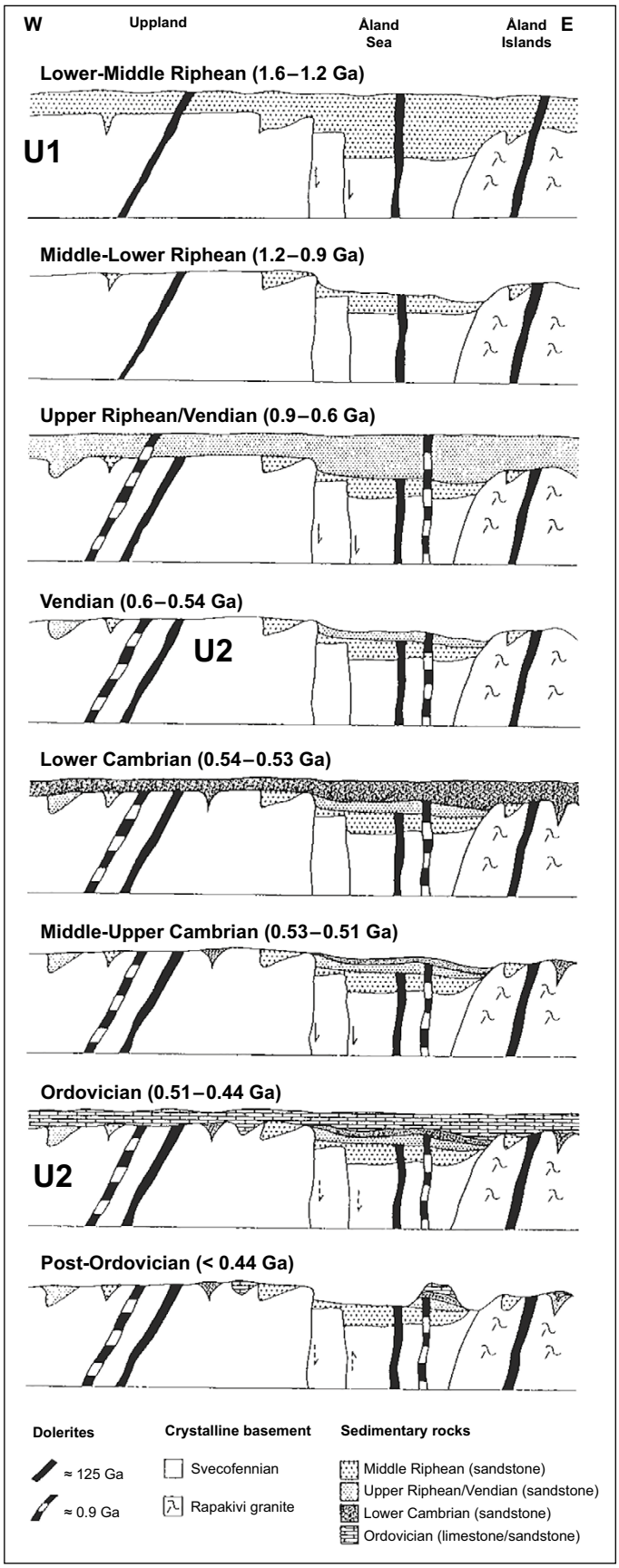

Figure 2-3. *The sequence of erosion and burial since 1.6 Ga in east-central Sweden, the Åland Sea and the Åland Islands during the Middle Riphean (late Mesoproterozoic), Late Riphean-Vendian (early-middle Neoproterozoic), Cambrian, Ordovician, and post-Ordovician. Modified to show U1 and U2 from Figure 8 in Söderberg and Hagenfeldt (1995).*

2.4 Glacial erosion

During the Pleistocene, the Fennoscandian Ice Sheet (i) eroded and thinned the sedimentary cover in the Baltic Sea basin, (ii) removed the sedimentary cover around its margins to re-expose parts of the sub-Cambrian unconformity and (iii) eroded the shield surface (Hall and van Boeckel 2020). A new assemblage of bedrock landforms of glacial erosion, including roches moutonnées, whalebacks and crag and tails developed across the basement lowlands of Sweden (Olvmo and Johansson 2002).

2.4.1 The sub-Cambrian unconformity: reference surface for Pleistocene denudation

Digital Elevation Models (DEMs) for lowland Sweden show extensive basement surfaces of low relief and low roughness at the regional scale (1–10 km). These landscapes are typical of much of Västergötland, comprises a mosaic of fault-bound blocks with flat or gently inclined top surfaces, separated by steeper steps or trenches, related to Phanerozoic faults with minor (< 20 m) throw. The surfaces carry mosaics of fault-bound rock blocks with flat or gently inclined tops that record minor Phanerozoic faulting. The smooth, low-relief top surfaces of these fault blocks have long been interpreted as slightly modified and lowered remnants of the *sub-Cambrian unconformity* (U2) and widely referred to as the *sub-Cambrian peneplain* (Rudberg 1970, Lidmar-Bergström 1988, Johansson et al. 2001b, Olvmo 2010, Lidmar-Bergström et al. 2017), although the latter term strictly refers to the present surface, eroded and lowered from the original unconformity (De Geer 1948, Hall et al. 2019a). In parts of southern Sweden, the unconformity surface shows metre-scale roughness and < 10 m per km relative relief over 1–10 km distances where it emerges from beneath Early Cambrian sandstones (Hall et al. 2019b). Summit relief on the emerging unconformity around the Early Palaeozoic outliers at Närke and Motala in south-eastern Sweden is slightly greater at 2–15 m over 2 km distances. Comparisons of models of the smooth, low relief U2 surfaces with the present basement surfaces around Early Palaeozoic outliers reveal increasing bedrock surface roughness and relative relief with increasing distances from outliers and allow the progressive development of glacial landscapes and landforms to be recognized (Hall et al. 2019b).

Strikingly similar features are found in Uppland. Early Palaeozoic covers are found in the Bothnian and Åland Seas and outliers on the seabed close to the present coastline (Figure 2-3). The present basement surface has low relief and low roughness (Hall et al. 2019a). A mosaic of fault blocks of various sizes dominates the regional relief (Beckholmen and Tirén 2010a, Grigull et al. 2019). Hence, the present basement surface has been long been referred to as part of the sub-Cambrian Peneplain in southern Sweden (Rudberg 1970, Tirén 1991, Lidmar-Bergström 1994)

The smooth, near-planar and block-faulted form of U2 allows the former unconformity to be used as a reference surface for identifying patterns and estimating depths of erosion of basement rocks since re-exposure (Hall et al. 2019a, b). In areas proximal to present-day outliers of Early Palaeozoic rocks, re-exposure of U2 occurred during the Pleistocene (Hall and van Boeckel 2020). Here, subsequent erosion of basement was by (i) glacial erosion beneath the Fennoscandian Ice Sheet and (ii) by weathering and fluvial erosion during ice-free periods. Slow weathering (Shakesby et al. 2011) and limited fluvial rock channel erosion (Jansen et al. 2014) during the Holocene in Sweden indicates that glacial erosion was strongly dominant.

2.4.2 Landscapes and landforms of glacial erosion

Mapping of landscapes and landforms of glacial erosion in Uppland at the regional (1–10 km) and local (0.1–1 km) scales using LiDAR-based DEMs has revealed the pattern of modification of the antecedent U2 topography and the development of new glacial landforms (Hall et al. 2019a). The new glacial landscapes retain the regional pattern of fault blocks, but the tops and edges of the fault blocks have been variably eroded. Some block tops retain the smooth relief of the U2 surface, but others have been lowered, dissected, and reduced in area by erosion, with increased surface roughness and relative relief (Figure 2-4). Examples of sequential glacial erosion of fault block tops at Alunda are given in Figure 4-16 of Hall et al. (2019a).

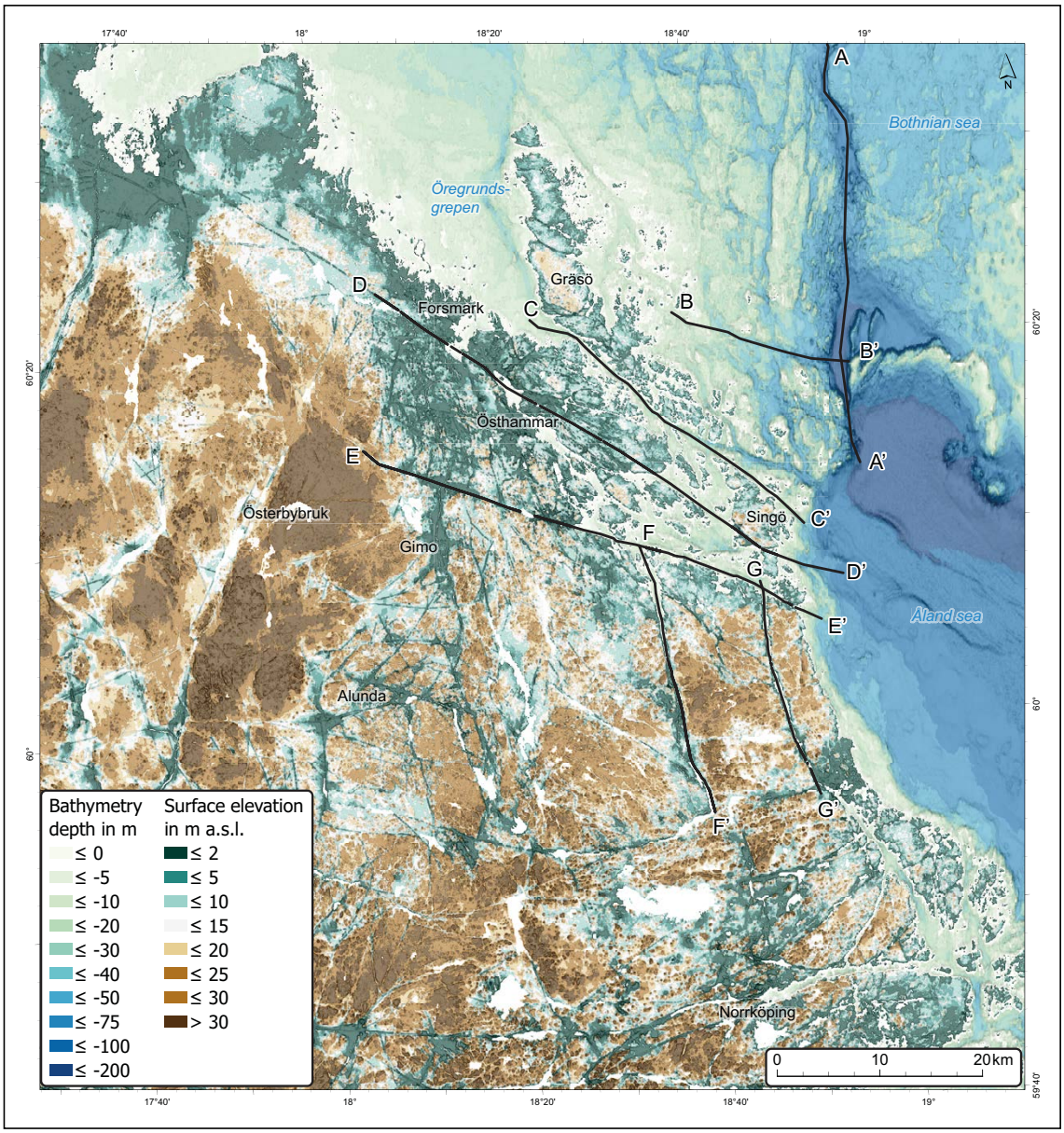

Figure 2-4. *Bedrock relief and bathymetry of Uppland, part of Stockholm County and adjacent areas of the seabed. The locations of major trenches are shown in NE Uppland and on the sea bed: long profiles for these trenches are shown in Figure 4-10.*

Mapping of local glacial landforms shows a strong zonation of features within three terrain types: (i) ice-roughened, (ii) weakly streamlined and (iii) disrupted terrain (Hall et al. 2019a). Ice-roughened terrain is dominated by box hills and roches moutonnées, with fracture-guided and till-filled rock trenches and box- and star-shaped rock basins. Weakly streamlined terrain has a similar general bedrock form but includes elongate hills, with till tails, which align with the direction of ice flow during the Late Weichselian glaciation. Glacially disrupted terrain is characterised by extensive shallow glaciotectonics, or *glacial ripping* (Hall et al. 2020, Krabbendam et al. 2022a, b) with hydraulic jacking and disruption in bedrock, and by spreads of large, angular boulders that mask the underlying bedrock surface. The depths of rock mobilized by ripping during the last deglaciation are estimated as 1–4 m, indicating that ripping can make a significant contribution to glacial erosion budgets in areas where ripping has operated (Hall et al. 2020, van Boeckel et al. 2022).

This study is focussed on areas of relatively deep (> 10 m) glacial erosion, specifically the rock trenches and rock basins found in and around the Öregrund archipelago. Evidence is lacking that these negative relief forms existed on the sub- Cambrian unconformity. In southern and eastern Sweden, the buried U2 surface around Early Palaeozoic outliers has a near-planar form, with depressions and hills maintaining 1–10 m relief over kilometre distances. No steep-sided, narrow and deep bedrock depressions are reported from the buried unconformity surface. Also, no small outliers of the basal Cambrian Mickwitzia Sandstone have been mapped infilling such depressions, Hence, the rock trenches and basins on the present surface in Uppland are not inherited landforms exhumed from the U2 surface. Instead, these rock depressions developed through glacial erosion beneath the Fenno-scandian Ice Sheet during the Pleistocene. Why was glacial erosion focussed on these locations?

3 Methods and datasets

This desk study synthesises published data on regional geology, fractures, the sub-Cambrian unconformity, the glacial geomorphology of Uppland and estimated depths of glacial erosion beneath the Fennoscandian Ice Sheet to assess the potential for headward erosion from the Öregrund archipelago towards Forsmark. New maps are provided for the distribution and topology of major fracture zones and rock trenches, the lines of weakness and the landforms most likely to relate to headward erosion. The collation of existing and new information provides insights into the processes by which ice sheets erode fracture zones to form rock trenches, valleys and basins in lowland basement terrains. We use U2 as a reference surface for estimating depths of Pleistocene denudation, of which glacial erosion constitutes the major part, for different geomorphological settings. We provide estimates of past rates of downwearing, backwearing and incision for various landforms in the Öregrund archipelago and its surroundings.

3.1 Data attribution

Digital geological data provided by the Swedish Geological Survey (SGU) and of digital elevation data from Lantmäteriet (The National Swedish Land Survey) have been extensively used in earlier studies (Hall et al. 2019a, b) and in the present study. Data sets include the bedrock elevation and depths of Quaternary sediment. Landforms have been superimposed in ArcGIS on SGU datasets for rock type, fractures, Quaternary geology and depth to bedrock. Soil depth data, representing the total depth of Quaternary deposits above bedrock, has been modelled by SGU from borehole, well and outcrop data. Bathymetric data was sourced from the Baltic Sea Hydrographic Commission, 2013, Baltic Sea Bathymetry Database version 0.9.3. Where necessary, the DEM's (2 m and 50 m) were resampled to a 10 m resolution, using ArcMap 10.6 to improve visual interpretation. Maps and diagrams from previous studies were first georectified using the overview map provided by SGU as a base map. Features such as faults and lithologies were then superimposed as a separate layer and modified in ArcMap 10.6 and Adobe Illustrator CS 6.

3.2 Fracture zone patterns and properties

The pattern of regional and local major deformation zones in Uppland and on the adjacent seabed has been mapped previously from topographic lineaments (Beckholmen and Tirén 2010a, Grigull et al. 2019) and includes results from SGU field mapping (Persson 1985). In Uppland, regional and local topographic lineaments have been mapped on the present land area and the adjacent seabed and interpreted as major fracture zones (Flodén 1977). Some local major and minor deformation zones may lack expression as topographic lineaments in areas where glacial erosion, with its associated incision, has remained relatively low. Here, we focus on the regional scale and on the erosion of major rock trenches.

We identify nodes on the regional fracture network mapped by Grigull et al. (2019) and apply a standard topology (Figure 3-1). The orientations of branches are shown in rose diagrams to identify the main regional fracture sets. Previous work at Finnsjön, Forsmark (Ahlbom and Tirén 1991), and beneath the seabed along the Singö deformation zone (Glamheden et al. 2007) has provided detailed measurements of the fracture and mechanical properties of rocks in different types of fracture zone. This information allows the observed characteristics and measured dimensions of fracture zones in the subsurface to be linked to trench dimensions and forms at the present rock surface. We apply topological descriptions to local fracture networks at Finnsjön and Forsmark.

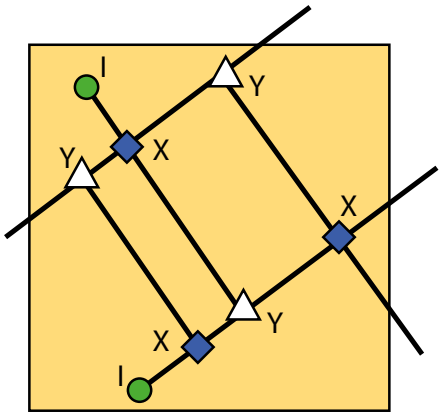

Figure 3-1. *A simple fracture topology with branches between crossing (X), abutting and splaying (Y) and terminating (I) nodes. Networks with high frequencies of I-nodes have low connectivity: networks with high frequencies and densities of X- and Y-nodes have higher connectivity.*

3.3 Glacial erosion in sedimentary rocks

The links between the distributions of sedimentary outliers and the basement relief are reviewed for the area of the Öregrund archipelago. A set of profiles were drawn from bathymetric data across the Åland Deep and the seabed E of Åland to illustrate differential erosion of basement and Jotnian cover and trench development along fracture zones in the basement. The elevations of small outliers of Jotnian sandstone and Ordovician limestone on the seabed are compared with those of adjacent upfaulted basement rock blocks interpreted previously as fault-bound to establish minimum depths of erosion in the sedimentary cover by the Fennoscandian Ice Sheet.

3.4 Glacial erosion in basement

3.4.1 Erosion patterns and landforms

Denudation depths below the sub-Cambrian unconformity have been estimated previously for Uppland and at Forsmark by comparing models of the U2 surface to the present bedrock surface (Hall et al. 2019a). Areas with relatively high erosion depths are seen as rock trenches, valleys and basins that are set below glacially modified fault block tops. These landforms are described in DEMs of the bedrock surface based on SGU data at the regional scale and in 5 sub-areas at Dannemora, Hargshamn, Öregrund, Forsmark and Finnsjön.

Various terms have been used to describe linear bedrock depressions in southern Sweden which include *fissure valleys* (Elvhage and Lidmar-Bergström 1987), *joint valleys* (Johansson et al. 2001a) and *fracture valleys* ('sprickdal' in Swedish). Here we use the term *rock trench* to describe long, narrow, linear, steep-sided valleys cut in bedrock which are typical forms of glacial erosion in basement terrain (Krabbendam and Bradwell 2014). The term is morphologically descriptive and can be applied across scales to cover valley forms from narrow, short clefts to wider, usually longer valleys. Rock trenches of different sizes at the landsurface can be linked to buried fracture zones that include those along master joints, fracture corridors, faults and deformation zones which potentially can strongly influence the positions and dimensions of trenches. The rock trench network can be described in terms of the same dimensionless topologies used for fracture networks. The term *valley* is used here in its general sense as a long, linear, partly sediment-filled depression set within higher ground and usually drained by a river or stream on land or wholly or partly submerged beneath the sea.

3.4.2 Fracture control on trench networks

The regional trench network and local sub-area networks are described and mapped from DEMs of bedrock surfaces. The same network topology used for fractures is applied to the regional trench network and the local trench network at Finnsjön. Fracture networks and trench networks are compared at the regional and local scales in terms of dimensions, morphology and topology.

3.5 Estimating denudation depths

In previous studies, U2 has been used as a reference surface for estimating depths of denudation and glacial erosion of basement rocks in lowland basement terrain (e.g. (Johansson et al. 1999, Sturkell and Lindström 2004, Gabrielsen et al. 2015). The method requires the following information:

- The form and elevation of U2, and depths of weathering across its surface before its re-exposure.
- The contribution, if any, of weathering and subaerial erosion to modification of the basement surface during the Phanerozoic but prior to the onset of Pleistocene glaciation.
- The form and elevation of the present bedrock surface.

The assumptions which underlie the use of U2 as a reference have been examined in detail previously (Goodfellow et al. 2019, Hall et al. 2019a, b). The methodology is outlined below.

In the Trollhättan area, U2 emerges from beneath Early Palaeozoic cover rocks. U2 has a near planar form (Johansson et al. 2001b) and weathering on the unconformity surface was limited to shallow patches (Hall et al. 2019b). U2 was dislocated by post-Early Permian fault movements, with vertical displacements of 5–50 m to form tilted fault blocks (Ahlin 1987, Hall et al. 2019a). The morphology, block faulting and weathering status of U2 is similar around Early Palaeozoic outliers at Närke and Motala (Hall et al. 2019b). Projections of buried unconformity surfaces in the vicinity of outliers allow estimation of patterns of downwearing and depths of incision.

Limited Phanerozoic erosion on the summits of resistant rock knobs allows bedrock summit elevations also to be used as pinning points for summit envelope surfaces that mimic the former U2 surface in Uppland. The procedure yields DEMs showing smoothed surfaces at different scales that represent models of U2 (the former, re-exposed unconformity surface). Subtraction of the present basement surface provides estimates of depths of rock removed since re-exposure of U2. Average erosion depths represent downwearing below the summit envelope surface; actual erosion depths also include rock missing from summits. The average lowering of summits around Forsmark is estimated to 10 m (Hall et al. 2019a), but some differential summit lowering may have occurred between fault blocks since re-exposure.

The fault scarps at the edges of rock blocks provide constraints on backwearing (Figure 3-2). As the fault scarps are exhumed features, the edges of the raised rock blocks were not exposed previously to weathering and erosion. Hence, the original fault scarp faces were likely sharp-edged, planar surfaces on re-exposure and so provide simple, step-like reference surfaces against which to compare the present rock slope form (Hall et al. 2019a, b). Backwearing is represented by the measured distance in bedrock profiles between the position of the former scarp face at the edge of the fault block and the point of inflexion on inclined fault block tops where wedge of rock removed from the scarp face tapers out.

Backwearing also occurs along trench, valley, and basin margins. The extent of backwearing is constrained by measured variations in width along these elongate bedrock depressions. The extent of trench widening beyond underlying fracture zones is constrained where subsurface information is available on fracturing, as at Finnsjön and Forsmark.

Headward erosion along river valleys is indicated by retreat of knickpoints and steepening of thalwegs in long profiles (Seidl et al. 1992). Similar steepening can be expected along rock trench floors that connect with deep bedrock depressions, as along tributary glacial valleys in mountains (MacGregor et al. 2000). In this study, long profiles are presented for major trenches formed along regional deformation zones on the rim of the Åland Deep and in the eastern part of the Öregrund archipelago.

Depths of incision are represented by measured elevation differences between neighbouring fault block surfaces and trench floors. Height differences are derived from DEMs of bedrock surfaces.

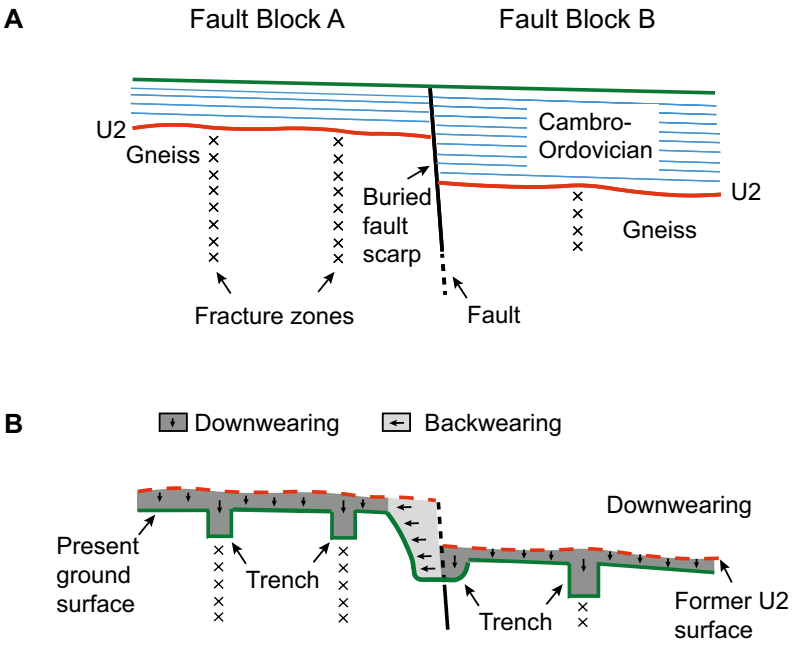

Figure 3-2. *Schematic model to illustrate how U2 and the fault scarps that dislocate its surface can be used to estimate downwearing and backwearing after re-exposure. A. Situation prior to re-exposure, with U2 and Phanerozoic fault scarps still buried by Cambrian-Ordovician sedimentary rocks. Fracture zones in the basement gneisses are indicated. B. Present-day basement surface. Downwearing of U2 has involved minor lowering on present summits and differential erosion along fracture zones to form trenches. Backwearing of the fault scarps is estimated from fault planes.*

3.6 Rates of glacial erosion in the Öregrund archipelago

Erosion depths were derived previously from comparisons of the sub-Cambrian unconformity modelled in summit envelope surfaces and the present basement surface in Uppland (Hall et al. 2019a). Here, we provide additional estimates for specific landforms in the Öregrund archipelago that include fault block tops, fault scarps and rock trenches. We assume that erosion dates from 1.2 Ma, the main period of glacial erosion in the Baltic Sea basin (Hall and van Boeckel 2020). Rates of downwearing and incision are expressed as m or km per 100 ka, the approximate lengths of glacial-interglacial cycles in the Middle and Late Pleistocene. We derive rates of backwearing over similar timescales for (i) fault scarps from the rock wedges lost to erosion after exhumation (Figure 3-2) and (ii) for headward erosion of trenches from the positions of knickpoints and where thalwegs steepen around the edge of the Åland Sea and in the eastern Öregrund archipelago.

4 Results

4.1 Fracture controls on basement erosion

Fracture properties exert strong influence over glacial lineaments and erosional landforms across scales in the basement gneisses of lowland Sweden (Lidmar-Bergström 1994). Major fracture zones seen in regional fracture patterns represent the most significant lines of weakness for deep erosion in the basement gneisses. The properties of different types of fracture zones at Finnsjön at Forsmark and the internal structure of the SDZ are important for understanding the links between fracture zones and patterns and processes of glacial erosion.

4.1.1 Regional fracture patterns

The regional and local major deformation zones in Uppland vary in length, with a few regional deformation zones exceeding 40 km (Figure 4-1). The fractures that delineate the main Phanerozoic fault blocks on U2 are generally > 10 km long (Tirén and Beckholmen 1989, Grigull et al. 2019). Some major fault blocks have a few, internal, shorter fractures; others are crossed by multiple short fractures. Areas with low fracture zone frequencies and high fracture zone spacings are found south and east of Gävle. In contrast, high frequencies and low spacings occur around Uppsala. Fracture zones also occur with high frequencies and low spacings in the Öregrund archipelago SE of Forsmark (Figure 4-1), part of a tectonic hinge zone between the basement and the sedimentary basins in the Bothnian and Åland Sea (Hall et al. 2019a).

The dominant orientations of the major lineaments are interpreted to represent 4 fracture sets (Figure 4-2): NNW-SSE, WNW-ENE, W-E and WSW-ENE.

The topology of major regional fracture zones is shown in Figure 4-2. Branches > 30 km long are few (n=10) and usually spaced 20–40 km apart. Terminating I-nodes are common, but Y- and X-nodes dominate, indicating significant connectivity between major deformation zones. Connectivity is greatest on long fractures, including the SDZ and other regional deformation zones, and in the Öregrund archipelago. Short fractures often abut longer fractures at T-junctions to form Y-nodes.

4.1.2 Fracture properties at Finnsjön

The Finnsjön area, ~15 km SW of Forsmark, was explored in the 1980s as a potential site for a nuclear waste repository (Ahlbom and Tirén 1991). The bedrock summits E of Finnsjön rise to 35–38 m a.s.l., and low-relief bedrock surfaces at these elevations suggest that the present surface stands close to the original erosional level of U2 (Tirén 1991). Rock trenches and rock basins have been eroded below the summit surface.

Detailed mapping of the dominantly granite-granodiorite rocks in surface exposures was accompanied by resistivity surveys and drilling of deep boreholes (Ahlbom and Tirén 1991). The exploration revealed the orientations and dimensions of main fracture zones and fracture corridors to depths of several hundred metres (Figure 4-3). Common fracture coatings at Finnsjön include three generations of calcite, together with laumontite, prehnite, quartz and chlorite (Tullborg and Larson 1982), similar to the generations of fracture coatings recognised at Forsmark.

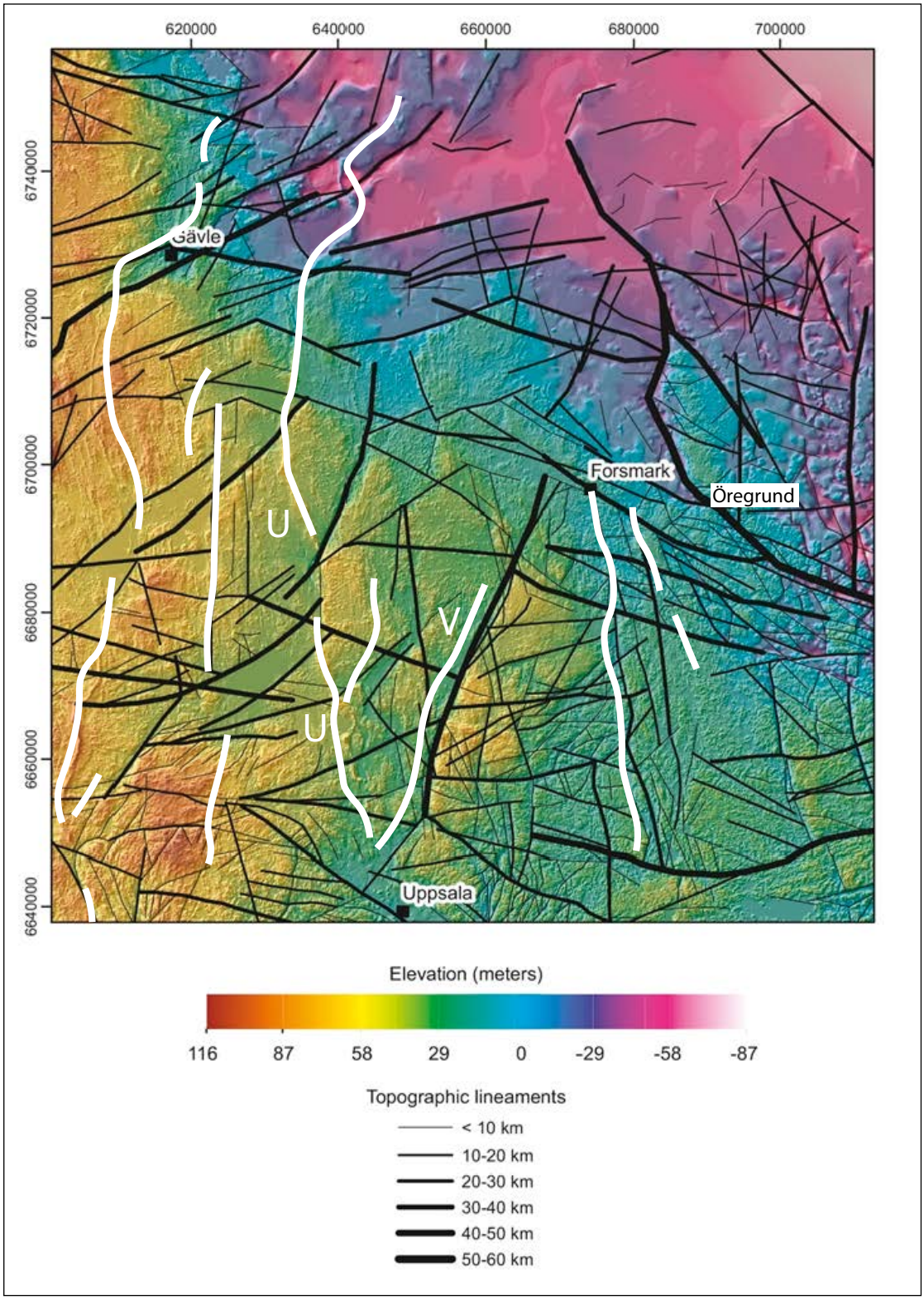

Figure 4-1. *Topographic lineament interpretation of the combined digital elevation model. Black lines are lineaments interpreted based on the DEM with 50 m grid resolution. The DEM represents the relief of both the bedrock surface and the Quaternary cover sediments. The lineament line thickness indicates different length categories. The white lines represent the main eskers, marking former major conduits for channelled glacial meltwater flow. U – Uppsala esker. V – Vattholma esker. The coordinate values are in meters (SWEREF99TM). Adapted from Figure 3-3 in Grigull et al. (2019).*

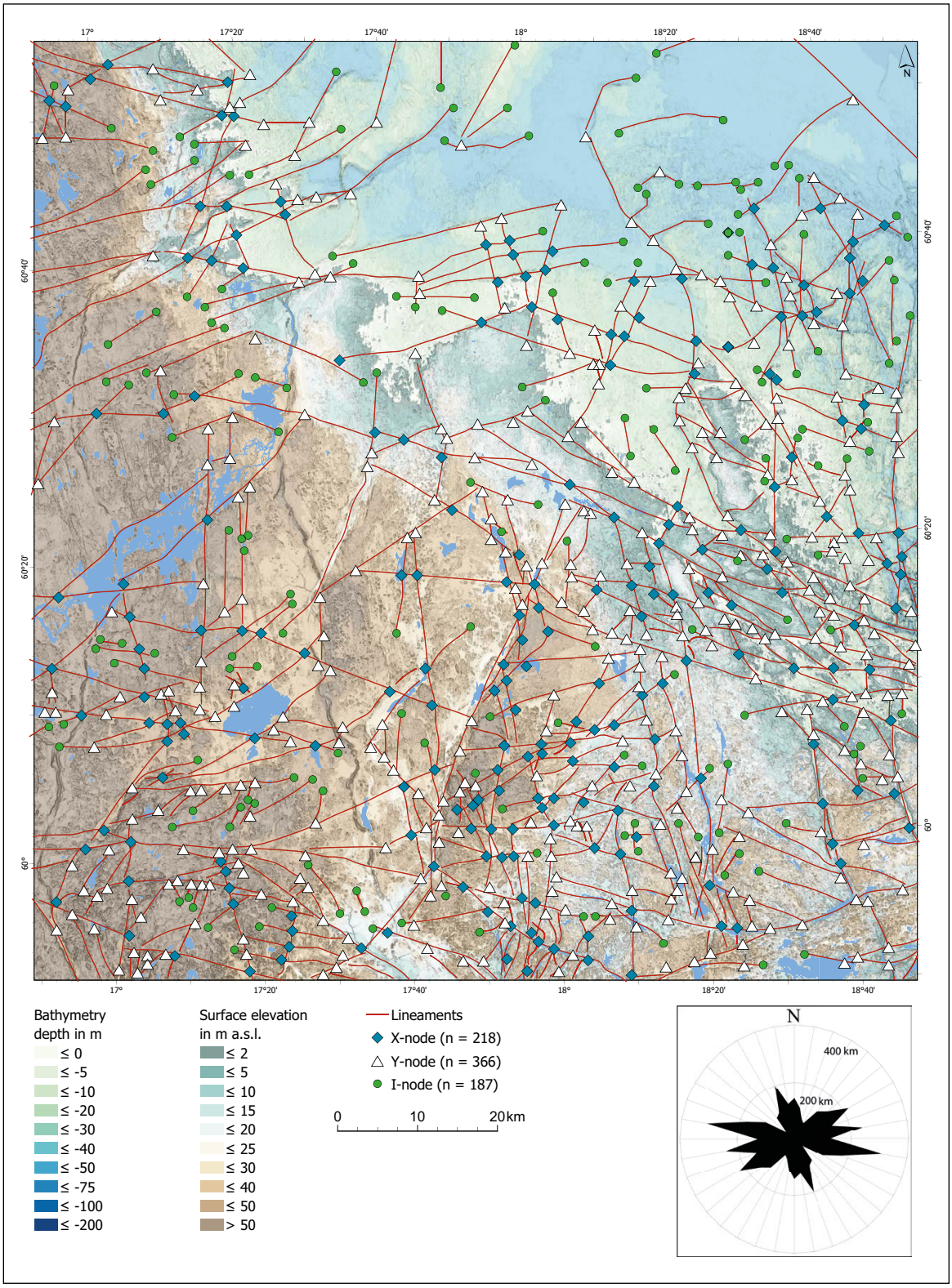

Figure 4-2. *Regional fracture pattern interpreted from topographic lineaments from Figure 3.3 in Grigull et al. (2019) redrawn as a topological network.*

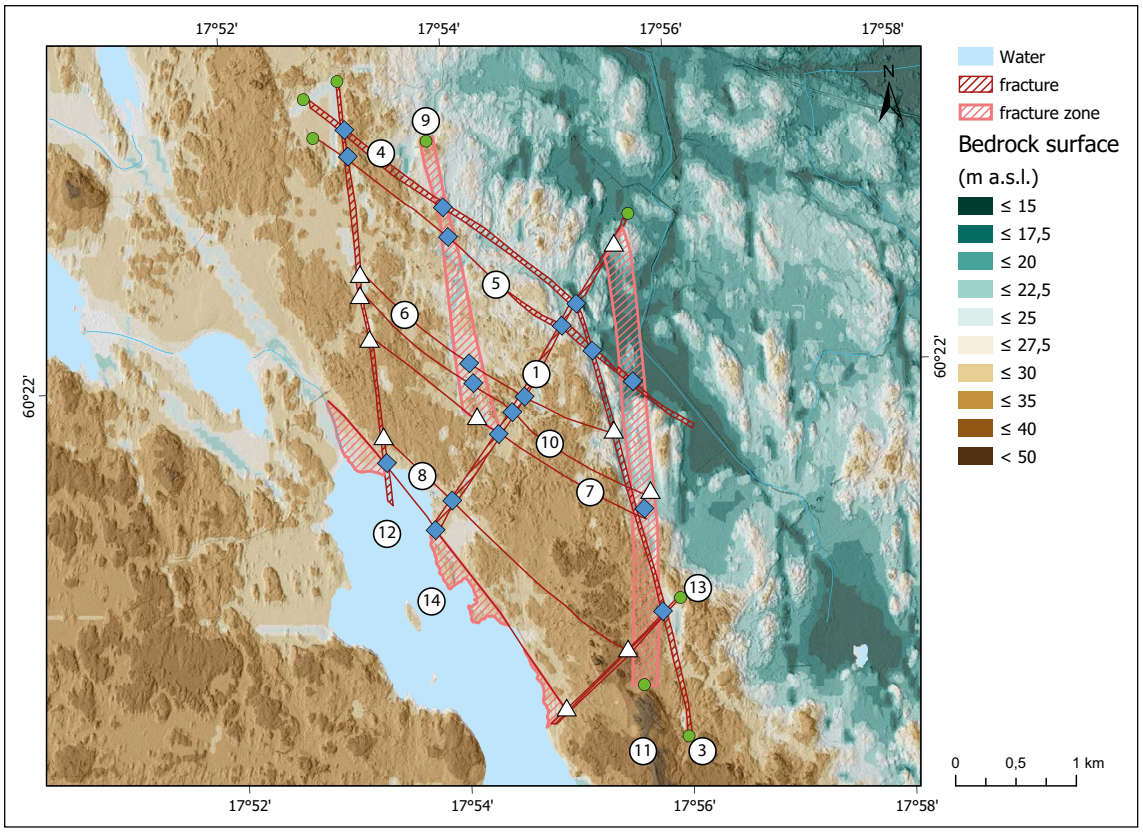

Figure 4-3. *Fractures and fracture zones at Finnsjön after Ahlbom and Tirén (1991) superimposed on a DEM. Topology of the fracture network as in Figure 4-2. Fracture descriptions in Table 4-1.*

Several fracture sets are recognised (Figure 4-3):

- The main fracture zone in the area is the Finnsjön regional deformation zone (labelled '14' in Figure 4-3), a regional structure with a length of > 50 km (Sjöström and Persson 2001) and a width of ~100 m (Ahlbom and Tirén 1991).
- NE-SW oriented fractures (1 and 13) have a steep dip towards SE (N10-70E). The fracture walls are altered, reddened by hydrothermal fluids and prehnite fracture coatings. The fracture zones are 5–7 km long and 20 m wide.
- For the N-S fractures and fracture zones (3, 9, 11, 12), fractures 9 and 12 are 2 and 6 km long, respectively, but remain narrow (5 m and 25 m wide, respectively). Fracture 3 is at least 5 kilometres long and 50 m wide; fracture 11 has a width of 100 m. The Gåvatsbo fracture zone (3) is intensely fractured with mylonite and breccia; common fracture minerals are epidote and chlorite.
- NW-SE oriented fractures (4, 5, 6, 7, 8 and 10) run parallel to the foliation in the granodiorite with a steep dip towards SW (N25-80W). NW-SE fractures are mainly 2–3 km in length and ~5 m in width. This fracture set resembles fracture zones or corridors found in many other settings with trace lengths of 10–1000 m and typical widths of 1–2 m, but up to 10 m (Questiaux et al. 2010).
- A set of subhorizontal fractures (2), dipping predominantly to the SW, is also recognised in the sub-surface (Tirén 1991). As these fractures are scarce at outcrop, they are not considered further here.

The NW-SE fracture set abuts against fractures 3 and 12. The fracture set orientations at Finnsjön resemble those at Forsmark (Ahlbom and Tirén 1991) and the regional pattern (Figure 4-2). The topology of the major fractures at Finnsjön indicates high connectivity, with a high proportion of X-nodes (Figure 4-3).

Table 4-1. Comparison of properties of fracture zones and rock trenches at Finnsjön (for location see Figure 4-14).

	Fractures							Trenches			
Lineament number	**Fracture zone name**	**Strike**	**Dip**	**Fracture length (km)**	**Fracture zone width (m)**	**Fracture spacing (m^{-1})**	**Block size (m)**	**Maximum trench length (km)**	**Maximum trench width (m)**	**Maximum trench depth (m)**	**Rock threshold Y/N**
1	Brändan	N30E	75SE	5	20	8–20	0.05–0.13	No trench	-	0	-
2	Zone 2	N28W	16SW	1.5	100	5	0.2	-	-	-	-
3	Gåvastbo	N15W	80W	> 5	50	-	-	0.9	36	10	Y
4	-	N50W	65SW	1	10	-	-	0.6	54	10	Y
5	-	N50W	60SW	5	2–6	-	-	0.4	64	5	Y
6	-	N55–65W	60SW	2	5	-	-	0.3	27	5	Y
7	-	N55W	60SW	2	5	-	-	No trench	-	0	-
8	-	N50W	90	3	5	-	-	No trench	-	0	-
9	-	N10W	15W	2	5	-	-	0.7	81	5	Y
10	-	NW	85SW	2.5	5	-	-	No trench	-	0	-
11	-	N5W	35W	2	100	-	-	1.3	109	7.5	Y
12	-	N-S	90	6	25	-	-	1.2	55	2.5	Y
13	-	N30E	75SE	7	20	-	-	No trench	-	0	-
14	Finnsjön	NW	90	> 50	100	-	-	> 10	200–825	> 20	Y

4.1.3 Fracture properties at Forsmark

Fracture patterns in the gneissic rocks around Forsmark have been mapped and modelled in detail (Stephens 2010). Models for all steeply dipping fracture sets on the present land area around Forsmark show 4 main orientations. Steeply dipping regional deformation zones at Forsmark show a dominance of NW-SE and NE-SW fracture orientations (Figure 4-4) (La Pointe et al. 2005). Shorter major and minor deformation zones are mainly oriented NW-SE, NNE-SSW and ENE-WSW (Stephens et al. 2007) and terminate against the SDZ and EDZ (Figure 4-4D). These major and minor deformation zones have widths of 3–64 m (Stephens et al. 2007). Collectively, the steeply dipping fractures delineate lath-shaped rock blocks with lengths of < 1.5 km and widths of < 0.5 km.

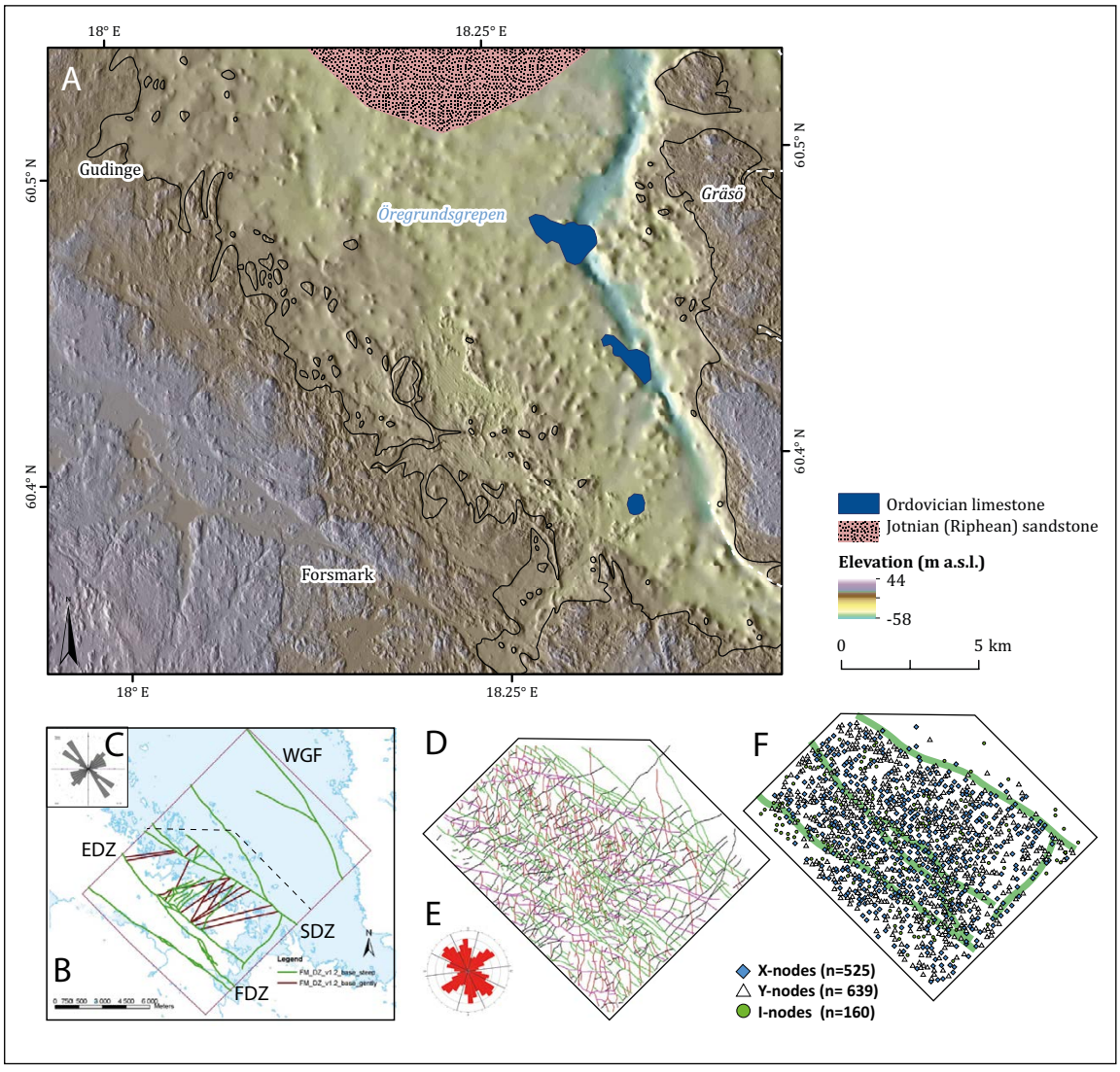

Figure 4-4. *A. DEM of the bedrock surface of the land area and the sediment-covered bedrock on the seabed between Forsmark and Gräsö. Sedimentary bedrock outliers included after Söderberg and Hagenfeldt (1995). B. Model for steeply and gently dipping deformation zones at Forsmark (Figure 7-1 in La Pointe et al. 2005). C. Deformation zone lineaments plotted in a rose diagram (Figure 7-2 in La Pointe et al. 2005). D. Lineaments colour-coded by the four main fracture sets (NE-SW and WNW-ESE sets dominant, with minor NNW-ESE and E-W sets) on the land area at Forsmark (Figure 6-9 in La Pointe et al. 2005). E. Lineament trace length rose diagram for the land area at Forsmark (Figure 6-7 in La Pointe et al. 2005). F. Topology of the onshore fracture network at Forsmark. Note that nodes are distributed independently of the regional deformation zones (shown in green).*

4.1.4 Fracture properties in the Singö deformation zone

The Singö deformation zone is a regional (at least 60 km long) deformation zone and fault line which extends from Gävle to the north to Singö in the S, one of several similar regional deformation zones in E Uppland (SKB 2005). The rock properties of the SDZ at Forsmark (Figure 4-5) have been examined in detail in 4 tunnel sections at ~50 m depth below the seabed and in boreholes (Glamheden et al. 2007 and references therein). The fracture properties at Forsmark are likely typical along the SDZ and for other deformation zones that extend to the SE through the Öregrund archipelago.

A general model is available for the description of deformation zones at Forsmark (Figure 4-6) which recognises (i) inner core zones flanked by (ii) transition zones, lying within (iii) host rocks (Munier et al. 2003). The SDZ is a 200 ± 50 m wide fracture zone which strikes WNW to NW, with a vertical or steep SW dip (SKB 2005). The SDZ is complex in its structure, locally branching, and with smaller, splayed crush zones (Carlsson and Christiansson 2007). Strike-slip faults run parallel to the SDZ and show both dextral and sinistral sense of movement, indicating reactivation of the SDZ under successive and contrasting stress regimes during and since the Palaeoproterozoic (Nordgulen and Saintot 2008).

Rock properties found in deformation zones at Forsmark are described in Table 4-2 (Glamheden et al. 2007). The core zone of the SDZ at Forsmark has a total width of up to 15–35 m (Glamheden et al. 2007). An axial, 2–12 m wide zone of crushed rock occurs, showing a high degree of alteration and disintegration. Fracture frequency is > 10 m^{-1}, with *in situ* block sizes of 2–20 cm. The crushed rock matrix consists of silt-, sand- and gravel-sized mineral and rock fragments. On one or both sides of the crushed rock zone, clay-filled fractures were observed, with apertures of a few cm to ~1 metre (Figure 4-7).

The core of the SDZ is flanked by transitional sectors that extend to the surrounding host rock. Glamheden et al. (2007) identified flanking (i) fractured sectors, closest to the core, with cubic fracture patterns and *in situ* block sizes of 10–50 cm, (ii) tabular sectors, with tabular shaped blocks striking across the tunnels, with a joint spacing of 5–50 cm, and (iii) altered sectors characterized by a gradual decrease in rock alteration and fracture frequency towards the host rock. In the host rock, fracture frequency is < 4 fractures per metre, comparable to measurements in nearby surface outcrops (Krabbendam et al. 2021). Whilst clay infills (Glamheden et al. 2007) and sealed fractures (Follin 2019) may inhibit water flow in core zones, the high intensities of open fractures in the adjacent transition zones are associated with high permeability (Carlsson and Christiansson 2007). In the SFR tunnel, the hydraulic conductivity of fractures in the SDZ is between 10^{-5} and 10^{-7} m/s. However, one half of the zone is dry; the hydraulic transmissivity within the zone is unevenly distributed. The hydraulic conductivity of fractures in the host rock outside and under the SFR tunnel is between 10^{-6} and 10^{-8} m/s (Palmqvist 1990). The tunnels in which these observations were made transect the SDZ; no information is available on variations in fracturing along the axis of the deformation zone.

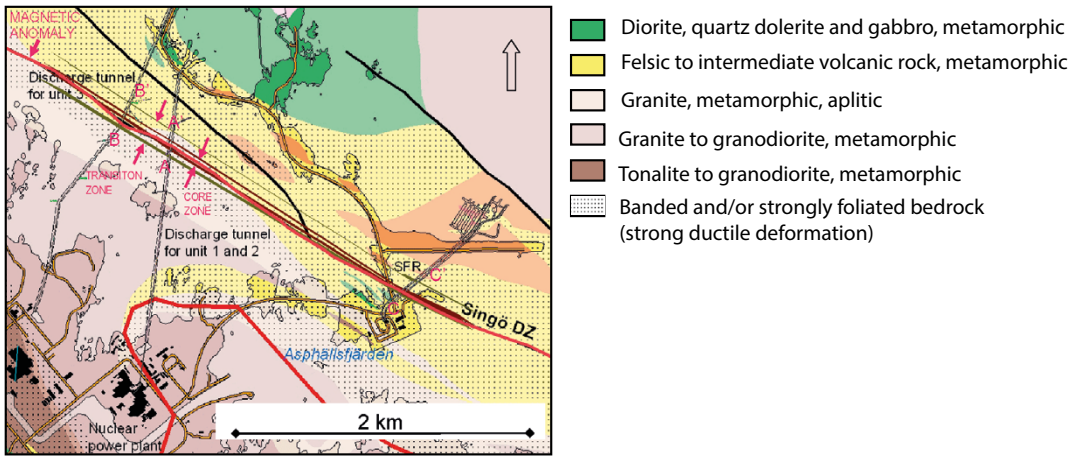

Figure 4-5. *The Singö deformation zone in the area around the SFR (the Final Repository for Short-lived Radioactive Waste) and the Forsmark Nuclear power plant. A model centre line (red) was derived from a geomagnetic anomaly map. The core and transition zone boundaries are indicated with arrows. Adapted from Figure 5-5 in Glamheden et al. (2007).*

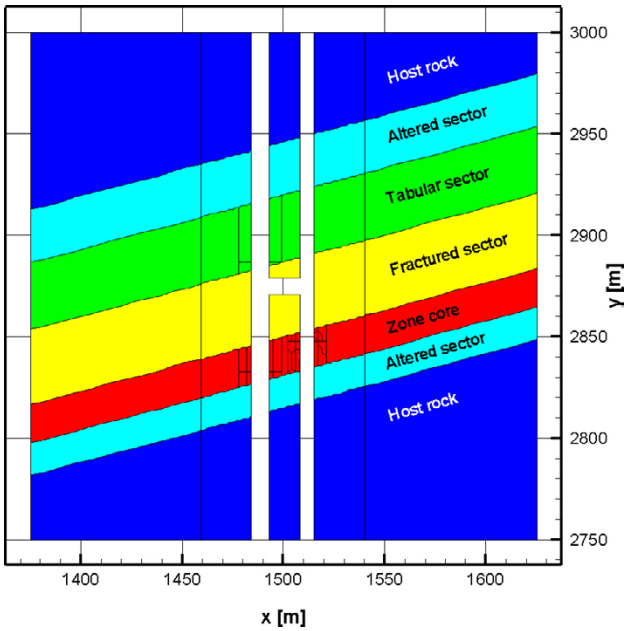

Figure 4-6. *Geometry of the Singö deformation zone at Forsmark (Figure 8-2 in Glamheden et al. 2007, based on the model of Munier et al. 2003). Two tunnels belonging to the SFR repository (white) intersect the core zone and the flanking sectors of the SDZ.*

Table 4-2. List of terms commonly used in tunnel mapping of mechanically weak rocks at Forsmark, after Glamheden et al. (2007).

Term	Explanation	Typical fracture frequency (number of fractures per metre)
Fractured zone	Zone with a considerably higher fracture frequency than the surrounding rock mass. Commonly, two block size grades: 20–50 cm and 10–20 cm. Block shape is described as cubic, tabular, or columnar, depending on joint sets and spacing.	2–5, and 5–10, respectively
Crushed zone	Zone where rock is crushed to cubic (“sugar cube rock”) or irregular pieces, generally less than 10 cm in size, and often with a fine grained, earth-like matrix between the rock pieces. A crushed zone is still in a state of disintegration, and never sealed, as can be the case for a fault breccia.	10 and over
Gouge	Soft fracture fill material, such as mica, chlorite, hydro-mica and other clay minerals.	Not applicable
Fault gouge	Soft fracture infilling material as above, caused by faulting.	Not applicable
Clay	Used as a general term for fine grained clay-silt sized fracture fills, not necessarily including clay minerals.	Not applicable

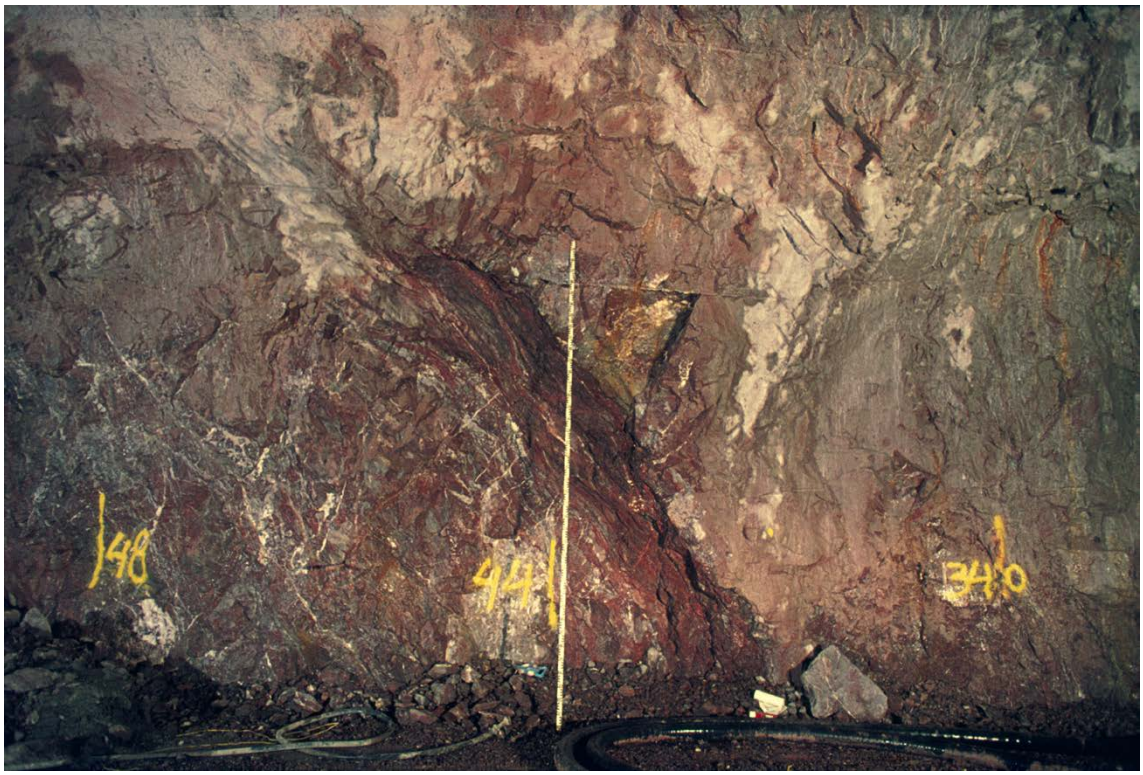

Figure 4-7. *Clay-filled fracture in brecciated metagranite within the core of the Singö Deformation Zone in the Forsmark 1 and 2 tunnels as described in Carlsson and Olsson (1977). Photo G Hansson/N.*

4.2 Denudation of sedimentary cover

This section examines the origins of the rock basin of the Åland Deep and the smaller rock basins between the islands of the Öregrund archipelago (Figure 4-8) in the context of former sedimentary cover.

4.2.1 The Åland Deep: a glacially eroded rock basin

The Åland Deep, or Södra Kvarken, is one of the deepest rock basins in the Baltic Sea, with a maximum depth of 301 m (Jakobsson et al. 2019). The Åland Deep approximately coincides with the Åland sedimentary basin, a down-faulted Proterozoic graben (Söderberg 1993). The interpreted tripartite sedimentary sequence is (i) a basal 1.2 km thick late Mesoproterozoic ('Jotnian') sandstone, (ii) Early to Mid Neoproterozoic sandstone and siltstone, and (iii) Early Palaeozoic rocks, composed of Lower Cambrian sandstones and Lower to Upper Ordovician limestones (Söderberg 1993, Hagenfeldt 1995). Seabed seismic profiles W of Åland indicate that U1 dips 2.5° towards the SW (Winterhalter et al. 1981). U1 and its Jotnian cover were tilted and eroded before formation of the sub-Cambrian unconformity. In the Åland Sea, U2 is imaged in sonar surveys as a gently inclined, even basement surface at ~90 m below sea level (Flodén 1977) that cross-cuts Jotnian sandstone. Formation of the Åland Deep has involved the removal of up to 210 m of Jotnian sandstone plus overlying Early Palaeozoic sandstone and limestone.

The crystalline basement rises close to present sea level W of a major fault that today delineates the western edge of the Proterozoic sedimentary basin and above sea level in the Åland archipelago to the E. Numerous Cambrian sandstone dykes are found across Åland (Bergman 1982), and in the Stockholm archipelago (Martinsson 1974); the dykes indicate proximity of the present land surface to U2. Hence, the low-relief basement surfaces that surround the Åland Deep (Figure 4-8) are inherited from U2, although the surfaces have been variously modified by Pleistocene glacial erosion.

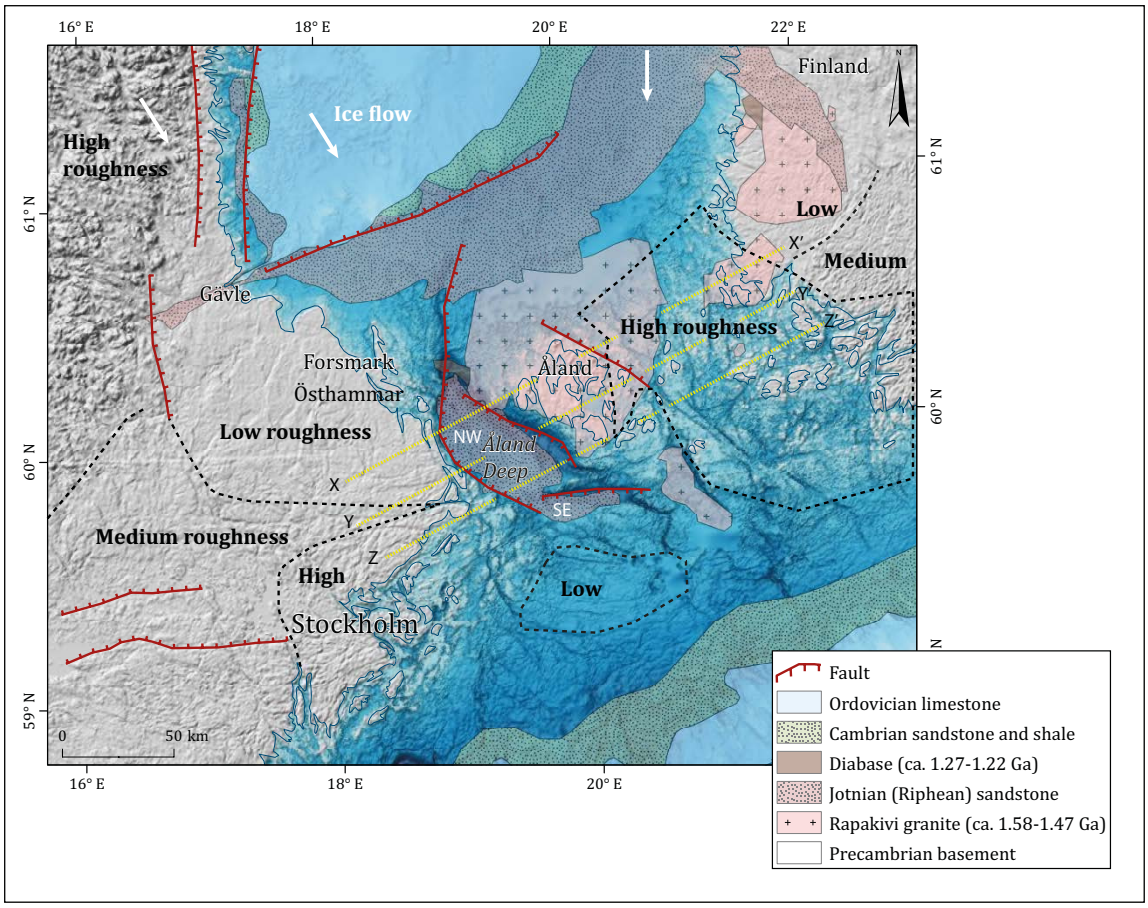

Figure 4-8. *Main elements of the bedrock topography and terrain roughness at the landscape scale in areas surrounding Åland. Yellow dashed lines refer to profiles shown in Figure 4-9. Adapted from Figure 4-12 from Hall et al. (2019a).*

The western boundary of the Åland Deep follows a major N-S fault (the Södra Kvarken fault) that delineates the edge of the Proterozoic graben (Beckholmen and Tirén 2010b). W of the fault, the basement forms small islands close to present sea level; rock slope retreat in the fault block W of the Södra Kvarken fault has been limited. The Åland Deep has two component rock basins, a larger northwestern basin (Ålandsdjupet), with a maximum depth of nearly 300 m, and a smaller south-eastern one, with a maximum depth of 220 m, separated by the ENE-WSW trending, fault-bounded basement ridge at Lågskar (Långskärsdjupet) (Winterhalter et al. 1981) (Figure 4-8). Shallow rock sills occur north and south of the Deep to 60 and 80 m depths, respectively (Jakobsson et al. 2019). Each sub-basin is partly enclosed (Holmlund et al. 2022); erosion has involved overdeepening by ~200 m below U2. As rivers cannot erode below base level (relative sea level), but glaciers can, the Åland Deep can be interpreted as a product of glacial erosion. The Fennoscandian Ice Sheet has selectively eroded the soft Mesoproterozoic and Early Palaeozoic sedimentary rocks in the Åland basin to form the Åland Deep; erosion in the surrounding hard, gneissic basement has been comparatively minor.

The bathymetry of the seabed around the Åland Deep reveals numerous deep rock trenches (Figure 4-9). The Södra Kvarken fault is followed by deep and narrow N-S trending trench (Figure 4-8) that acted as a major conduit for glacial meltwater released southwards from the Bothnian Sea basin (Shackleton et al. 2018) . To the E of Åland, trench systems are cut in fracture zones in the rapakivi granites and basement gneisses and form interconnected branches with dominant orientations of NNW-SSE and NW-SE (Beckholmen and Tirén 2010b). Trenches are narrow, with 1–3 km wide cross-sections. Rock channel *thalwegs* (the lines which connect the lowest points along the course of a valley) steepen to the S.

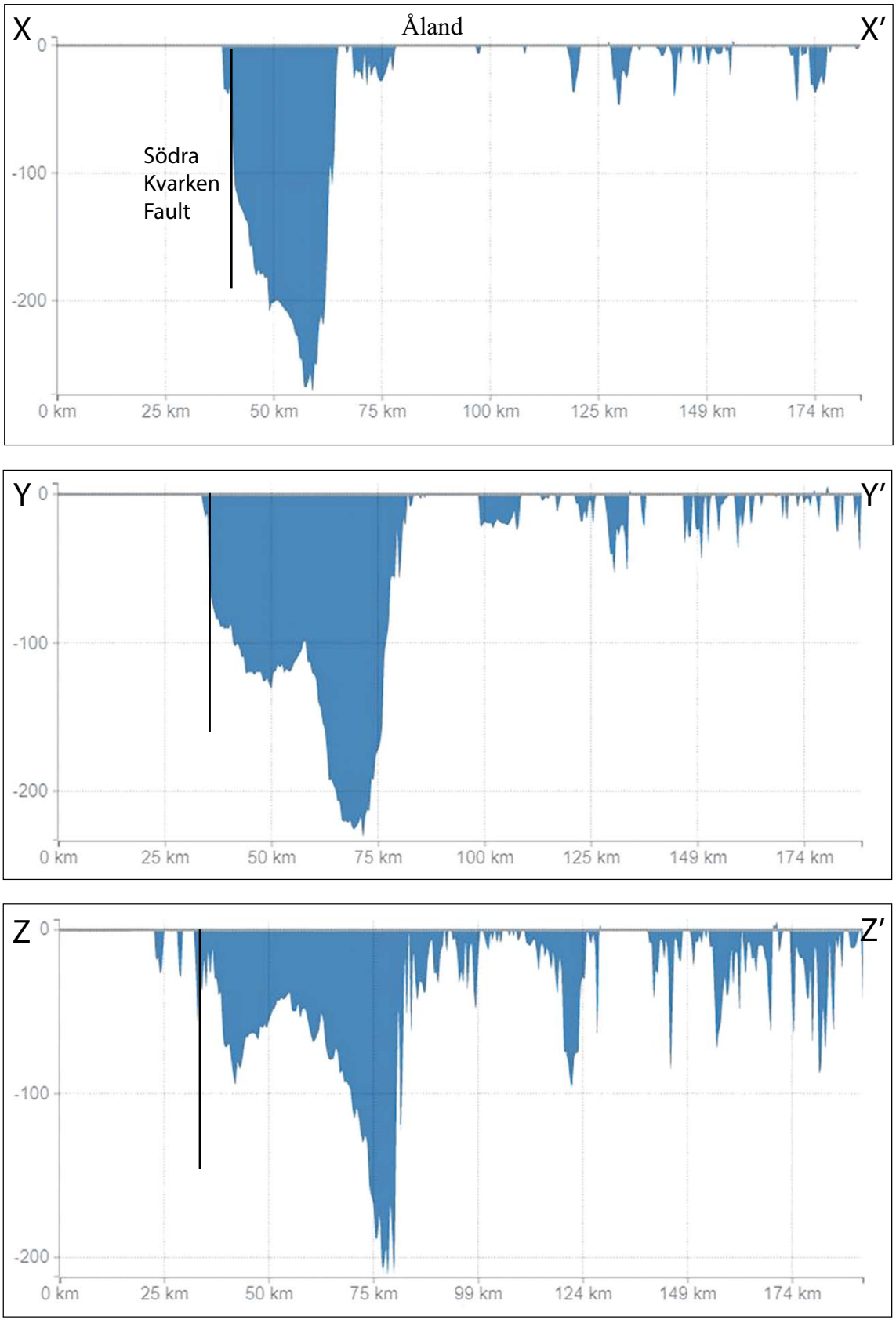

Figure 4-9. *Three WSW-ENE cross-sections of the Åland Deep. Lines of section X-X', Y-Y' and Z-Z' (shown on Figure 4-8) indicate changes in trench width and depths from N-S. Data from the Baltic Sea Hydrographic Commission, 2013, Baltic Sea Bathymetry Database version 0.9.3. Downloaded from http://data.bshc.pro/ on 04/04/2021.*

Long profiles show that the trenches deepen southward from 40 to 100 m over a distance of 40 km towards the basement shelf edge that forms the rim of the Baltic proper (Figure 4-10). Overdeepening of the Åland basin is associated with similar steepening along Profile A-A' along the main N-S oriented fault along the western edge of the basin. The 4 km wide trench marked as A-A' is cut in Jotnian sandstone and basement and shows an overdeepened section in its long profile. Profiles B-B' to E-E' are incised into the western rim of the Åland Deep and follow mainly WNW-ESE deformation zones. Profile C-C' follows the SDZ and its northern splay. Each trench floor steepens towards the edge of the rock basin, with knickpoints at a maximum distance of 5–10 km from the rim. For most of the length of Profile C-C' and D-D', however, and for the N-S oriented trenches F-F' and G-G', the trench floors remain close to present sea level and depths of rock basins along the trench floors are mainly < 20 m. The rock floors are also highly irregular, with 10–20 m relief over 1–5 km distances, giving up-down profiles to thalwegs. Whilst there is some evidence of headward erosion of trenches around the Åland Deep, rock-trench incision has not extended deeply into the Öregrund archipelago and rock trench floors maintain an elevation with a few tens of metres of present sea level towards the S.

4.2.2 The Öregrund archipelago: glacial erosion in sedimentary bedrock and basement

The Öregrund archipelago comprises low rock islands that rise out of sounds and fjärds (Figure 4-13). *Fjärd* is part of many local place names. Previous usage in geomorphology refers to shallow, glacially eroded inlets and bays found on lowland rocky coasts (Werth 1908, Embleton 1982). Water depths in the sounds and fjärds are generally < 25 m, but reach 50 m in trenches, and generally deepen along trenches towards the SE and the rim of the Åland Deep (Figure 4-10).

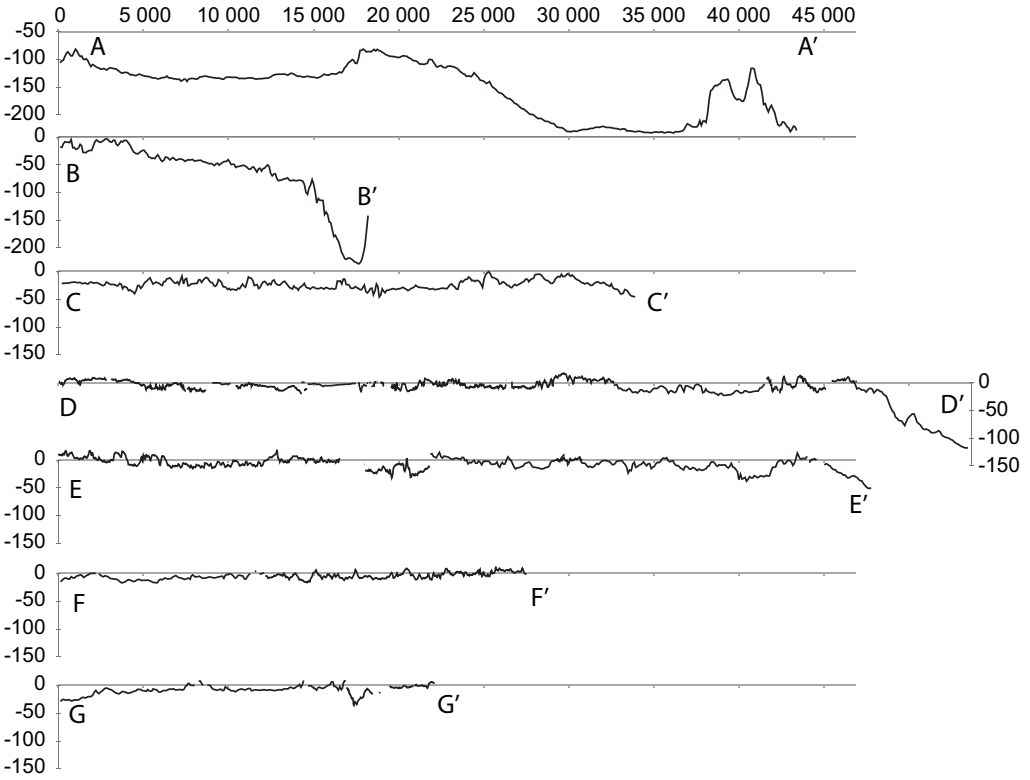

Figure 4-10. *Long profiles along major trenches around the western margin of the Åland Deep. For the profile lines see Figure 2-4.*

The area is crossed by the regional deformation zones present at Forsmark, namely the Singö, Forsmark and Eckarfjärden deformation zones and associated fault splays (Figure 2-1). Several regional faults also occur which include the West Gräsö fault. Collectively, the major fractures in the basement are more closely spaced than in areas to the west and south (Figure 4-1). Consequently, most fault blocks around Östhammar are small, except for the Gräsö block, and resemble the minor rock blocks found at Forsmark.

Outliers of Proterozoic sandstone and Ordovician limestone occupy down-faulted positions along regional deformation zones (Söderberg and Hagenfeldt 1995). The outliers lie along hanging walls that demarcate the edges of raised and tilted fault blocks (Figure 4-11). The Jotnian sandstone outlier in the Öregrundsleden is seen in seismic sections to infill a shallow linear depression across the Singö deformation zone (Figure 4-12); the fracture zone was already excavated close to its present erosion level in the Mesoproterozoic. In Raggaröfjärden and in Singöfjärden, small outliers of Ordovician limestone are also found at shallow depth on the seabed.

The basement rock types around Östhammar are dominated by the suite of Precambrian granitic gneisses with minor amphibolites in common with adjacent parts of Uppland (Persson 1985).

The large fault blocks at Gräsö (Figure 2-11 in Hall et al. 2019a) and between the Herräng and Väddö Faults (Figure 2-9 in Hall et al. 2019a) found north and south of the archipelago retain gently inclined basement surfaces interpreted as inherited from U2 (Hall et al. 2019a). Within the archipelago area, however, the original surface of U2 was developed across basement and Proterozoic sandstones (Figure 2-3). Here, the differences in elevation between (i) the summits of the basement blocks that stand above sea level and (ii) the beds of the sounds and fjärds between the islands represent the minimum depths of Pleistocene glacial erosion below U2. Singöfjärden has an average depth of 11 m, and a maximum depth of 49 m and neighbouring basement tops, which represent U2, rise above 20 m a.s.l. Thus, the maximum depth of excavation in Jotnian and Ordovician sedimentary rocks is ~70 m, with an average depth of 30 m. At Raggaröfjärden, the surrounding basement tops reach elevations of 15 m whereas the submerged Ordovician outlier has a surface at −16 m, indicating removal of more than 30 m of limestone. In the eastern part of the Öregrundsleden, near the island of Vässarön, > 45 m of Jotnian and Ordovician cover is missing. A minimum of 40 m of Ordovician limestone is missing from NW of the Gräsö block (Figure 2-11 in Hall et al. 2019a). To these 30–40 m totals should be added unknown thicknesses of sedimentary cover removed from above the upper surfaces of upstanding basement fault blocks that remain at or close to the level of the U2 unconformity. In contrast, fracture-aligned trenches and basins developed in basement are shallower (Figure 4-11) with water depths in fjärds between islands of ~10 m. Hence, glacial erosion in basement fracture zones after removal of former sedimentary cover has remained relatively shallow.

Erosion by the Fennoscandian Ice Sheet in the Öregrund archipelago has involved mainly the removal of Proterozoic sandstones and Early Palaeozoic limestones from the block-faulted basement surface. The large numbers of Proterozoic sandstone erratics found along parts of the coast in eastern Uppland and in eastern Stockholm County support significant glacial erosion of this sedimentary cover (Hagenfeldt 1995). These depths exceed the average 22 m erosion depths of glacial erosion in basement estimated in the Forsmark area (Hall et al. 2019a). The relatively deep glacial erosion in the Öregrund archipelago and the development of drowned trenches and rock basins, therefore, is largely a result of differential glacial erosion of sedimentary rocks in small fault grabens.

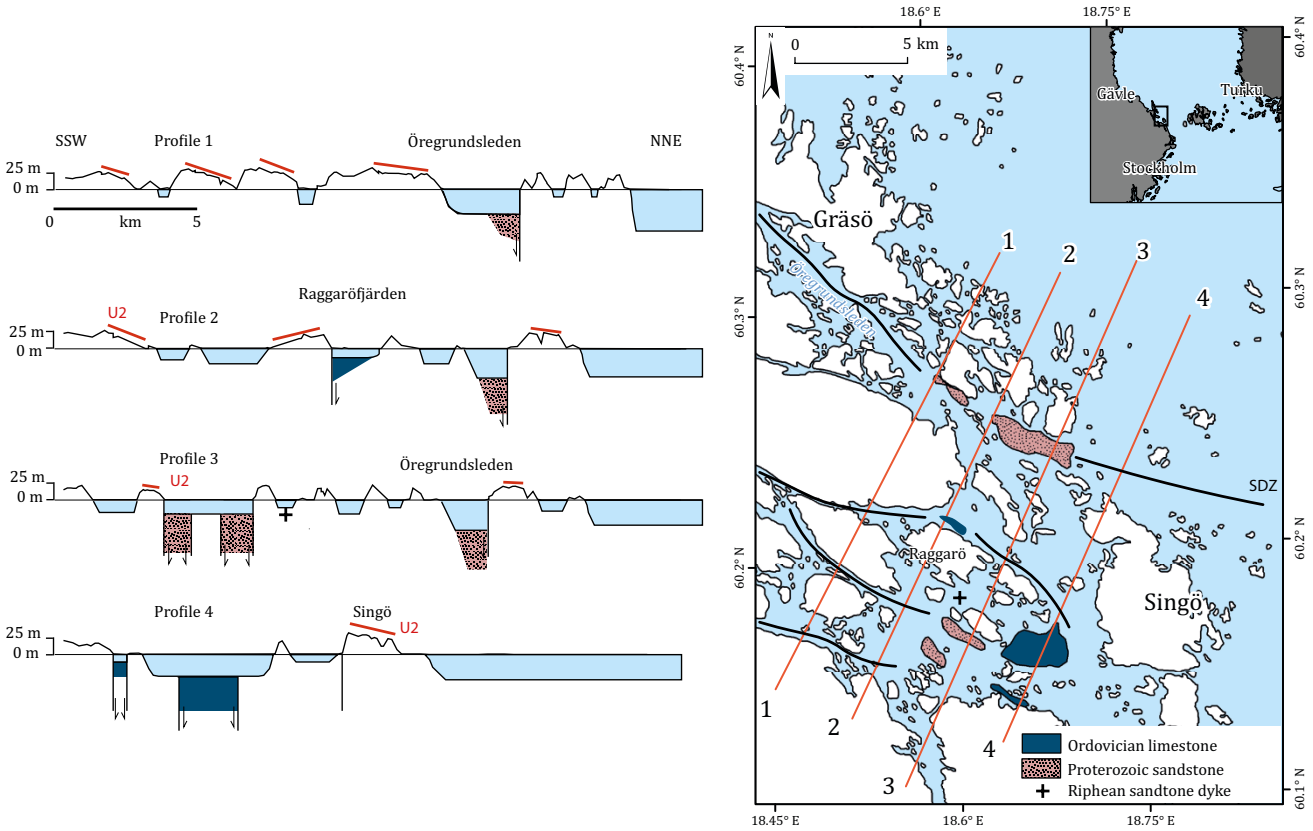

Figure 4-11. *Schematic profiles of block-faulted basement W of Singö, with the position of U2, and Proterozoic and Ordovician sedimentary rocks after Söderberg and Hagenfeldt (1995). Adapted from Figure 2-8 of Hall et al. (2019a). Major deformation zones and faults indicated by black lines.*

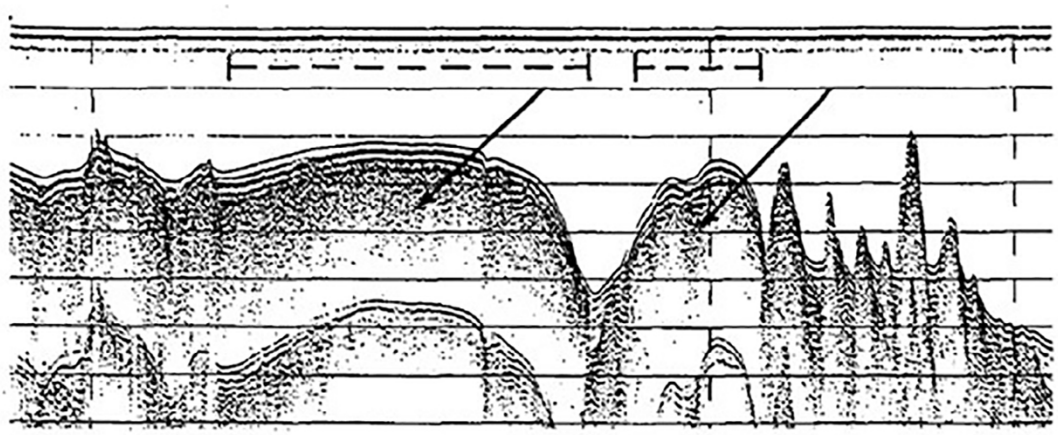

Figure 4-12. *Seismic reflection profile indicating sedimentary rock in the Öregrundsleden. The trench likely marks the trace of the SDZ. The disturbed reflectors with short lateral extension (arrows) were interpreted as Upper Proterozoic sedimentary rock. The horizontal extent of the sedimentary bedrock is indicated by broken lines. Modified from Söderberg and Hagenfeldt (1995).*

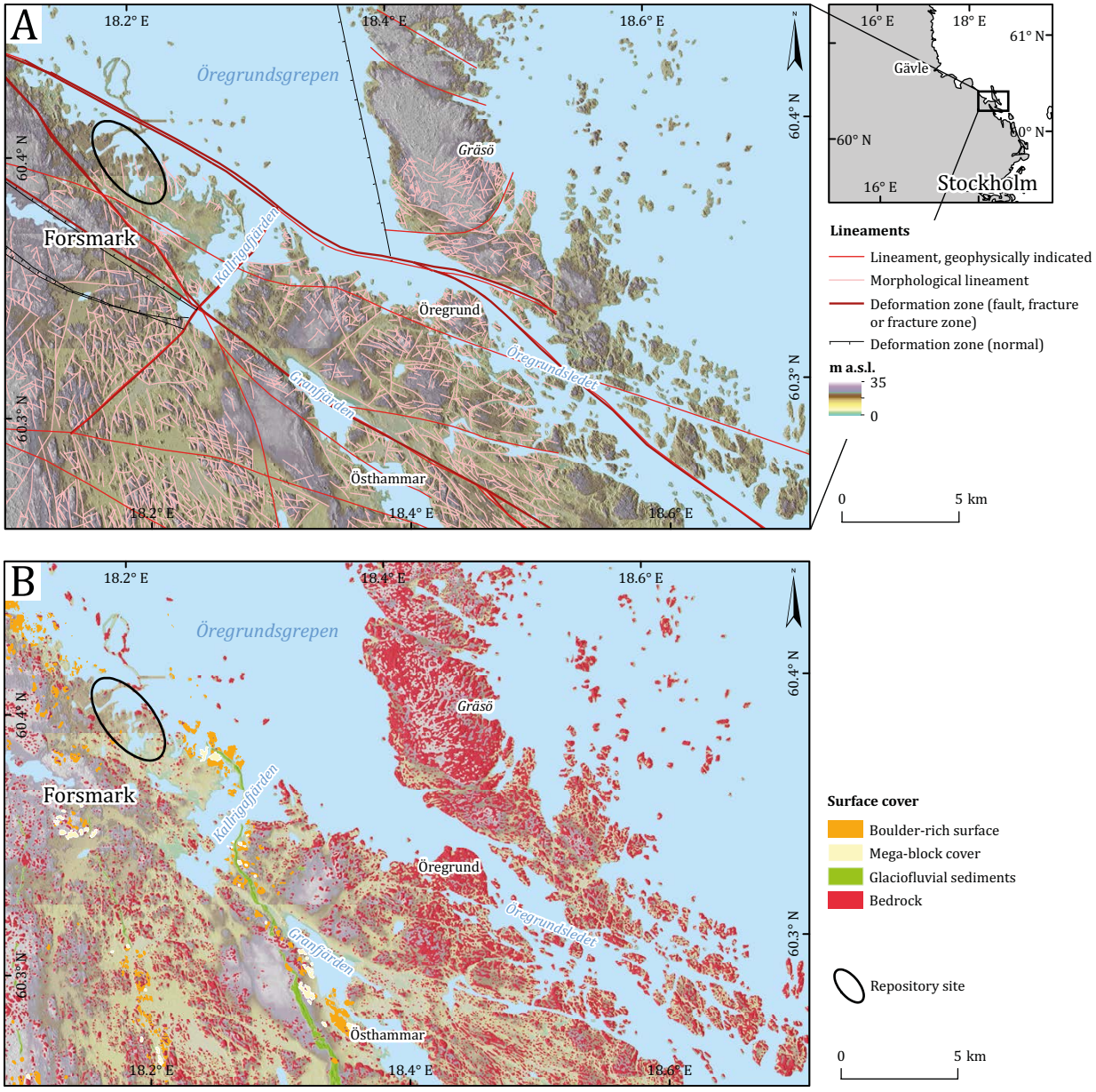

Figure 4-13. *Topography and Quaternary geology in the western part of the Öregrund archipelago. A. DEM based on Lantmäteriet data with lineaments based on SGU data. EDZ Eckarfjärden deformation zone, FDZ Forsmark Deformation Zone SDZ Singö Deformation Zone WGF West Gräsö Fault. B. DEM overlain by selected SGU data on boulder spreads, glaciofluvial deposits and exposed bedrock.*

4.3 Glacial erosion of basement

West of the coastal hinge zone, there are few candidates for grabens on the basement surface from which significant thickness of sedimentary rock have been removed. The basement surface shows similar smoothness (Figure 4-8), low relief and elevation (Figure 2-4), absence of deep rectilinear basins (Figure 2-4) and limited differential movement across faults between rock blocks (Grigull et al. 2019) to the unconformity surfaces around Early Palaeozoic outliers further S in Sweden. Hence, U2 in northern Uppland had a similar near-planar, block-faulted form. Support for this interpretation is found in the Öregrundsgrepen, where a gently inclined basement surface is overlain by Ordovician limestone (Fig 2-11 in Hall et al. 2019a). Summit envelope surfaces for the present basement surface approximate to the original form and level of U2. Subtraction of present basement surfaces from summit envelope surfaces indicates patterns and depths of erosion since re-exposure. In northern Uppland, including the Öregrund archipelago, re-exposure of U2 occurred after 1.2 Ma (Hall and van Boeckel 2020). The lack of weathering and limited erosion under Holocene interglacial environments indicates that non-glacial

erosion in the Middle and Late Pleistocene was similarly limited. Hence, erosion of basement after re-exposure of U2 was dominated by glacial erosion. In Uppland, bedrock depressions represented loci for relatively deep glacial erosion in past glacial phases and, potentially, sites for further excavation and extension in future glaciations.

4.3.1 Regional patterns of erosion

Based on the assumptions and measurements outlined above, the regional pattern of estimated depths of glacial erosion in basement rocks in Uppland can be mapped (Figure 4-14). Average depths of erosion tend to increase southwards across Uppland and into Stockholm County. The linear zones of deep erosion correspond to the positions and planforms of the main rock trenches.

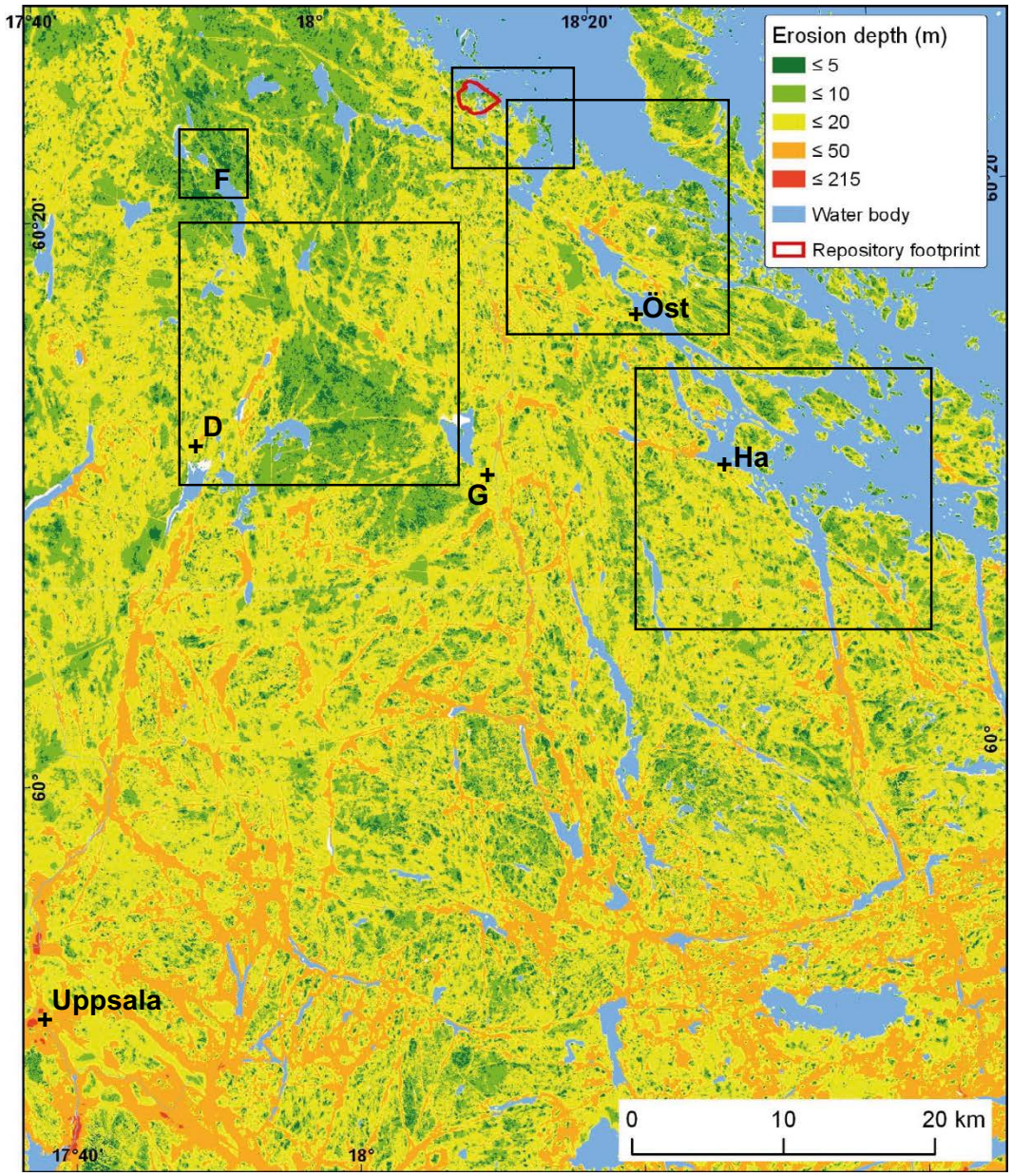

Figure 4-14. *Modelled erosion depth (m) across NE Uppland based on Figure in Hall et al. (2019a). Modelled by subtracting the present bedrock surface from the MAX MEAN surface of the bedrock surface (the summit envelope surface representing U2), based on a circular window with 500 m radius. Category values selected to emphasise the distribution of end members of minimum and maximum erosion. D Dannemora. F Finnsjön. G Gimo. Ha Hargshamn. Öst Östhammar. The boxes show the locations of Figures 4-18 to 4-21 and 4-23.*

4.3.2 Regional patterns of rock basins

The main rock basins include parts of the shallow seabed between islands in the Öregrund archipelago, lake-filled depressions, and the isolated, broad depressions that lie between blocks of high ground. A line approximately from Dannemora to Hargshamn divides northern and southern areas which show different basin configurations.

In the northern area, rock basins are typically elongate and filled by lakes. Basin depths are generally < 20 m, lengths are 1–5 km and widths are 1–2 km. Several rock basins lie along regional deformation zones, including Finnsjön (Figure 4-3), Bruksdammen (Figure 4-15 in Hall et al. 2019a) and the fjärd at Östhammar (Figure 4-15). However, the basin margins often extend beyond the known margins of major fracture zones, as in the shallow basins E of Östhammar and at Bruksdammen. Some basin margins are not aligned with the edges of mapped fracture zones.

In the southern area, the total surface area occupied by topographic depressions is relatively high, but lakes, such as Erken, are mainly confined to the south-eastern sector. Basin depths are generally 20–50 m, lengths are 2–7 km and widths are 1–3 km. Many basins connect with neighbouring basins via rock trenches. Deep basins SE of Uppsala have developed in zones with closely-spaced, parallel trenches. Hence, rock basins in the southern area, when compared to the north, are deeper, and slightly longer and wider, and more intricately connected to surrounding rock depressions.

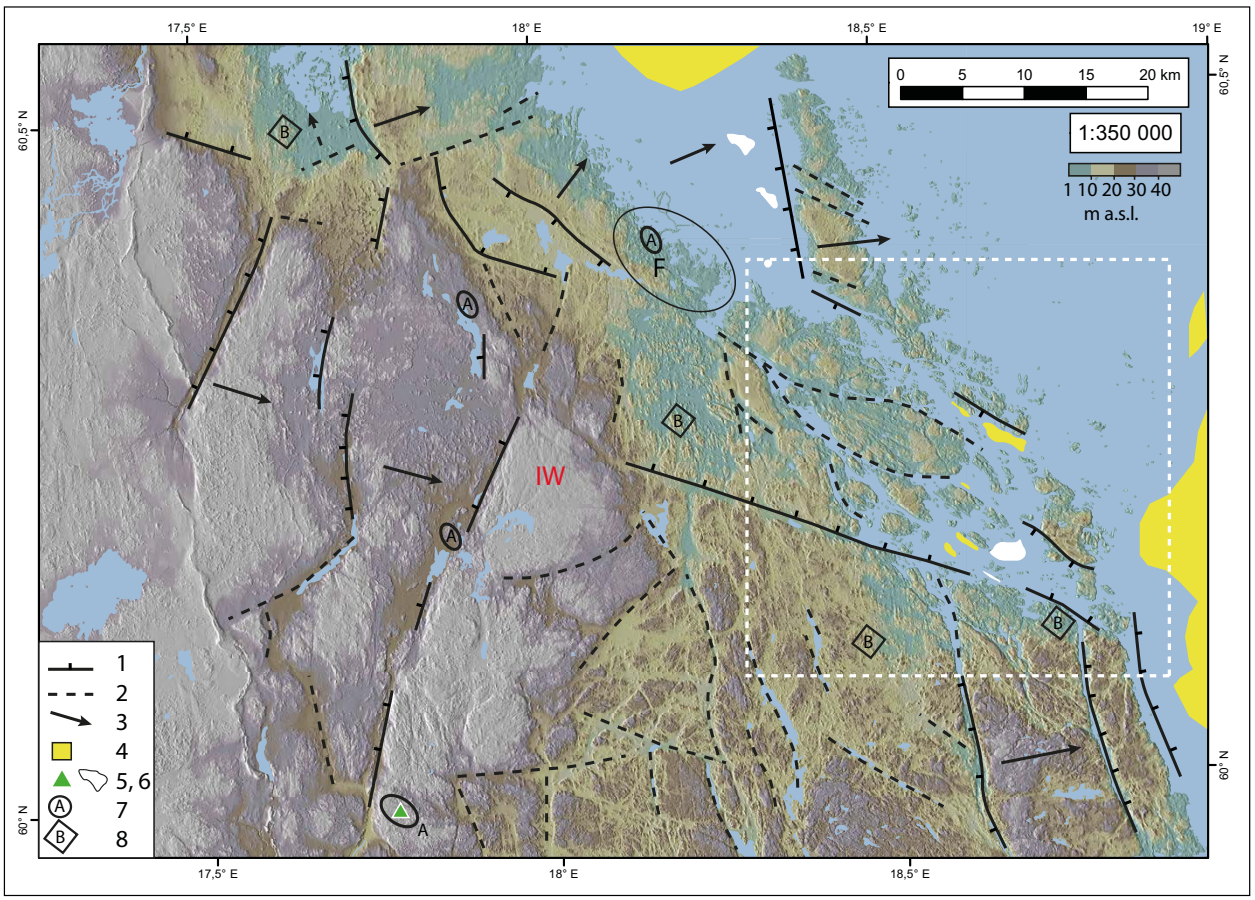

Figure 4-15. *DEM of the glacial modified U2 surface in NE Uppland. 1. Exhumed fault scarp along edge of fault-bound rock block. 2. Fracture without clear dislocation of opposing rock blocks. 3. Direction of tilt of fault block. 4. Proterozoic sandstone. 5. Early Cambrian sandstone. 6. Early Ordovician limestone. 7. Asphaltite fracture coatings derived from a former cover of Late Cambrian to Early Ordovician Alum Shale. 8. Shallow, open basin developed from glacial erosion. F Forsmark repository site. IW Ironworks. Broken line denotes the area of the Öregrund archipelago. Revised from Figure 2-22 in Hall et al. (2019a).*

4.3.3 Rock trenches at the regional scale

Rock trenches are seen as long, narrow corridors in DEMs of the bedrock surface. Parts of the trenches are filled by finger lakes and in the E by fjärds. Rock trenches mapped from DEMs of the bedrock surface are unevenly distributed (Figure 4-16). Trenches are absent from the Jotnian basin of the Åland Sea. Trenches appear to be relatively widely spaced on the seabed around Gräsö, but the resolution of the bathymetric data (100 m pixel size) is lower than for the land area (10 m pixel size). A DEM with a 10 m pixel size was used to map the trenches within the base map; short, narrow trenches are likely under-represented in the marine area. Post-glacial sediment may also fill trench floors. On the present land area, areas with low trench frequencies and short trench lengths include the smooth fault block tops identified previously as facets of U2, little modified by glacial erosion (see, for example, Figure 4-42 in Hall et al. 2019). In contrast, the frequency of trenches is high in a W-E belt across north-east Uppland (Figure 4-16). This belt includes the Öregrund archipelago where long, WNW-ESE oriented trenches are aligned along the Singö and Forsmark deformation zones. Other long trenches on the present land surface are generally found south of the Österbybruk-Gimo line, extending for distances that may exceed 20 km. Six N-S trenches follow, from W-E, the Österbybruk-Skyttorp and Gimo deformation zones and the Vällen, Gisslaren, Herräng and Väddö faults. In areas SE of Uppsala, and around Lake Erken, the trenches are interconnected with other trenches and basins. The depths of rock trenches are mainly 20–50 m south of Dannemora and Gimo; the widths of long trenches are generally < 2 km. Large volumes of basement rock have been removed from these rock depressions by erosion.

The regional trench network (Figure 4-16) is dominated by short trenches, many of which terminate at I-nodes. Y-nodes are most frequent along the lines of the main trenches but crossing X-nodes are relatively few. The density of nodes is high in the Öregrund archipelago and towards the southern boundary of the map area. Large areas remain distant from trenches. Network connectivity is low over wide areas, with many short trenches terminating along a single branch. Trench segments may terminate at I-nodes along the broader valleys. The long corridors of the main regional trenches have the highest connectivity, with many short trenches joining at T- and Y-junctions.

Trench orientations show a dominance of NNW-SSE trends, with a lesser ENE-WSW trend (Figure 4-16). Whilst the preferred orientations approximate to that of former ice flow, many main and subsidiary trenches have orientations transverse to ice flow. In section 4.4, this will be compared against the dominant trends of the fractures.

Eskers mark the locations of former subglacial channels which discharged large volumes of meltwater from beneath the retreating margin of the Fennoscandian Ice Sheet (Boulton et al. 2007). In Uppland, large eskers were part of a dendritic subglacial drainage system (Figure 4-1). Many eskers lie on the sediment-filled floors of north-south oriented valleys. Only some eskers, however, follow trenches excavated along regional major deformation zones, notably the Vattholma esker which follows the Österbybruk-Skyttorp deformation zone. The Uppsala esker north of Uppsala city (Figure 4-1) does not align with regional deformation zones except along short segments. The SGU-BGS 3D geological model of the esker includes cross-sections based on borehole data (Jirner et al. 2016). North of Uppsala city, cross-sections show that the sediments of the Uppsala esker and the Vattholma esker do not infill rock trenches. However, a major sediment-filled rock trench appears from the confluence of the two esker systems a few kilometres north of Uppsala city. This trench is locally > 40 m deep and can be traced for 15 km to south of the city. The Uppsala city trench is not associated with a major ductile deformation zone, but fault control on its position is likely (Stålhös 1972). Till occurs on the flanks of the rock trench but not widely on its floor (Stölen et al. 2019) suggesting that till was eroded prior to esker deposition. Deposition of the Uppsala esker during final deglaciation was not generally accompanied by bedrock incision north of the city but removal of till cover may have been accompanied by limited bedrock erosion south of the city.

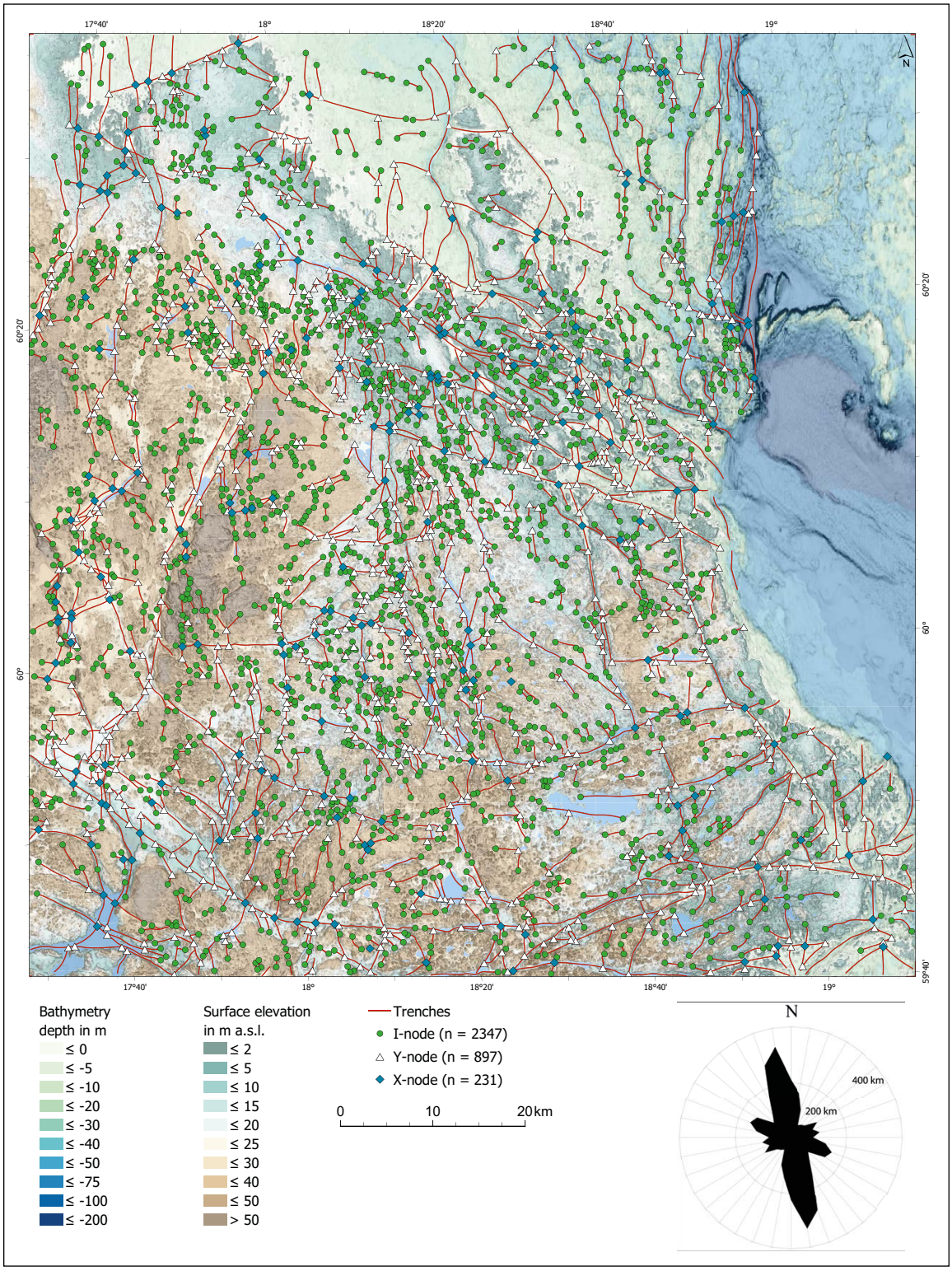

Figure 4-16. *Trench network topology in Uppland and part of Stockholm County.*

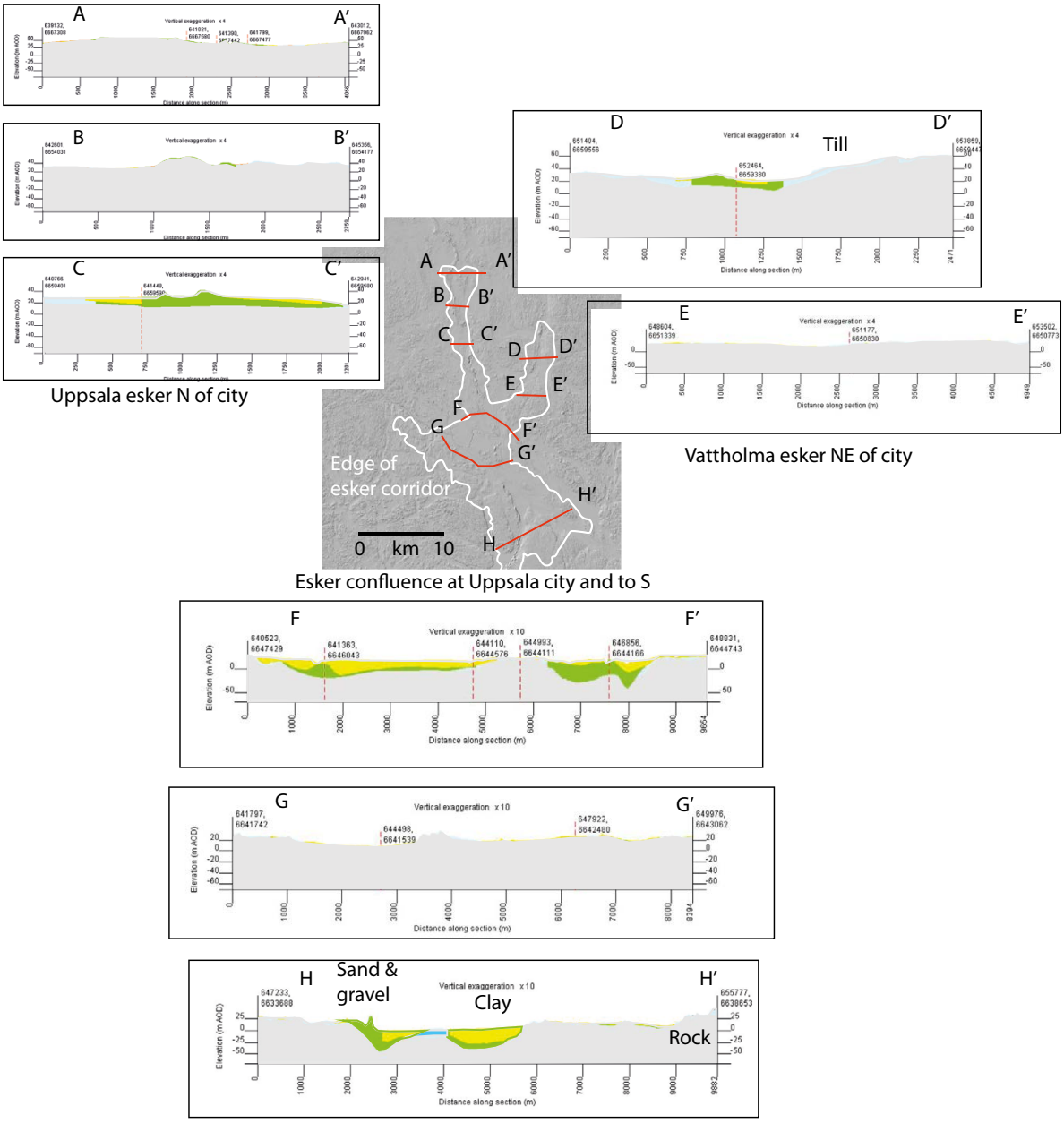

Figure 4-17. *Cross-sections of the Uppsala esker system. Data from SGU-BGS 3D geological model of the esker at http://mapapps.bgs.ac.uk/sweden_esker_pilot/ .*

4.3.4 Rock trenches at the local scale

The spatial variability of trench forms at the local scale is described below for five case-study areas: Dannemora, Hargshamn, Öregrund, Forsmark and Finnsjön.

Dannemora

The Dannemora study area (Figure 4-18 and 4-14) is crossed by the Österbybruk-Skyttorp (ÖSDZ) deformation zone (see (1) in Figure 4-17). The ÖSDZ includes a younger fault zone (Malehmir et al. 2011). The latest movement along this fault, likely in the Permian (Sandström et al. 2006a), raised and gently tilted the eastern fault-bound rock block, termed the *Ironworks Block* by Hall et al. (2019a), and its former sedimentary cover. A fault scarp up to 20 m high faces to WNW (2) with a broad fault-line trench. The upper surface of the Ironworks Block retains a smooth, near-planar form with < 5 m local relief (9), interpreted previously as a little-modified facet of U2 (Hall et al. 2019a). The rock trenches on the upper surface of the Ironworks block are shallow, short, and closed features.

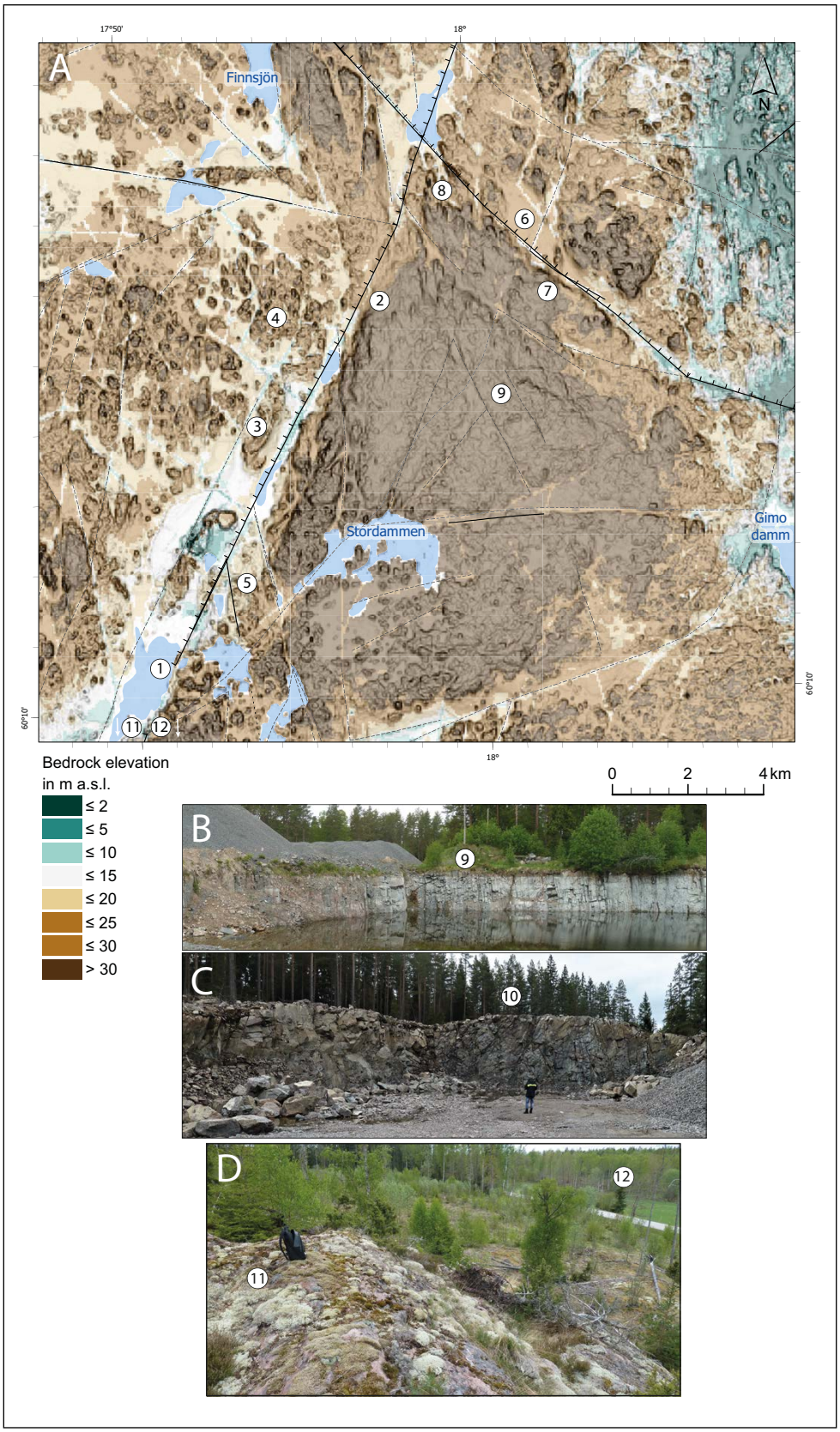

Figure 4-18. *A. The bedrock terrain NE of Dannemora and Österbybruk ('Ironworks fault block'). For location, see Figure 4-14. Localities 1–12 are described in the text above. B. Krapelås Quarry. C. Eastern edge of the valley along the ÖSDZ at Linddalsvreten Quarry (60.13167N; 17.81605E). D. The valley flank at Gränboda mast, 1.3 km S. This is cosmogenic nuclide sample site FORS 16-18 in Hall et al. (2019a).*

At Krapelås, exposures in a quarry and on surrounding rock surfaces, show that fracture spacing is widely < 1 m; a fracture corridor in the quarry with < 0.5 m spacing has not been exploited by differential erosion (9). Glacial erosion has been limited on the top of the Ironworks Block despite relatively high fracture intensity.

The rock trenches that delineate the Ironworks fault block have been eroded along major fracture zones. The main fault-line trench along the ÖSDZ (the Dannemora valley) varies in its width, reaching 800 m (1), and it branches around small bedrock highs and ribs (3). The trench narrows where its western part terminates north of Lillbyasjön (4) and terminates against a 2 km wide rock threshold before resuming to the north (2). Short fracture zones oriented NNW-SSE terminate against the main deformation zone SW of Stordammen (5). The NW-SE oriented rock trench at Vigelsbo also varies in its width and broadens into an elongate basin at (6). The Vigelsbo valley has several rock thresholds that divide the valley into separate, closed trench sections (7). The valley terminates towards the NW (8) without connection to the ÖSDZ. Each of the major rock trenches is joined by shorter trenches at T-junctions (5 and 6). On the southern, lee-side edge of the block, a shallow rock basin is developed at Stordammen (10); here several major fracture zones intersect.

Erosion depths along the Dannemora trench are 15–20 m. Quarries and exposures on the eastern flank of the ÖSDZ south of Dannemora (11 and 12) show strong contrasts in fracture spacing. Linddalsvreten Quarry exposes rocks in the flank of a 150 m wide trench which runs parallel to the ÖSDZ and terminates to SW. Here, fracture corridors run parallel to the main trench, with *in situ* block sizes of < 0.5 m. At Gränboda mast, glacially abraded, coarse-grained to porphyritic granite gneiss surfaces descend towards the valley floor (11). Two fracture sets dominate: a vertical set at 010/190 and a steeply inclined set that is subparallel to flank rock slopes. Fracture frequency is low (0.25–0.5 m^{-1}). A sediment-filled trench (12) marks one branch of the ÖSDZ, with a 300 m-wide rock ridge separating this trench from the main valley. Hence, the Dannemora trench is largely confined to branches of the ÖSDZ. At Gränboda, trench widening may have been arrested by tabular zones in the host rock with wide fracture spacings. At Linddalsvreten, however, closely fractured rock remains *in situ*. Glacial bedforms along the Dannemora valley are not fully adjusted to fracture controls.

Hargshamn

The terrain around Hargshamn lies at the boundary between the Öregrund archipelago to the north and the low relief of E Uppland to the south (Figure 4-19). The boundary is delineated by the Hargshamn-Herräng deformation zone (H-HDZ) (see 13 to 23) in Figure 4-19) which extends westward towards Finnsjön. The rocks in the south are mainly granitic gneisses, with a corridor of metavolcanic rocks around Gisslaren (Bergman et al. 1998). A major fault set within a wider shear zone along the trend of Gisslaren (14) crosses the H-HDZ and extends NNW towards Kallrigafjärden; the fault trace along Edeboviken terminates against this deformation zone (15).

The H-HDZ also divides an area of seabed to the north with its down-faulted outliers of Jotnian sandstone and Ordovician limestone from the exposed basement to the south. The northern edge of the basement along the H-HDZ is lower than further south. Here, shallow rock basins, with uneven floors, are partly open to the north (16). The surrounding terrain has high surface roughness (Figure 4-23 in Hall et al. 2019a), with up to 30 m of relative relief and many small rock knobs (Figure 4-19a). Smooth, low-relief surfaces persist on fault blocks to the south (Figure 4-13 in Hall et al. 2019a); the estimated average erosion depths below summit envelope surfaces south of Hargshamn are generally < 20 m (Figure 4-14).

Rock trenches and basins are common. North of the H-HDZ, the sounds between the islands follow the WNW-ESE trends of major deformation zones (15 and 17) and the crossing NNW-SSE oriented faults (18). The widths of the trenches that follow the SDZ, EDZ, FDZ and H-HDZ are 200–820 m, with the SDZ widening to 1 050–1 300 m at Singö. To the S, long trenches along the NNW-SSE oriented faults are dominant. The north end of Edeboviken is up to 700 m wide compared to the 300–400 m width of the straight-sided fjärd that extends to the south (19). Väddöviken also maintains a 300–400 m width for most of its 13 km length (Figure 4-20) Short trenches terminate against longer trenches (20), but the connectivity of trenches and basins is locally high (21).

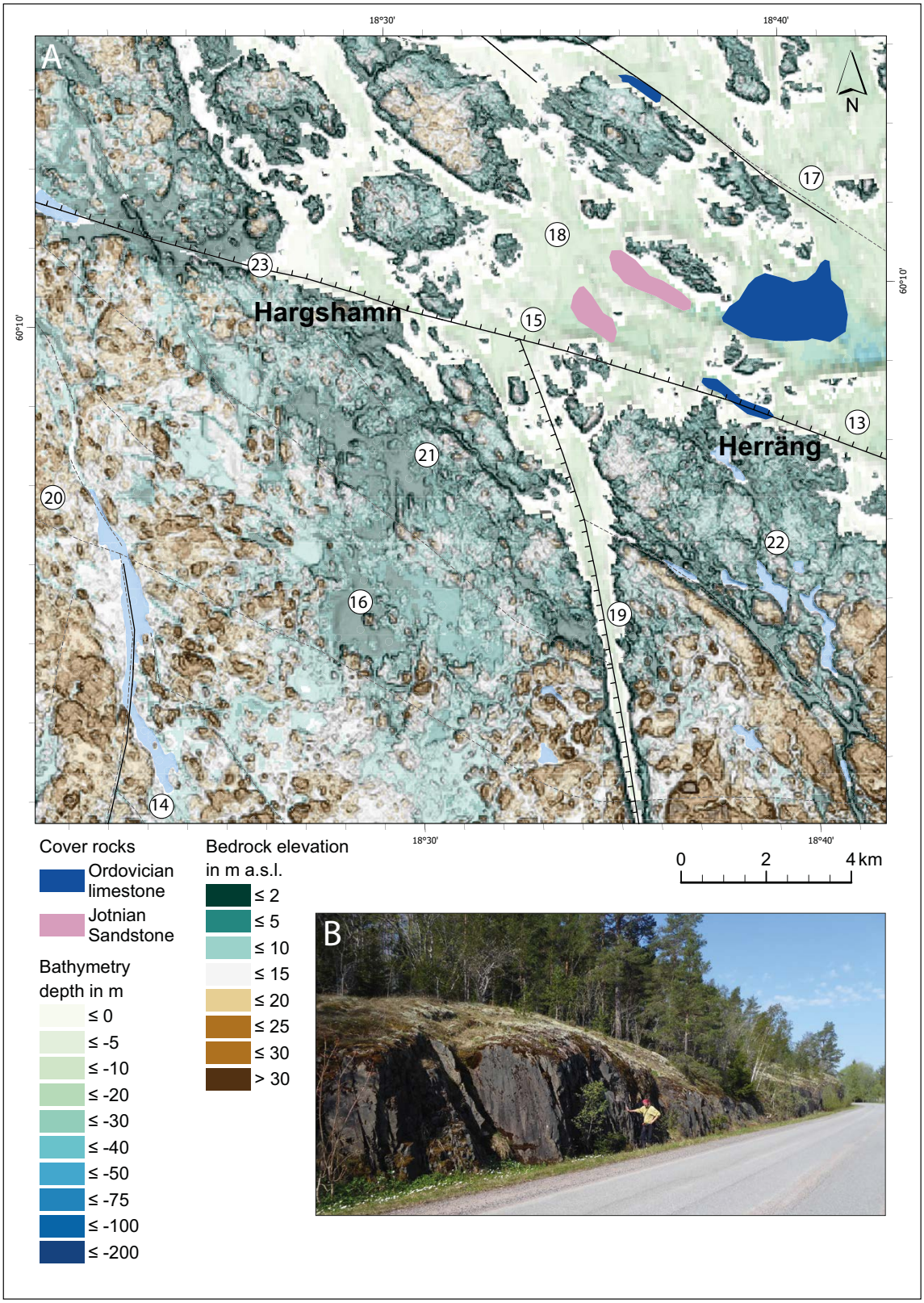

Figure 4-19. *Hargshamn. For location, see Figure 4-14. A. DEM of the bedrock surface. B. Järnboden (23) located on the S side of the Hargsviken fault zone. Positions of main faults and directions of throw shown as black lines.*

Figure 4-20. *View north along Väddöviken fjärd, a submerged rock trench excavated along the Väddö fault.*

Öregrund

The area W of Öregrund is crossed by the WNW-ESE oriented Singö (24), Forsmark (25) and (26) Eckarfjärden deformation zones (Figure 2-1). The latter deformation zone terminates against the N-S deformation zone in Kallrigafjärden (27) which itself terminates against the SDZ. A major fault marks the edge of the raised fault block that forms the W edge of Gräsö, one of several NW-SE oriented faults.

The gently inclined rock ramp on the seabed of the Öregrundsgrepen is overlain by Ordovician limestone (Hagenfeldt and Söderberg 1994) and remains close to the U2 surface. The island of Gräsö is part of a raised fault block which rises to 27 m a.s.l. (Figure 4-21). Glacial erosion of the fault scarp along the West Gräsö fault has removed a triangular rock wedge 1–1.5 km wide along the edge of the fault scarp. Low relief summit surfaces are, however, of restricted extent elsewhere around Öregrund (29 and 30). Glacial erosion of fault block tops has been high compared to the Dannemora area, with high surface roughness and relative relief, but equivalent to that found in the archipelago in the northern part of the Hargshamn area.

The close spacings of the deformation zones and faults has allowed formation of a well-connected network of partially drowned basins and trenches in this part of the Öregrund archipelago, with numerous intersecting trenches (34). Kallrigafjärden occupies a fault-guided (Stålhös 1991), shallow rock basin open to the north (27), in a similar position to other basins along the present coastline (Figure 4-13 in Hall et al. 2019a), including the low elevation terrain at Herräng. The drowned valley along the FDZ is segmented by two rock bars or thresholds (31 and 32).

Forsmark

At Forsmark, the deepest erosion is along regional deformation zones (Figure 4-47 in Hall et al. 2019a). The main trenches are developed along (i) the Singö, Eckarfjärden and Forsmark deformation zones, (ii) the Kallrigafjärden deformation zone with its NE-SW orientation, and (iii) the West Gräsö fault (Figure 4-4). The associated trenches and basins have lengths of several kilometres, widths of up to 1.5 km and depths of up to several tens of metres. The major and minor deformation zones at Forsmark have trace lengths of 1–10 km (Stephens et al. 2007) but are not associated with continuous trenches of similar length. On the Klubbudden coast, east of Forsmark, the major local deformation zones ZFMENE0060A and ZFMENE0062A have widths of 3–45 m and 10–64 m, respectively (Stephens et al. 2007), but limited or no topographic expression at the bedrock surface. Other major and minor deformation zones delineate groups of low bedrock hills located on lath-shaped rock blocks; trenches along these fracture zones are < 1.5 km long and 20–110 m wide. Seismic reflection velocities along shallow trenches are low, consistent with high fracture densities on trench floors (Brojerdi et al. 2014).

The topographic expression of the SDZ in the Forsmark area is muted. The trace of the SDZ on the seabed is marked by a trench with a floor in rockhead at −5 m a.s.l. at the SFR repository and which deepens to the SSE to −25 m a.s.l. (Figure 4-22). The trench is not continuous but broken into segments

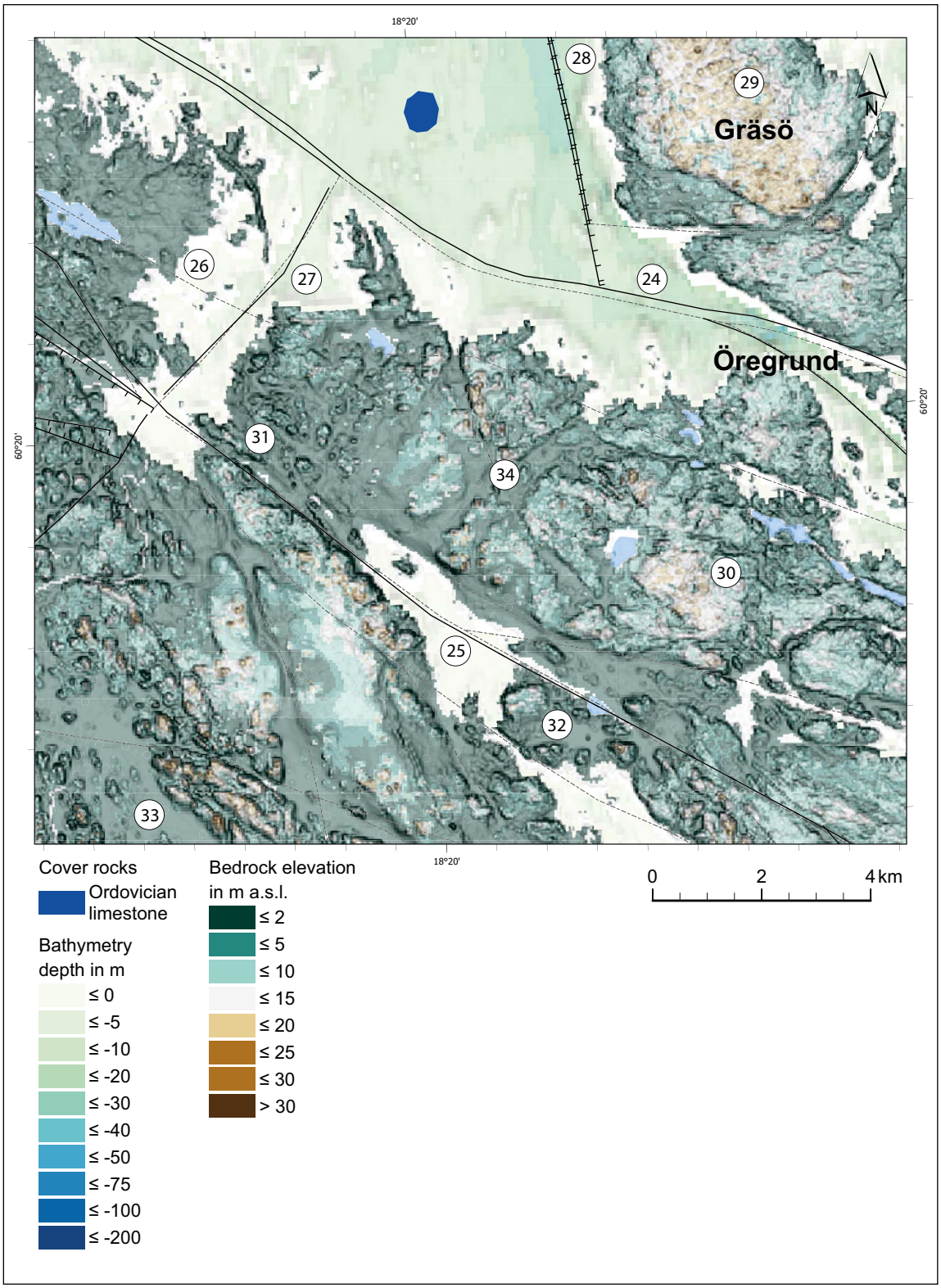

Figure 4-21. *DEM of the bedrock surface and seabed around Öregrund. For location, see Figure 4-14.*

by rock thresholds, giving an uneven thalweg. A north-south oriented trench that crosses the SDZ outside Kallrigafjärden is a deeper, wider, and more continuous topographic feature. Despite high fracture frequencies and small block sizes extending over a width of 200 ± 50 m for many kilometres, the WNW-ENE oriented SDZ has not been deeply eroded by the Fennoscandian Ice Sheet flowing generally in a N-S direction.

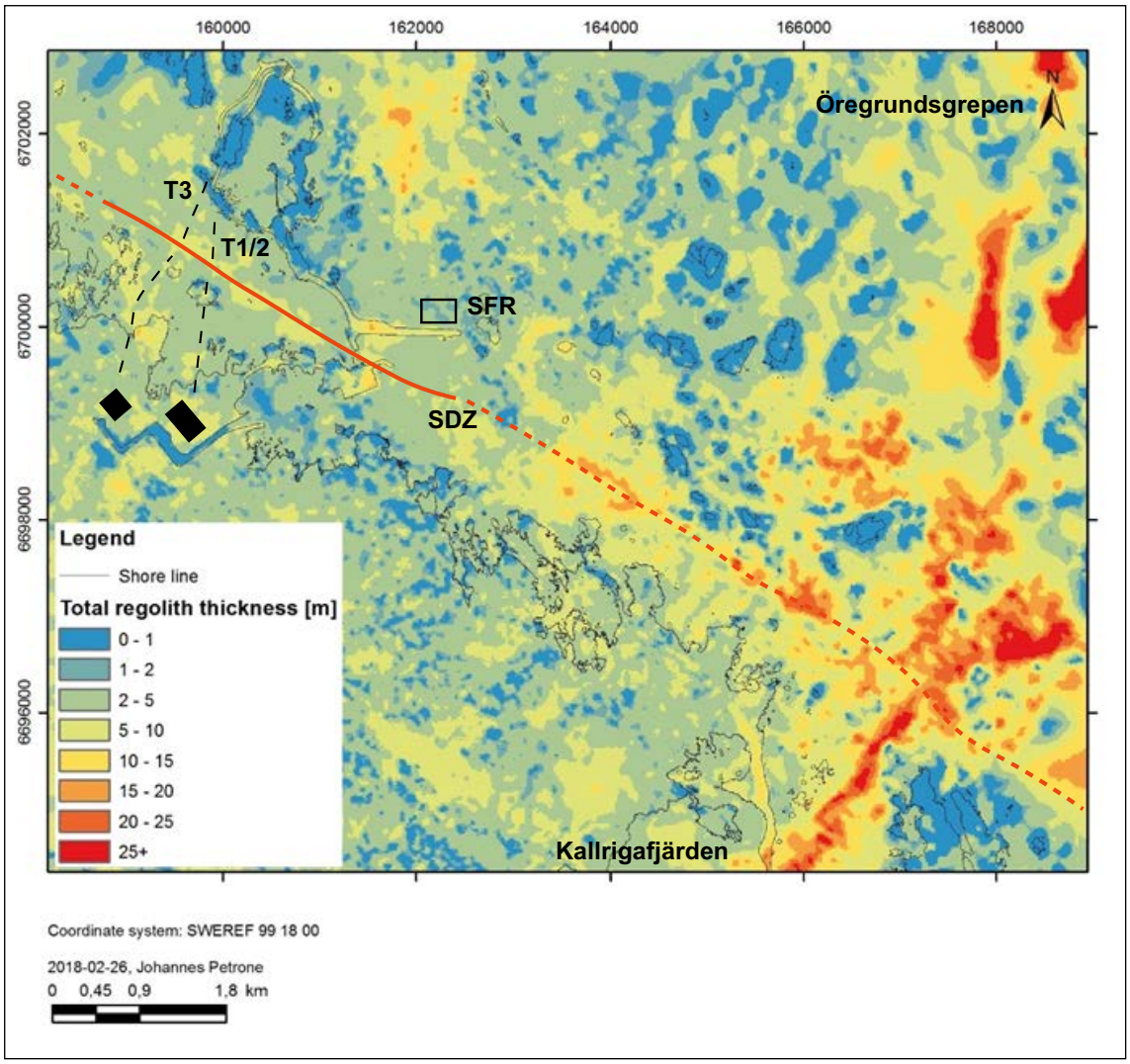

Figure 4-22. *The modelled regolith depths in the onshore and offshore area around Forsmark, illustrating the general form of the bedrock surface. The present shoreline is marked by a black line. For orientation, the "w-shaped" object just above the legend is the intake canal to the nuclear power plant and the SFR peninsula and pier can be identified some distance to the northeast of the canal. SDZ: Singö deformation zone trace. SFR: repository for low- and intermediate level waste. T1/2 and T3: tunnels for cooling water discharge from the nuclear power plants, marked as black boxes. Modified from Figure 5-2 in Petrone et al. (2020).*

Finnsjön

Rock trenches at Finnsjön are seen in DEMs of the bedrock surface as long, narrow, linear depressions (Figure 4-23) which are coincident with mapped fracture zones (Figure 4-9). However, segments of some fracture zones, and Fractures 1, 7–9 and 13 lack expression as topographic lineaments. The rock trenches have irregular thalwegs and numerous, broad rock thresholds rise along the lineaments that hold the trenches, separating the trench floors into discrete segments (Fractures 3 4, 9, 11, 13). These segments form individual branches in the rock trench network topology. Most rock trenches are short (0.3–1.3 km) (Table 4-1). The Finnsjön basin is exceptional, extending for over 10 km in length. The rock trenches are shallow, with depths of < 10 m. Rock trenches have widths of 27–109 m which are generally several times wider that the underlying fracture zones. Again, the exception is the Finnsjön regional deformation zone which forms a linear, lake filled depression up to 825 m wide. Most rock trenches are < 10 m deep.

The dominant trench orientations are north-south. Fractures oriented NW-SE and NE-SW have more limited topographic expressions. However, several NW-SE oriented trenches and basins are found east of the main area of geological mapping (Figure 4-23). In the Finnsjön area, the glacial erosion has been focussed along the Finnsjön deformation zone, the only major regional fracture zone to cross the area.

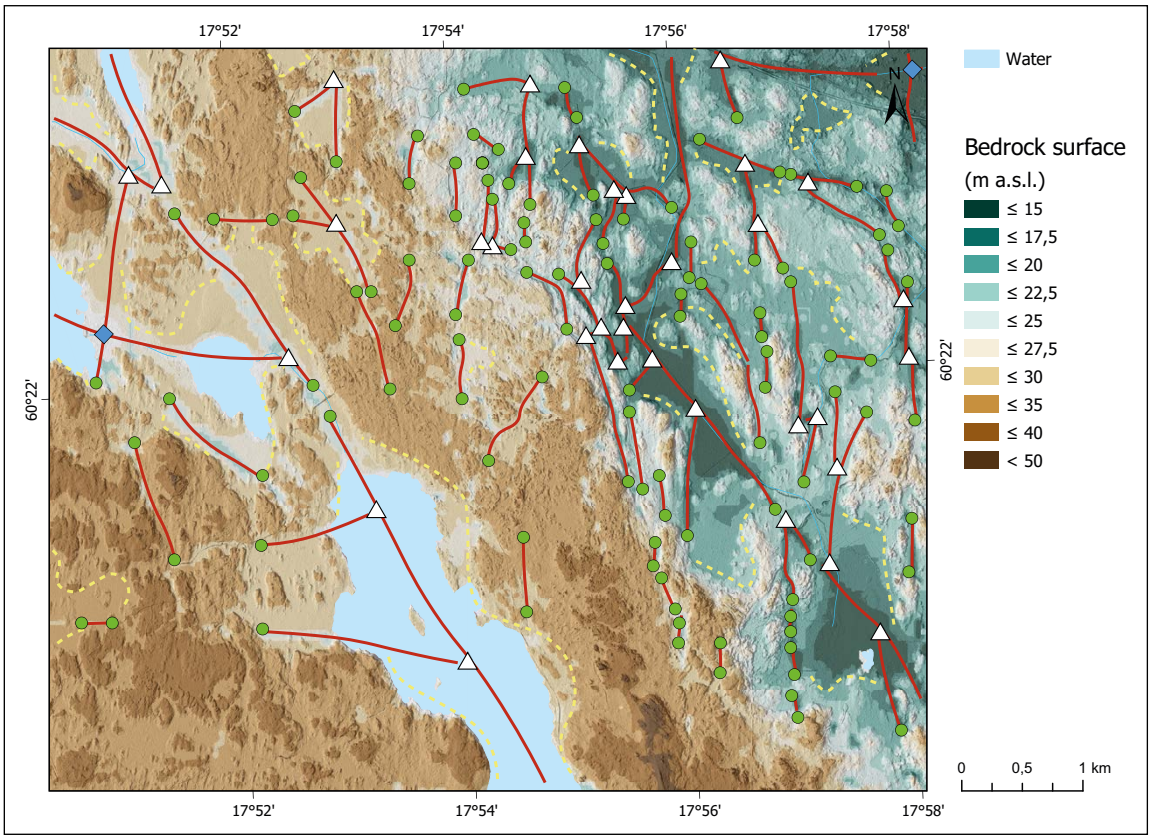

Figure 4-23. *Trenches and basins around Finnsjön. For location, see Figure 4-14. Trenches are shown by red lines. Edges of basins and depressions are indicated by yellow dashed lines. Nodes as in Figure 4-16.*

Table 4-3. Topology of fracture and trench networks at Finnsjön.

Nodes	I	Y	X	Total
Fractures	7	10	18	35
%	20.0	28.6	51.4	
Trenches	111	34	2	146
%	76.0	23.3	1.4	

4.4 Contrasting topologies of fracture and trench networks

Comparison of the regional fracture network topology and the regional trench topology reveals important differences (Table 4-4). For the regional fracture network, terminating I-nodes are relatively few and low in density whereas splayed Y-nodes and crossing X-nodes are common. For the trench network, there is a strong dominance in the number and density of I-nodes and X-nodes are few. The connectivity of the regional trench network is low compared to the fracture network. The number of rock trenches is also much higher than the number of major fracture zones, suggesting that trench erosion has also exploited minor fracture zones. At Finnsjön (Table 4-3), the percentage of closed I-nodes is low (20 %) in the fracture network. At Forsmark, the fracture network also has few I-nodes (12 %). Hence, similar relationships between fracture and trench topologies exist at the local scale.

Table 4-4. Topology of regional fracture and trench networks.

Nodes	I	Y	X	Total	Area (km^2)
Fractures (n)	**187**	**366**	**218**	**711**	**653.2**
%	24.3	47.5	28.3		
Density (n/km^2)	0.29	0.56	0.33		
x/y ratio			0.6		
(x+y)/i ratio	3.1				
Trenches (n/km^2)	**2347**	**897**	**231**	**3475**	**699.5**
%	67.5	25.8	6.6		
Density	3.36	1.28	0.33		
x/y ratio			0.3		
(x+y)/i ratio	0.5				

Significant variations exist in the connectivity of the trench network between areas. At the regional scale, trench connectivity is high at the coastal hinge zone and between Uppsala and Norrtälje (Figure 4-16). The lowest connectivity is on the Ironworks Block (Figure 4-18), and other low-relief block tops (Figure 4-15) interpreted previously as low glacial erosion zones (Hall et al. 2019). Trench connectivity is also low NE of Finnsjön. At Forsmark, in the Öregrund archipelago (Figure 4-21:34) and north of Hargshamn, trenches and basins show high connectivity where the spacings of fracture zones are low (2–3 km). These variations in connectivity appear to relate to regional differences in the intensity of glacial erosion combined with the spacing of major fracture zones. In the regional trench pattern and in DEMs of the local case study areas, the highest connectivity between trenches exists along the main trenches developed in regional deformation zones.

The positions of trenches in the study area align with known or inferred fracture zones, indicating that the trench network is controlled by underlying fracture patterns. Other important features of fracture networks are closely replicated by the trench network:

(i) the low frequency and wide spacing of both fracture zones and trenches,

(ii) the limited widths of both fracture zones and trenches,

(iii) the abutment of short fractures and termination of short trenches against longer features, and

(iv) the terminations of some short fractures and trenches without network connection.

Significant differences also exist, namely:

(v) the connectivity of the fracture network is higher than the trench network,

(vi) many major fracture zones carry trenches along only part of their length, and

(vii) whereas the fracture network shows 4 dominant fracture sets, with broadly equal dominance (Figure 4-24A), the trench network is dominated by a single NNW-SSE trend (Figure 4-24B).

The strong dominance of NNW-SSE oriented trenches indicates that fracture zones along this trend have been preferentially exploited by glacial erosion. Ice-flow direction, as indicated by regional striation patterns, was predominantly to the south-southeast.

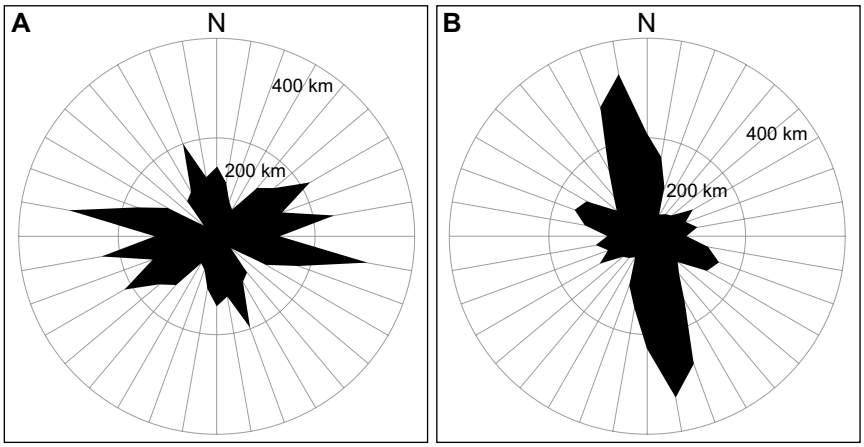

Figure 4-24. *Comparison of fracture orientations (A) and trench orientations (B).*

4.5 Summary of depths and rates of erosion in the Öregrund archipelago and its surroundings based on geomorphological criteria

Erosion depths and rates of downwearing, backwearing and incision in various geomorphological contexts are listed in Table 4-5. The broad estimates for erosion depths and rates in the Öregrund archipelago and its surroundings rest on two assumptions: (i) that the present basement topography in NE Uppland is largely inherited from the sub-Cambrian unconformity, with its near-planar surface broken into fault blocks (Grigull et al. 2019, Hall et al. 2019a) and (ii) that this surface was re-exposed progressively after 1.2 Ma by glacial erosion beneath the Fennoscandian Ice Sheet (Hall and van Boeckel 2020).

4.5.1 Erosion in former sedimentary cover rock

Erosion depths in former sedimentary cover in the Åland Deep are high. The minimum erosion is constrained by the amount of overdeepening (which can only be achieved by glacial erosion) and amounts to ~ 200–300 m (Section 4.2.1). In the Öregrund archipelago, the minimum depths of erosion in the former sedimentary cover are represented by height differences between basement fault block tops and basement surfaces on the seabed with and without sedimentary outliers. The minimum erosion depths are ~31–45 m.

4.5.2 Erosion in basement

Denudation depths in basement, which are overwhelmingly dominated by glacial erosion, are constrained by the difference in height of the former U2 surface and the present-day rock surface. The estimated average depths of erosion at Forsmark are 12 m and in Uppland are 14 m (Hall et al. 2019a). An estimate of 10 m is added to these depths to include average summit erosion.

Backwearing of fault scarps is < 1.5 km in the Öregrund archipelago, slightly higher than comparable figures for Västergötland (Hall et al. 2019b).

4.5.3 Erosion of trenches

Assuming that the U2 surface contained no trenches (see Section2.4.2), the depth of trenches is a direct constraint on their glacial erosion. Trench deepening is most pronounced around the rim of the Åland Deep. In the Öregrund archipelago, trench depths lie in the 10–50 m range (see Section 4.3.3–4.3.4). Similar trench depths are present at Trollhättan (Hall et al. 2019b). Trench widths rarely exceed 1 km and trenches are more usually ~100 m wide. Knickpoints in the eastern Öregrund archipelago indicate steepening of thalwegs over distances of 5–15 km (Figure 4-10) but similar steepening is not seen in the western part of the archipelago or along trenches to the S.

Table 4-5. Summary of Pleistocene glacial erosion depths and rates in lowland Sweden and SW Finland based on geomorphological criteria.

Location	Downwearing			
	Sedimentary cover	**Minimum depth of erosion (m)**	**Erosion rate (m/100 ka)**	**Reference**
Åland	Åland Deep	200–300	17–25	
Öregrund	Singöfjärden	39	3.3	Hall et al. (2019a)
	Raggaröfjärden	31	2.6	
	Vässarön	45	3.8	
	Gräsö	40	3.3	
	Basement gneisses	**Average depth of rock removed (m) below U2**	**Erosion depth (m/100 ka)**	
Uppland	Forsmark	22	1.8	Hall et al. (2019a)
	Uppland	24	2.0	
Västergötland	Trollhättan	20	1.7	Hall et al. (2019b)
	Back wearing			
	Retreat of fault scarps	**Distance (km) from former fault plane**	**Retreat rate (m/ 100 ka)**	
Uppland	Gräsö	1.0–1.5	83–125	Hall et al. (2019a)
	Ironworks	0.5	42	
	Hallstavik	0.75	63	
Västergötland	Trollhättan	0.3–0.8	25–67	Hall et al. (2019b)
	Incision			
	Trench deepening	**Depth of erosion (m) below U2**	**Erosion rate (m/100 ka)**	
Åland	East Åland	40–100	3.4–8.3	
	Södra Kvarken	100–130	8.3–10.8	
Uppland	Öregrundsleden	15–25	1.3–2.1	
	Östhammar fjärd	10–25	0.8–2.1	
	Väddöviken	10	0.8	
	south Uppland and north Stockholm County	10–50	0.8–4.2	
Västergötland	Trollhättan	10–80	0.8–6.7	Hall et al. (2019b)
	Närke	20–50	1.7–4.2	Hall et al. (2019a)
	Motala	10–60	0.8–5.0	Hall et al. (2019b)
	Trench widening	**Width (m)**	**Widening rate (m/100 ka)**	
Uppland	SDZ	450–850	38–71	
	EDZ	150–330	13–28	
	FDZ	500–1 000	42–83	
	H-HDZ	310–630	26–53	
	Headward erosion of rock channels	**Distance (km)**	**Retreat rate (m/100 ka)**	
Åland	East Åland archipelago	40	3.3	This report
	Åland Deep	60	5.0	
Öregrund	Öregrund archipelago	5–15	0.4–1.2	

5 Discussion

Erosion of the Precambrian gneisses in Uppland from the Palaeoproterozoic onwards led to the development of three major unconformities: the sub-Jotnian unconformity (U1), the sub-Cambrian unconformity (U2) and present basement surface (e.g. Hall et al. 2019a). Remarkably, these unconformities remain at similar elevations in the present landscape so that inherited topographic elements from the earlier unconformities are widespread. During the Pleistocene, glacial erosion by the Fennoscandian ice sheet acted to re-expose parts of the sub-Jotnian and sub-Cambrian unconformities and to modify and reshape the basement surface. Glacial erosion was strongly influenced by the distribution of Proterozoic and Early Phanerozoic sedimentary cover and by the pre-existing fracture patterns in the basement.

5.1 Controls on glacial erosion in Uppland

The main controls on rates and patterns of erosion beneath ice sheets are geology, topography, glaciology, and time.

5.1.1 Geology

Geological controls on the effectiveness of glacial erosion operate mainly through rock type (hardness, permeability and mineralogy) and structure (mainly the orientation and spacing of fractures and bedding planes). In Uppland, there is a strong contrast in rock resistance between the remaining and former sedimentary cover rocks and the Precambrian gneisses. There is a broad relation between uniaxial compressive strength and Schmidt Hammer hardness, and hence with abrasion resistance (Aydin and Basu 2005). Proterozoic sandstones have high uniaxial compressive strength (247 MPa) but low abrasion resistance (Sahlin et al. 2000) and very high fracture intensities, with bedding plane spacings of 2–64 cm (median fracture intensity ~10 m^{-1}) in the Jotnian sandstones in a borehole of Gotska Sandön in the Baltic Sea (Gorbatschev 1962). The Ordovician limestones have lower uniaxial compressive strength (190 MPa) but higher abrasion resistance (Sahlin et al. 2000) but, again, fracture intensities are high due to the close spacing of bedding planes (Milnes and Gee 1992).

The gneissic bedrock at Forsmark includes granite gneisses, amphibolites and metavolcanics. Testing of rock types found in the so-called ‘Forsmark tectonic lens’ has yielded values for uniaxial compressive strength of 175–275 MPa (SKB 2008) and 226–373 MPa (Glamheden et al. 2008). Borehole KFM01A yielded rock samples with a mean value for uniaxial compressive strength of 239.2 ± 25.9 MPa (Jacobsson 2004). The mean uniaxial compressive strength of borehole samples of granite and granodiorite is higher (225 MPa) than that of the tonalite (156 MPa) (Lanaro and Fredriksson 2005). For three samples from borehole FFM01 of pegmatitic granite in the vicinity of a deformation zone, the uniaxial compressive strength of samples ranged between 158 MPa and 187 MPa (Glamheden et al. 2008), slightly lower than for the surrounding host rock. Hence, the gneisses are generally very strong in engineering terms, but show variability in strength between different rock types and between intensely fractured deformation zones and neighbouring host rocks.

At Forsmark, the mean fracture frequency in host rocks outside deformation zones and measured at outcrop is 2.9 m^{-1} (Darcel et al. 2006). In shallow rock excavations, fracture frequency is 1–3 m^{-1} (Krabbendam et al. 2021). Fracture frequency and rock permeability often drop sharply beneath the uppermost few metres of the rock column (Min and Stephansson 2011, Follin 2019).

Weathering acts to reduce the mechanical strength of rock and to open microfractures. In many formerly glaciated areas, shield surfaces were already extensively weathered at the onset of the Pleistocene glaciations (Elvhage and Lidmar-Bergström 1987, Hall and Migoń 2010, Krabbendam and Bradwell 2014). In southernmost Sweden, deep weathering developed over long periods in the Mesozoic and Cenozoic (Lidmar-Bergström 1995). The deepest penetration of preglacial weathering was within fracture zones of high permeability (Hall et al. 2015). Saprolitic materials can be readily excavated by Pleistocene ice sheets to form rock trenches and basins (Krabbendam and Bradwell 2014). However, where Early Palaeozoic and younger sedimentary cover rocks persisted into the late Cenozoic the

basement was largely protected from chemical weathering. Where U2 remained buried into the Pleistocene the only significant weathering on its surface was that inherited from the sub-Cambrian unconformity. Pre-Cambrian weathering depths varied from zero to tens of metres on basement surfaces across Baltica (Liivamägi et al. 2014), with negligible weathering recorded from the buried unconformity in Västergötland (Hall et al. 2019b). At Forsmark, and by extension in the Öregrund archipelago, there are no traces of sub-Ordovician or younger Phanerozoic weathering (Hall et al. 2019a). Hence, the re-exposed U2 basement surface in these areas was in hard, unweathered rock.

In addition to the character of the bedrock, the availability and hardness of clasts at the glacier sole is an important control on rates of abrasion (Sugden and John 1976, Krabbendam and Glasser 2011). The greater hardness of gneissic clasts is likely to have increased abrasion rates on sandstone and limestone rock surfaces at the Fennoscandian Ice Sheet bed. Contrasts in hardness between different gneiss rocks are less marked but likely led to differential abrasion of rocks with low uniaxial compressive strength from harder clasts.

In summary, the sedimentary cover rocks are generally softer and have higher fracture intensities than the Precambrian gneisses. Hence, the resistance of the sedimentary rocks to glacial erosion by abrasion and block removal is significantly lower than for the basement gneisses. The gneisses are generally very hard and so are resistant to glacial abrasion. However, the heterogeneous orientations, spacings and lengths of individual fractures render the gneisses mechanically anisotropic and hence spatially variable to glacial erosion by block removal.

5.1.2 Topography

Topography acts to guide ice and meltwater flow, with valleys providing conduits for faster ice flow, high meltwater discharges and more efficient erosion (Margold et al. 2015). Due to inheritance of relief from U2, the topography of the basement surface has only a few tens of metres of regional relief. Hence, the low relief topography probably exerted limited control on the flow of the overriding Fennoscandian Ice Sheet. Bed roughness is another important control on ice flow (Rippin 2013). In Uppland, bed roughness and relief increase southward, implying higher resistance to ice flow in this direction.

5.1.3 Glaciological variables

Glaciological controls on erosion include basal thermal regime, basal ice flow velocity, and groundwater and meltwater fluxes. The glaciological conditions beneath the Fennoscandian Ice Sheet varied through time during the last and earlier glacial phases (Kleman et al. 2008, Quiquet et al. 2016). Ice sheet modelling suggests, however, that spatial variations were limited beneath the last Fennoscandian Ice Sheet in (i) glacier dynamics (Patton et al. 2016a) and (ii) cumulative basal sliding distances (Näslund et al. 2003) over 10–100 km distances in east-central Sweden. Possible exceptions to this general uniformity of glaciological conditions include subglacial meltwater routing, with channelling along major valleys indicated in ice sheet models (Shackleton et al. 2018).

5.1.4 Time

Time is required for rock surfaces and landforms originally shaped by non-glacial processes to become adapted to ice flow. The timing of re-exposure of basement surfaces on the sub-Cambrian unconformity in southern Sweden was diachronous, latest at locations close to present outliers (Hall et al. 2019b). A similar situation likely existed in Uppland during the Pleistocene. Here, the higher surface roughness and relative relief in the present basement surface found southwards is transitional to the fissure-valley landscapes identified in the Stockholm area (Elvhage and Lidmar-Bergström 1987). The change in landscape character has been linked to (i) a greater magnitude of pre-Cenozoic faulting (Wiman 1942), (ii) prior exposure of the basement to deep chemical weathering before Pleistocene glaciation (Lidmar-Bergström 1995), and (iii) a longer period of exposure to glacial erosion (Hall et al. 2019a). However, the Öregrund archipelago and the Forsmark area are located a few kilometres from outliers of Ordovician limestones. Hence, the timing of removal of cover rocks was likely broadly similar at these two locations. Around the Baltic Sea basin, re-exposure of the U2 surface dates mainly or entirely from the last 1.2 Ma (Hall and van Boeckel 2020).

In summary, basement rock type, topography and the different glaciological variables are unlikely to have significantly influenced the observed patterns of glacial erosion in the basement in Uppland. Instead, the key controls on glacial erosion were (i) the contrasting resistance between the basement and its former sedimentary cover and (ii) unevenly fractured basement gneisses.

5.2 Glacial erosion in sedimentary cover

The relative softness and high fracture intensity of Mesoproterozoic and Neoproterozoic sandstones, Cambrian sandstones and shales, and Ordovician limestones render these rocks less resistant to glacial erosion than the basement gneisses. These sedimentary rocks are typically preserved in fault-bounded basins of various dimensions on the beds of the Bothnian, Åland and Baltic Seas. Fault-bounded Phanerozoic sedimentary basins are loci for large and deep rock basins and trenches on the seabed (Hall and van Boeckel 2020).

Around the Åland basin, the basement surfaces at present sea level retain the low regional relief of U2 (Figure 4-8), but the Åland Deep, excavated in Jotnian sandstones and younger sedimentary rocks, attains a maximum depth of 301 m. The Åland Deep is an enclosed rock basin, excavated below present sea level. This overdeepening is a product of differential glacial erosion between the sedimentary basin and the surrounding basement. The timing of the onset of overdeepening is uncertain but the absence of marine sediments from the southern Baltic Sea in the Early Pleistocene and much of the Middle Pleistocene indicates that a marine Baltic basin did not exist until perhaps as late as the Holsteinian interglacial (~ 420–395 ka) (Hall and van Boeckel 2020). By the Late Weichselian, the Åland Deep had become a locus for ice streaming (Patton et al. 2017) and for high meltwater discharges (Shackleton et al. 2018) beneath the Fennoscandian Ice Sheet.

In the Öregrund archipelago, shallow grabens and half grabens hold remnants of former Mesoproterozoic and Neoproterozoic sandstones and Ordovician limestones (Hagenfeldt and Söderberg 1994). Based on an interpretation that the upper surfaces of fault blocks and the basement around Ordovician outliers on the seabed stand close to U2, the differences in elevation of 30–40 m between neighbouring upstanding basement fault blocks and the rock floor beneath the seabed indicates the removal of at least an equivalent thickness of sedimentary rock to re-expose the block faulted basement surface. The submarine rock basins within the Öregrund archipelago are mainly a product of the removal of this former sedimentary cover by glacial erosion. Along the regional deformation zones and major faults within the archipelago, there has been additional erosion in basement, forming trenches that cut below the U2 surface.

5.3 Patterns and depths of glacial erosion in basement in lowland Sweden

The pattern of erosion depths across Uppland and in its surroundings (Figure 4-4) indicates that (i) most of the rock volume removed from below the former unconformity comes from rock trenches, valleys and basins and (ii) average erosion depths increase southward. Average depths of glacial erosion have been estimated at 14 m across north-east Uppland and 12 m in the Forsmark area (Hall et al. 2019a).

Similar erosion patterns and depths have been recognised in southern Sweden close to Early Palaeozoic outliers (Hall et al. 2019b). Extensive areas near Trollhättan show removal of < 5–10 m depths of basement. Glacial erosion is greatest in rock trenches and basins that reach depths of 80 m along the Göta trench. South of Trollhättan, where average depths of erosion below summit envelope surfaces are relatively high (~20 m), ~75 % of rock removed comes from topographic depressions > 10 m deep (Table 3-2 in Hall et al. 2019b). Significantly for this study, the buried unconformity and the edge of the exposed basement in southern Sweden display only broad (> 1 km), shallow (< 10 m) topographic depressions. No deep rock basins or buried valleys are reported that hold outliers of basal Cambrian sandstone (Hall et al. 2019b). Hence, rock depressions are products of glacial overdeepening during the Pleistocene and represent the most likely sites for enhanced glacial erosion in future glaciations.

5.4 Glacial erosion in basement terrain in relation to properties of fracture networks and rock trenches

The links between fracture networks and rock trenches are important for understanding why glacial erosion has exploited fracture zones to form rock trenches.

5.4.1 General relationships of fracture networks

The capacity for glacial erosion to exploit individual fractures, fracture corridors and fracture zones is influenced by their lengths, spacings and widths.

- *Fracture lengths* commonly follow power laws (Marrett et al. 1999, Reeves et al. 2012). At Äspö, median fracture-trace lengths are short, estimated at 2.3 m in tunnels (Munier 1993). At Forsmark, fracture-trace lengths for the four dominant, steeply dipping fracture sets over trace lengths of 1 m to 10 km plot as straight trend-lines on log-log plots (La Pointe et al. 2005, Follin et al. 2013). Similar results are derived from maps of fractures with multiple orientations on outcrops (Darcel et al. 2006). Hence, general power law relationships between fracture length and frequency also apply to fractures in Precambrian gneisses. A consequence is that fracture zones with > 5 km length are few in Uppland (Figure 4-2).
- *Fracture spacings* along lines, planes or in 3D, or fracture intensities, commonly follow log normal distributions (Munier 1993). Fracture corridors typically occupy < 5 % of 100 m long scanlines, requiring modal spacing of tens of metres (Sanderson and Peacock 2019). Individual major regional fracture zones are separated by distances of 2–15 km (Figure 4-2).
- *Local deformation zones and other fracture zones are narrow*. Local major deformation zones are 5–100 m wide at Forsmark (Table 2-1). Local minor deformation zones have widths of 0.1–5 m (Table 2-1) and resemble fracture corridors (Questiaux et al. 2010). At Finnsjön, deformation zone widths are 3–100 m (Table 4-3). Similar relationships exist at the local scale at Äspö where major fracture zones with lengths of 2–5 km have widths of 12–49 m (Stanfors et al. 1999).
- *Fracture zones are deep*. Most subvertical fracture zones extend to depths of at least several hundred metres (Ahlbom et al. 1986, Follin et al. 2007).
- *Short fractures often terminate* without connection to long fractures or *abut* long fractures (Davy et al. 2010, Sanderson et al. 2019).
- *Fracture apertures* scale with fracture length to the 1/2 power across fracture lengths of 0.1–1 km in sedimentary rocks (Olson 2003). Similar power law relationships apply in many rocks (Gudmundsson et al. 2012), including basement gneisses (McCaffrey et al. 2020).
- *In situ joint-bound rock block sizes* in general are controlled mainly by fracture length and fracture spacing and show log normal distributions (Wang et al. 1991). In the field area, fracture corridors and fracture zones are distinctive, with significantly higher fracture intensities (Glamheden et al. 2008, Sanderson and Peacock 2019) and smaller block sizes (Munier 1993).

Regional and local deformation zones and regional faults represent fractures that are > 5 km in length and widely separated but few in number. The major fracture zones are narrow (mainly < 100 m wide) but are of great depth. Fracture apertures are likely high and fracture intensities are very high, forming long corridors with small joint block sizes along major fracture zones.

5.4.2 Fracture network and trench network topologies

Topographic lineaments are routinely mapped in crystalline terrain as indicators of underlying fracture patterns, with potential for circular reasoning about the co-relationships between the two features. Where topographic lineaments run parallel to field-mapped fracture orientations, a causal relationship may be inferred based on the assumption that differential weathering and erosion has exploited permeable fracture zones (Ericsson et al. 2005, Henriksen and Braathen 2006). Topographic lineaments have been mapped previously at various scales in NE Uppland (Section 4.1). At Forsmark (La Pointe et al. 2005), and to a lesser extent, at Finnsjön (Ahlbom and Tirén 1991), topographic lineaments run parallel to fracture sets mapped at outcrop. This provides confidence that topographic lineaments in Uppland generally follow fracture zones. In this study, fracture patterns inferred from topographic

lineaments (Section 4.1) and trench patterns mapped from DEMs (Section 4.3.3) are compared in terms of distribution and topology (Section 4.4).

The similar distributions of fractures inferred from topographic lineaments and of rock trenches (Figures 4-1, 4-3 and 4-4) indicate that fracture zones generally underpin trenches. Similar patterns of termination, junctions and grouping in parallel sets are also seen in the fracture and trench topologies (Figures 4-2 and 4-16). However, fractures subparallel to ice-flow were preferentially eroded out to form trenches (Figure 4-24). Short trenches ending at I-nodes in the trench topological network (Figure 4-16) are seen in DEMs to terminate at facing rock walls on the distal flanks of long fractures (Figure 4-19B). This type of termination is likely controlled by the tendency of short fractures to abut longer fractures.

A key difference in connectivity exists between the topologies of the fracture and trench network. Numbers of X- and Y-nodes are high for fracture networks, but I-nodes dominate in trench networks; network connectivity is high in fracture networks relative to trench networks. Several reasons may be proposed for this. Firstly, fracture zones interpreted from valley lineaments are assumed to be continuous but actually may be locally discontinuous where fracture zones become constricted or deviate from the present erosion level. Secondly and more certainly, valleys along fracture lineaments are seen in DEMs to be segmented by rock thresholds that separate the valley floors into shorter trenches (Figures 4-18, 4-19, 4-21 and 4-23). Thirdly, short trenches may terminate a short distance from a long trench, without forming a T-junction or I-node, and leave a narrow rock rib between the two trenches (Figure 4-18). The rock thresholds and rock ribs likely relate to tabular zones of relatively wide fracture spacing that run parallel or transverse to major fracture zones. Finally, several fracture zones at Finnsjön and Forsmark lack continuous or deep trenches at the land surface; glacial erosion has not exploited these lines of weakness and trench connectivity remains low. Hence, the lower connectivity of the trench network is in part a result of the uneven and limited exploitation of the underpinning fracture network by glacial erosion.

The trench network in Uppland is one of (i) low connectivity, (ii) where many long valleys are segmented by rock thresholds into individual trenches, (iii) short trenches join the main trenches at various angles determined by fracture sets, (iv) junctions between trenches include splay- and T-junctions and (v) trenches may intersect and cross each other. This partial mesh network is unlike simple drainage networks which gather and transport water via dendritic or trellis networks. Viewed from the perspective of subglacial hydrology, the trench network has long, continuous trenches which are suited to efficient discharge of channelled meltwater towards the ice margin, shorter, connected but discontinuous trenches that may channel water towards or away from these main conduits and isolated trench segments that may act as stores for meltwater.

5.4.3 Major fracture zones and rock trenches in Uppland

Close spatial associations exist between the regional distributions of major regional fracture zones (Figure 4-2) and long rock trenches (Figure 4-16). Long trenches (> 5 km) are confined to long fracture zones. Examples include the trenches along the WNW-ESE-oriented SDZ, EDZ and FDZ in the Öregrund archipelago, the NNE-SSE trenches along the Österbybruk and Kallrigafjärden and the fault-guided trenches south of Gimo. Trenches remain narrow (< 0.1–2 km). Regional major deformation zones, such as the SDZ, underpin trenches where fracture zone width is equal to or less than trench width. Examples include the Finnsjön deformation zone (~100 m) and its trench (200–825 m), the Forsmark deformation zone (3–63 m) and its trench (220–330 m) at Bruksdammen and the Singö deformation zone (200 ± 50 m) and its trench (1 050–1 300 m at Singö). The Kallrigafjärden deformation zone underlies only the axial part of a broad, shallow basin (Figure 4-8). Hence, the trenches have been significantly widened beyond the initial confines of major fracture zones. Trenches remain shallow, with maximum depths of 50 m. Erosion has not extended deeply into major regional fracture zones.

Whilst fracture patterns at the regional scale in Uppland show 4 main orientations, it is the ice-flow parallel NNW-SSE set has been selectively exploited to form trenches (Figure 4-16; Fig. 4-24)). At Dannemora (Figure 4-18), Hargshamn (Figure 4-19) and Finnsjön (Figure 4-23), NNW-SSE trenches also dominate at the local scale. Similar selectivity is reported for fracture sets subparallel to ice flow in southern Sweden (Tirén and Beckholmen 1990). Selective erosion of fracture zones along ice flow is also recognised in regional streamlining in basement terrains (Krabbendam et al. 2016). The occupation

of dominantly N-S trenches by post-glacial streams and rivers has generated a sub-regional drainage network of parallel type (Zernitz 1932) that extends south into parts of Stockholm County.

In the tectonic hinge zone occupied by the Öregrund archipelago, rock trenches follow the ENE-WSW oriented set of regional deformation zones (Figure 4-2). This trench set, and the W-E major trenches between Uppsala and Norrtälje, are transverse to former ice flow. Short but narrow minor fracture zones which run transverse to ice flow were less frequently, or less deeply eroded to form trenches. In these cases, glacial erosion appears to have selectively exploited relatively wide regional deformation zones that lie across the line of former ice flow. Hence, both the orientation and width of fracture zones have influenced the potential for glacial erosion of major trenches.

5.4.4 Progressive adjustment of the basement surface to fracture patterns under glacial erosion

The sub-Cambrian unconformity surface developed under non-glacial environments in late Precambrian times; it was eroded across different rock types and shows limited or no fracture control over its form over wide areas (Hall et al. 2019b). In contrast, the present basement surface shows close fracture control on the geometry of its landforms (Hall et al. 2019a). The glacial bedforms developed on U2 represent a progressive adjustment of the glacier bed to fracture controls in response to Pleistocene glacial erosion.

Progressive glacial erosion of fault blocks after Pleistocene exhumation has been examined previously on three adjacent fault blocks at Alunda in Uppland (Figures 4-16 and 4-17 in Hall et al. 2019a). Fault block tops were first lowered by loss of rock sheets from areas with relatively high fracture intensities, leading to the excavation of shallow basins. The top surfaces were dissected by the excavation of long (1–2.5 km), narrow (20–40 m) trenches along fracture zones of similar dimensions. This early stage of erosion is also represented on the Ironworks Block (Figure 4-18 here). As fault block tops were further lowered, residual high points became increasingly confined to widely-spaced rock kernels with > 5 m fracture spacings. Large box hills emerged. Rock surface roughness and relative relief increased across the fault block tops as zones with small rock blocks were differentially eroded. Most erosion occurred along fracture zones along block edges, with erosion of trenches with lengths of 4–10 km and depths of 10–20 m. The exposed edges of the fault blocks were transformed from straight margins along fracture-guided trenches to crenulated and then indented edges. Whilst the outlines of the original fault blocks were obscured, backwearing from fault zones rarely exceed 1 km. Similar sequences of progressive erosion on fault blocks are identified at Trollhättan and Närke (Hall et al. 2019a, b).

The progressive development of trenches is seen on U2 at increasing distances from the edges of Early Palaeozoic outliers in Västergötland (Hall et al. 2019b). At Nordkroken, 1–2.5 km from the Halleberg outlier, rock trenches occur on granite gneisses which are ~4 m deep, 15–25 m wide and 0.6–1.6 km long. The trenches are mainly oriented N-S and NE-SW along vertical fracture zones and, respectively, parallel and transverse to former ice flow (Figure 3-23 in Hall et al. 2019b). At Sjuntorp, 20 km S, many trenches are > 20 m deep, 150–400 m wide and 2–5 km long (Figure 3-21 in Hall et al. 2019b). The main Göta River valley follows the Göta Fault; this valley is 50 m deep, 2 km wide and 75 km long. Assuming that Sjuntorp, remote from the outlier edge, has been exposed to glacial erosion for longer than Nordkroken, close to its edge, the differences in trench dimensions indicate the progress of erosion at Sjuntorp. Shallow and short trenches appeared at Nordkroken early in the downwearing of U2 soon after its re-exposure and the onset of glacial erosion of basement. Over time, the trenches became wider, deeper and better connected. The Göta valley, the main discharge route for meltwater from the Vanern basin, formed the widest, deepest, and longest trench in the region.

5.4.5 Rock block size and glacial erosion

General fracture properties (Section 5.4.1) generate fracture patterns that, in turn, control *in situ* rock block sizes. The log-normal distribution of fracture spacings requires a similar frequency distribution of rock block sizes (Reeves et al. 2012). In southern Sweden, measurements in gneiss quarry faces confirm that block sizes in Precambrian gneisses also have log-normal distributions (Jern 2004). Most

(70–90 %) block sizes fall in the intermediate 0.5–2.0 m range, with low frequencies of larger and smaller boulders. The spatial distribution of *in situ* block sizes is highly uneven. Visualisations of modelled fracture patterns in host rocks based on empirical relationships between fracture length, spacing and orientation show a few clusters of large *in situ* joint-bound, rock blocks or *rock kernels* that are set within much larger volumes of rocks with variable block sizes that remain within the normal, intermediate range (Elmouttie and Poropat 2012). Because spacings of individual joint sets show clustering (Wichmann et al. 2019), crossing joint sets with short fracture spacings may produce small zones at intersections with small *in situ* block sizes. More amorphous zones with low fracture spacings (> 10 fractures/m^2) may also occur, such as cover 0.1 ha areas of jointed granodioritic gneisses in the Eastern Alps (Wichmann et al. 2019). The broad, shallow topographic basin at Kallrigafjärden may occupy a submerged area with similarly closely spaced fractures. In summary, the first order spatial distribution of block sizes in Precambrian gneisses in lowland Sweden is for (i) a few, widely spaced rock kernels set within (ii) large areas of the dominant intermediate-sized blocks and (iii) small areas of small blocks mainly along fracture corridors and at fracture set intersections and (iv) larger areas independent of major fractures.

These general host rock distributions are interrupted by transecting major fracture zones. In the core zone of the SDZ, fracture frequency is > 4 m^{-1} and locally > 10 m^{-1} (Glamheden et al. 2007). In the Brändan fracture zone at Finnsjön, block volumes are ca. 1 dm^3. At Äspö, block volume in the peripheral host rock is typically ca. 1 m^3 but drops to ca. 1 dm^3 in the core of deformation zones (Munier and Talbot 1993). Small block sizes are a result of repeated shearing, faulting and crushing along the regional deformation zones (Hudson et al. 2011). At Dannemora, fracture zones which run parallel to the ÖSDZ increase the width of the closely fractured corridor along this regional major deformation zone (Figure 4-18). Similar damage zones are suggested by linear depressions that flank regional deformation zones at Finnsjön (Figure 4-23), Dannemora (Figure 4-18) and Bruksdammen (Figure 5-1).

Block and kernel sizes are critical for rock resistance to detachment and entrainment of blocks at the glacier bed (Flint 1971, Krabbendam and Glasser 2011, Anderson 2014, Krabbendam et al. 2022a). Hence, block size distribution influences differential glacial erosion in the basement. On fault block tops, intermediate block sizes dominate, rock kernels are widely spaced and marked by box hills, and intensely fractured rocks are of small extent. Fracture zones within the fault block tend to be short, narrow, and often terminate within the confines of the fault block. The limited extent and isolation of zones with small *in situ* rock blocks has provided limited potential for excavation of deep basins and long trenches; glacial erosion of the fault block tops has been dominated by areal erosion through lowering. Within major fracture zones, rock block size remains a key control over glacial erosion. Rock ribs of different widths occur on trench floors within fracture zones (Figure 4-18A). Rock thresholds are significant even along major fracture zones, segmenting trenches. For example, rock thresholds are seen at Östhammar (Figure 4-21), Dannemora (Figure 4-18) and near Forsmark (Figure 4-15 in Hall et al. 2019a). Limited air photo evidence and field observations suggest that rock thresholds are tabular zones with widely spaced fractures where the main fracture zone splits, or is interrupted, or closely constricted at the present erosion level. Variable trench widths link to contrasts in fracture spacings between fracture zones and host rocks. Where host rocks with wide fracture spacing form the margins of fracture zones, a rock wall may occur (Figure 4-19B). Where sharp contrasts in fracture spacing persist over long distances along a fracture zone, the trench walls may remain parallel over several km (Figure 4-20). Where host rocks with close fracture spacings occur alongside the fracture zone (Figure 4-18C) there is potential for further widening of the fracture lineament into a broad valley or elongate basin, as at Kallrigafjärden. The presence of closely spaced fractures along the sides of major regional fracture zones (Figure 4-18B) indicates, however, that trench widening may remain incomplete. At Finnsjön and Forsmark, fracture zones of 1–3 km length, and with measured small block sizes, have weak topographic expression. Whilst differential removal of small blocks typically found in fracture zones has strongly influenced trench positions and forms, block removal has operated unevenly in space and time.

5.4.6 Rock trenches and meltwater channels

An important question is to what degree the rock trenches are eroded by subglacial erosion processes such as abrasion and plucking as compared to subglacial meltwater erosion. Rock-cut meltwater channel systems formed by erosion from subglacial meltwater have several distinctive features, namely:

(i) bifurcating and anastomosing channel segments (Sissons 1961),

(ii) abrupt channel terminations and initiations (Price 1963) and

(iii) undulating thalwegs formed as water locally flowed upward under hydrostatic pressure (Sissons 1961, Kirkham et al. 2020).

(iv) meltwater channels are box-shaped (Pair 1997) with fresh, unabraded rock walls from which blocks have been removed or fallen (Sutherland 1993, Tirén et al. 2001, Johansson 2003).

(v) many meltwater canyons are associated with glaciofluvial deposits and other glaciofluvial landforms at exits (Olvmo 1992).

These morphological elements are apparent in parts of the trench systems in Uppland. Trenches may split, and start and end abruptly (Figures 4-18, 4-21 and 4-23). Thalwegs are irregular (Figure 4-10). However, key differences also exist, namely:

(vi) the trench systems in Uppland have poor connectivity compared to integrated meltwater channel systems.

(vii) rock trenches display a partial mesh network topology (Figure 4-16). In contrast, rock-cut meltwater channels typically form parts of former subglacial hydrological networks, with dendritic, subparallel or anastomosing patterns (Jansen et al. 2014).

(viii) branched and anastomosing trenches are largely confined to well-connected trench and basin systems in the Öregrund archipelago and south of Lake Erken and to narrow zones along the main trenches that follow regional deformation zones.

In contrast to meltwater-cut rock channels, the rock trenches in Uppland have glacially abraded sides that descend towards valley floors (Figures 4-17D and 4-18B) and generally lack glacifluvial deposits at trench exits. Moreover, whilst meltwater-cut rock channels are common in the Swedish uplands (Olvmo 1985, Jansen et al. 2014) and important, but isolated examples also occur in the lowlands (Tirén et al. 2001), few, if any, meltwater canyons have been recognised in Uppland (Olvmo 1992). The orientations of several long trenches also lie oblique or transverse to former ice and meltwater flow, as between Uppsala and Norrtälje (Figure 4-16). The trench systems are not simple equivalents to meltwater channel systems.

Circulation of overpressurized subglacial water is significant in the formation of subglacial channels (Sissons 1961). Such channels include tunnel valleys (Lelandais et al. 2016). Tunnel valleys, however, are largely confined to layered soft rocks and sediments and are not characteristic features of hard, relatively impermeable shield rocks (Boulton et al. 2007) and so are not considered further here.

The regional N-S esker systems were major conduits for meltwater flow beneath the last ice sheet. Cross-sections along the Uppsala esker indicate that erosion of rock trenches below the esker gravels is limited in depth (Figure 4-17). An important exception occurs where a broad, buried trench occurs beneath Uppsala city at a confluence of two large esker systems where meltwater discharges were likely exceptional high. Eskers in Uppland follow routes that do not closely match the trench network (Figure 4-2). However, trench orientations show a dominance of NNW-SSE trends subparallel to former ice flow (Section 4.3.3). Trenches parallel to ice flow may operate as axial subglacial canals for meltwater discharge (Gao 2011, Burke et al. 2012). The main N-S trenches in Uppland have been identified in glaciological models as potential meltwater routeways beneath the Fennoscandian Ice Sheet (Shackleton 2019). It is likely that selective erosion of trenches was the result of a combination of meltwater and ice-induced erosion (see Section 5.4.7).

5.4.7 Processes of glacial erosion in rock trenches

The main processes of glacial erosion as currently recognised are abrasion, plucking and ripping from glacier ice and abrasion, cavitation, and block removal by glacial meltwater. The term *quarrying* has been used to refer to general block removal beneath glaciers (Iverson 2012), but it is often used synonymously with plucking (Fu and Harbor 2011) and risks confusion with man-made block excavation (Wang et al. 1991). Hence, we use here the term *block removal* to refer to the group of processes by which individual, joint-bound rock blocks may be removed on the glacier bed.

Rock trenches have close spatial and directional associations with fracture zones indicating that glacial erosion has selectively exploited the fracture zones across scales. Yet understanding the processes involved in glacial erosion along rock trenches is challenging because trench floors are hidden from direct observation by sediment or water. Available observational evidence suggests that the operation of different processes of glacial and meltwater erosion in trenches has been uneven in space and time. In this section, we make a preliminary assessment of the potential importance of different processes of glacial erosion in trench formation.

The following processes are considered in relation to trench erosion:

Abrasion. Many rock trenches in Uppland have abraded and striated sides that descend beneath the present sediment cover on valley floors (Figures 4-17D and 4-18B).

Block removal. Several processes have been identified previously with potential for block removal on trench floors that include:

- *Plucking*, the loss of single or small numbers of large (> 256 mm boulder size) blocks mainly from lee- and flank-side cliffs (Krabbendam and Glasser 2011). In trenches, plucking was likely confined to cliffs on trench sides and to rock risers on trench floors. However, abraded surfaces are widespread on trench flanks, indicating a limited impact for this process.
- *Ripping*, the removal of large numbers of blocks after hydraulic jacking and disruption of rock hills and rock sheets in response to subglacial groundwater overpressure (Hall et al. 2020). Ripping led to development of extensive boulder spreads in Uppland, including along the Lake Vällen depression. A lack of exposure prevents assessment of the impact of ripping on trench floors.
- *Removal of small joint blocks*. The process(es) by which small (< 256 mm boulder size) blocks may be removed by glacial erosion in topographic lows are uncertain. We may infer erosion by this process from the isolation of rock ribs and knolls with wide fracture spacings on trench floors and flanks which follow regional major deformation with generally small block sizes (Figure 4-18) and from the excavation of narrow fracture zones.

Channelled flow of glacial meltwater also has potential to erode trenches in rock. Two main processes may be involved:

Abrasion and cavitation. Rapid and turbulent meltwater flow (Dürst Stucki et al. 2012), with high sediment loads, is capable of cutting meltwater channels in hard, crystalline rocks (Olvmo 2010, Fagherazzi et al. 2021). These processes collectively form streamlined microforms such as various s-forms (Shaw et al. 2020). However, these microforms are not common in Uppland (Hall et al. 2019a Appendix 1).

Extraction of fracture-bounded rock blocks. Hydraulic action along sub-marginal tunnels may remove blocks from the sides and beds of rock-cut gorges (Tirén et al. 2001, Johansson 2005). Trench flanks in the study are widely abraded and generally lack unabraded sockets from which blocks were extracted at a late stage of the last glaciation. Few observations are available however on trench floors which are concealed beneath glacial and postglacial sediments.

In summary, glacial abrasion, plucking and ripping were extensive in their erosional impacts on the ice sheet bed and likely contributed general lowering of rock surfaces on trench margins and floors. Channelled subglacial meltwater erosion is potentially effective in eroding rock gorges yet many trenches lack evidence for meltwater erosion. Moreover, the trenches do not closely resemble meltwater channels in their morphology and trench networks have distinctive partial mesh topologies that differ from drainage networks. Hence, selective erosion of trenches along fracture zones mainly involved poorly understood processes that required the removal of the small fracture-bounded rock blocks.

Small block removal along fracture zones was potentially enhanced by several factors acting in combination including:

- High potential for water storage in ponds and lakes on trench floors. Low, water-gathering topographic positions on the ice sheet bed offer sites for transient storage of subglacial water (Hiester et al. 2016).
- Large fracture apertures, with high permeability leading to enhanced groundwater flow in fractures and fracture zones at the glacier bed (Banwart et al. 1994). Detailed estimates of hydraulic transmissivity by Vahlund et al. (2006) from eastern and south-eastern Sweden give values of between 10 and 10^4 m^2 y^{-1} in 1–10 km wide deformation zones and between 10^{-1} and 10^2 m^2 y^{-1} in less deformed zones of similar width.
- Transient development of groundwater overpressure beneath the ice sheet (Röthlisberger and Iken 1981) by application of ice overburden pressure on trapped water (Peters et al. 2007) or by large inflows of meltwater to the subglacial system (Boulton et al. 1995).

Such processes may have interacted to dilate rock fractures (Leith et al. 2014), brecciate parts of the rock mass (Gegg et al. 2020) and loosen blocks in response to fluctuating groundwater pressures in hydraulically transmissive fracture zones (Follin et al. 2013). The reduced resistance of the rock surface to drag from sliding glacier ice or tractive forces from fast meltwater flow may then allow extraction of closely brecciated rock (Anderson 2014, Leith et al. 2014). Conversely, erosion on trench floors may have been periodically suppressed by ice-rock bed separation by sediment fills in bedrock lows (Alley et al. 2019). Also, seasonal meltwater flow can potentially excavate significant bedrock volumes over timescales of several thousand years (Beaud et al. 2018). Further work is required to identify and quantify the impact of the various processes by which ice and meltwater may remove small blocks from fracture zones on the glacier bed.

5.5 Past depths and future rates of glacial downwearing, backwearing and incision in the Öregrund archipelago

Glacial erosion in the lowlands of southern and eastern Sweden has involved the stripping of Early Palaeozoic cover rocks, downwearing and roughening of fault block surfaces developed in gneisses, the backwearing of fault scarps and the incision and headward erosion of trenches. Estimated depths and rates of erosion are summarised in Table 4-5.

5.5.1 Differential downwearing between sedimentary rocks and basement gneisses

The bedrock depressions in the Öregrund archipelago have significantly greater extent and depth than those found in terrain to the W and S. The relatively high volumes of the topographic depressions have been interpreted previously (Hall et al. 2019a) as a product of differential erosion between former sedimentary and gneissic rocks in the archipelago. The differences in erosion rates derive from the relative softness and high fracture intensities of the Jotnian sandstones and Ordovician limestones compared to the Precambrian gneisses.

The minimum depths of sedimentary rock missing are 31–45 m (Table 4-5), but an unknown thickness of sedimentary rock may also have covered the exposed fault block tops earlier in the Pleistocene. Average thickness of gneissic bedrock eroded from below U2 in Uppland are estimated at 24 m and include major contributions of rock volumes from trenches and basins (Hall et al. 2019a). Hence, erosion depths across fault block tops were low; the thicknesses of sedimentary rocks removed are at least twice those of basement. The actual disparity is likely to be larger. Differential erosion of the Åland Deep rock basin involved the excavation of 100–300 metres of Jotnian sandstone and younger sedimentary rocks yet the surrounding basement surface retains a morphology inherited from U2 (Figure 4-8). Source-sink sediment budgets indicate average losses of 40 m of sedimentary rocks from around the Baltic Sea basin (Hall and van Boeckel 2020).

The residual sedimentary outliers in the Öregrund archipelago are today confined to small outcrops and narrow fault grabens which lie along the main regional deformation zones. The restricted extent of residual sedimentary rocks means that future differential glacial erosion between sedimentary rocks and basement has limited potential to increase the total volume of the bedrock depressions in the archipelago. Future erosion in this area will be largely confined to basement and can be projected to be slow.

5.5.2 Potential for extreme erosion in basement

It has been suggested that glacial erosion of bedrock by mega-flood events would be capable in future glaciations of the erosion of depths of up to 400 m in a single glacial episode at Forsmark (Talbot 2014). The proposed mechanism for this extreme erosion involves a process sequence envisaged as follows: (i) deep-seated hydraulic jacking (ii) along subhorizontal fractures many km long (iii) shall cause catastrophic headward erosion in response to (iv) proglacial mega-floods from (v) the drainage of meltwater from large supraglacial lakes and (vi) lead to the formation of channelled scablands (Talbot 2014).

The proposed mechanism is highly implausible because observational evidence is lacking for similar effects developed beneath the Fennoscandian Ice Sheet in the multiple glacial cycles of the Pleistocene on the Fennoscandian shield. No extensive, overdeepened rock basins with depths of several hundreds of metres are known *cut in gneissic basement* in eastern Sweden. Where deep rock basins exist, as in southern Sweden at Lake Vättern and the Åland Deep, the basins are sited on sedimentary grabens and are products of differential erosion of the sedimentary rock fill, relative to more limited erosion in surrounding basement terrain. No extensive channelled scablands are known in lowland Sweden, apart from small areas around Baltic Ice Lake drainage channels (Johnson et al. 2022). Even here, most meltwater erosion has removed previous glacial sediment (till and outwash) and basement bedrock incision was negligible. Whilst some of the key processes may have operated beneath and in front of the Fennoscandian Ice Sheet during the Pleistocene, the modes of operation differed in key respects from those envisaged by Talbot (2014). For example, hydraulic jacking is confined to the uppermost 1-11 m of the bedrock at Forsmark (Carlsson and Christiansson 2007, Krabbendam et al. 2021). Subhorizontal fractures are rarely, if ever, continuous in the near-surface for > 1 km distances (Carlsson and Christiansson 2007). The lateral connectivity of rock fractures is low at depth, preventing rapid transmission of water through rock fractures over km distances and attenuating water pressure transients (Hökmark and Lönnqvist 2014). Where hydraulic jacking, rock disruption and disintegration triggered by groundwater overpressure are observed in lowland Sweden, the depth of erosion by glacial ripping is 1–4 m, except in large roches moutonnées where most or all of a rock hill may be disrupted to depths of 10–15 m (Hall et al. 2020). The ripping process sequence operated beneath the retreating margin of the Fennoscandian Ice Sheet, rather than in the proglacial zone. The lack of clear analogues for past operation of the mechanism and the implausible operations proposed for key processes suggested by Talbot (2014) means that the potential for such extreme erosion during future glaciations can be regarded as negligible. Hence, we focus below on providing estimates of past depths and future rates of glacial erosion and rates based on observations from a range of landforms and measurements of cosmogenic nuclide inventories.

5.5.3 Erosion in basement on fault block tops

In Uppland and on the neighbouring seabed, erosion by the Fennoscandian Ice Sheet through the Pleistocene of the re-exposed basement gneisses on U2 has been spatially variable and has 4 components: *downwearing*, *backwearing*, *incision* and *headward erosion*.

Fault block tops with low surface roughness and low relative relief are of restricted extent in the Öregrund archipelago. The small sizes of the fault and rock blocks, the close spacing of intersecting major fracture zones and the local relief generated during differential erosion of the narrow sedimentary grabens likely led to relatively higher average erosion depths on fault blocks in the Öregrund archipelago than in areas to the south and west in Uppland.

5.5.4 Backwearing of fault scarps

Based on an assumption that fault movement of the basement, the unconformity and its Early Palaeozoic sedimentary cover formed sharp, planar fault scarps, the volume of rock removed by glacial erosion can be estimated, along with the distance of backwearing. For fault scarps in Uppland, the distances of backwearing are 0.5–1.5 km (Table 4-5). These distances are comparable to estimates for fault scarps at Trollhättan of 0.3–0.8 km (Hall et al. 2019b). More generally, backwearing of fault block edges has lowered and indented, rather than eliminated the edges. The mapping of exhumed fault scarps at the regional scale across southern Sweden confirms that glacial modification of these 10–50 high edges features has been limited (Hall et al. 2019b). The open, shallow basins at Herräng and Kallrigafjärden are exceptional; here, glacial erosion has eroded backward by 2–4 km, perhaps due to extensive areas of rock with relatively small *in situ* rock block sizes in these areas.

5.5.5 Incision, widening and headward erosion of trenches

Based on an assumption that rock trenches were not components of the U2 surface and represent wholly glacial landforms of Pleistocene origin, the depths of rock trenches below fault block tops constrain the depths of glacial erosion in the fracture zones that guide these valleys. On the rim of the Baltic Sea proper and the Åland Deep, trench depths may exceed 100 m. In the Öregrund archipelago, however, and across Uppland, trench depths lie in the 10–50 m range (Table 4-5).

The trench widths rarely exceed 1–2 km except in areas where host rocks are themselves closely fractured. In comparison to measured fracture zone widths, a trench may be several times wider but strong contrasts in fracture spacing between fracture zones and host rocks tend to maintain narrow widths.

The trenches on the rim of the Åland Deep steepen eastward, with knickpoints standing 10–15 km W of the rock basin rim. This steepening is likely a result of headward erosion in adjustment to the glacial overdeepening of the main Deep. However, trenches in the Öregrund archipelago to the south show no clear knickpoints and instead maintain highly irregular thalwegs (Figure 4-10). Headward erosion has not extended into this area along rock trenches.

5.5.6 Rates of past erosion and implications for future erosion in the Forsmark area

Modelling of future climate at Forsmark suggests that the climate of the next 100 ka will be different from that of the past 100 ka and that the duration of glaciation will be relatively short (Lord et al. 2019). Climate cycles more similar to those of the last 100 ka may develop thereafter, with longer periods of glaciation (Lord et al. 2019). Over the next 100 ka the long duration of subaerial conditions, with surface weathering, fluvial and coastal erosion, is unlikely to have a similar impact to that of glacial erosion over the past 100 ka and 1 Ma because the observed impact of subaerial processes on rock surfaces since deglaciation has been slight. Moreover, downwearing, backwearing, incision and headward erosion operate differently under subaerial conditions. Erosion below sea level is negligible. Below we focus on future 100 ka glacial periods with a re-established ice sheet behaviour.

In the vicinity of Forsmark, no sedimentary rocks remain at the present erosional level. Hence, the extent and depth of the bedrock depressions found in the Öregrund archipelago cannot be replicated by future glacial erosion at Forsmark because future erosion here will be entirely in basement, characterised by much lower erodibility.

Past downwearing rates: average depths of extensive total basement erosion around Forsmark based on geomorphological evidence were ~22 m (Hall et al. 2019a), with an average rate of 2.0 m per 100 ka glacial cycle.

At Forsmark, additional constraints on downwearing in basement are available from paired ^{10}Be and ^{26}Al cosmogenic nuclide data. Results are available for 32 surface bedrock samples, mainly from bedrock highs, along a transect that extends south from Forsmark for ~50 km, and three boulder samples at the coast (Hall et al. 2019a, Heyman et al. 2019). Under the assumption that all glaciations that covered the Forsmark area and Uppland region eroded the basement with similar mode and intensity, the typical values for denudation are 1.6–3.5 m over the last 100 ka and 13–27 m erosion

over the last 1 Ma. The cosmogenic nuclide data demonstrate significant differences in erosion depths between neighbouring localities. Hence, glacial erosion has varied spatially on separate bedrock highs. Non-glacial subaerial erosion rates on exposed rock surfaces in cosmogenic isotope models were assumed to be 0–5 mm/ka (Heyman in Hall et al. 2019a). Measured Holocene erosion rates on bare rock surfaces in northern Sweden are 0.2 mm/ka (André 2002), at the low end of this range, indicating that any contributions from non-glacial erosion to total downwearing were small. Constraints from cosmogenic nuclides on erosion rates in topographic depressions, including rock trenches, are lacking due to shielding by present and former sediment.

Past backwearing rates: the edges of fault blocks of Gräsö, at Ironworks and Hallstavik involved erosion of rock wedges with 0.75–1.5 km widths, equivalent to rates of backwearing of 68–136 m/100 ka.

Past incision rates: incision was mainly confined to excavation of trenches along major regional fracture zones. The trenches have depths of 10–50 m, equivalent to incision at 1–5 m/100 ka. Trench widening is limited, with maximum trench widths of 1–2 km, represented maximum widening rates of 100–200 m/100 ka. Trench floors are today typically buried by sediment, or covered by freshwater lakes (Figure 5-1) or submerged by the sea (Figure 4-20); the contribution of non-glacial subaerial erosion to trench floor lowering is regarded as negligible at the present day.

Past headward erosion: significant headward erosion was restricted to the western rim of the Åland Deep. Here average rates of headward erosion were ~1 km in each 100 ka glacial cycle. Headward erosion was entirely a product of glacial and meltwater erosion.

Future glacial erosion at Forsmark over future 100 ka periods can be projected on the basis of (i) past patterns of erosion and (ii) rates of erosion estimated from geomorphological evidence at Forsmark, in the Öregrund archipelago and in neighbouring parts of Uppland. Potential future depths of glacial erosion at the Forsmark site (iii) also have been derived (Heyman in Hall et al. 2019) through a combination of simulations of glacial erosion based on cosmogenic ^{10}Be and ^{26}Al nuclides with simulated scenarios of tentative future periods of ice sheet coverage at Forsmark over the coming 1 Ma based on IPCC emission scenarios and future variations in insolation (Lord et al. 2019).

Future downwearing: geomorphological and terrestrial cosmogenic nuclide data constrain past denudation to the range of 1.6 to 3.5 m/100 ka, dominantly from glacial erosion. Under different scenarios, projected depths of total denudation of rock surfaces for the Forsmark site over the coming 100 ka are less than 1 m (Heyman in Hall et al. 2019a). Hence, future downwearing of fault block tops at Forsmark is likely to be slow over the coming ~100 ka.

Future backwearing: past backwearing rates indicate retreat of scarps by 68–136 m in the last 100 ka glacial cycle. The modelled brief duration of glaciation in the coming 100 ka suggests that backwearing will be less than these estimates. Potentially more significant is the backwearing indicated by the open basins at Kallrigafjärden and Herräng. However, the downwearing involved in basin extension is ~10 metres. Hence, geomorphological evidence indicates that backwearing of fault block edges has operated slowly and to shallow depth in the past; future rates may be lower.

Future incision: past incision rates are 1–5 m/100 ka, with trench widening at maximum rates of 100–200 m/100 ka. As trench incision requires glacial conditions and these conditions are likely to be of short duration in the coming 100 ka, future incision will likely be limited.

Future glacial erosion is likely to (further) excavate trenches along regional deformation zones at Forsmark due to the presence of wide zones of intensely fractured rock with small *in situ* rock block sizes. Past glacial erosion, however, has had uneven impacts along regional and local deformation zones at Forsmark. The Forsmark deformation zone has been excavated to form an elongate basin at Bruksdammen with a maximum depth of 20 m (Figure 5-1). The trace of the Singö deformation zone remains marked only by a shallow, intermittent trench. Future incision is likely to be similarly uneven. More certainly, the limited widening of trench of the SDZ in the Öregrund archipelago, and of similar sized deformation zones, indicates that any future trench will remain restricted in its width to a few multiples of the width of the underlying fracture zone. The candidate area for the spent nuclear fuel repository at Forsmark is situated in a tectonic lens between the Singö and Eckarfjärden regional deformation zones (Stephens et al. 2007). Hence, trench erosion will likely remain confined to the regional deformation zones outside the tectonic lens. Within the tectonic lens at Forsmark, future erosion rates (downwearing) are predicted to be up to 2 m/100 ka on the basis of past erosion rates on fault block tops.

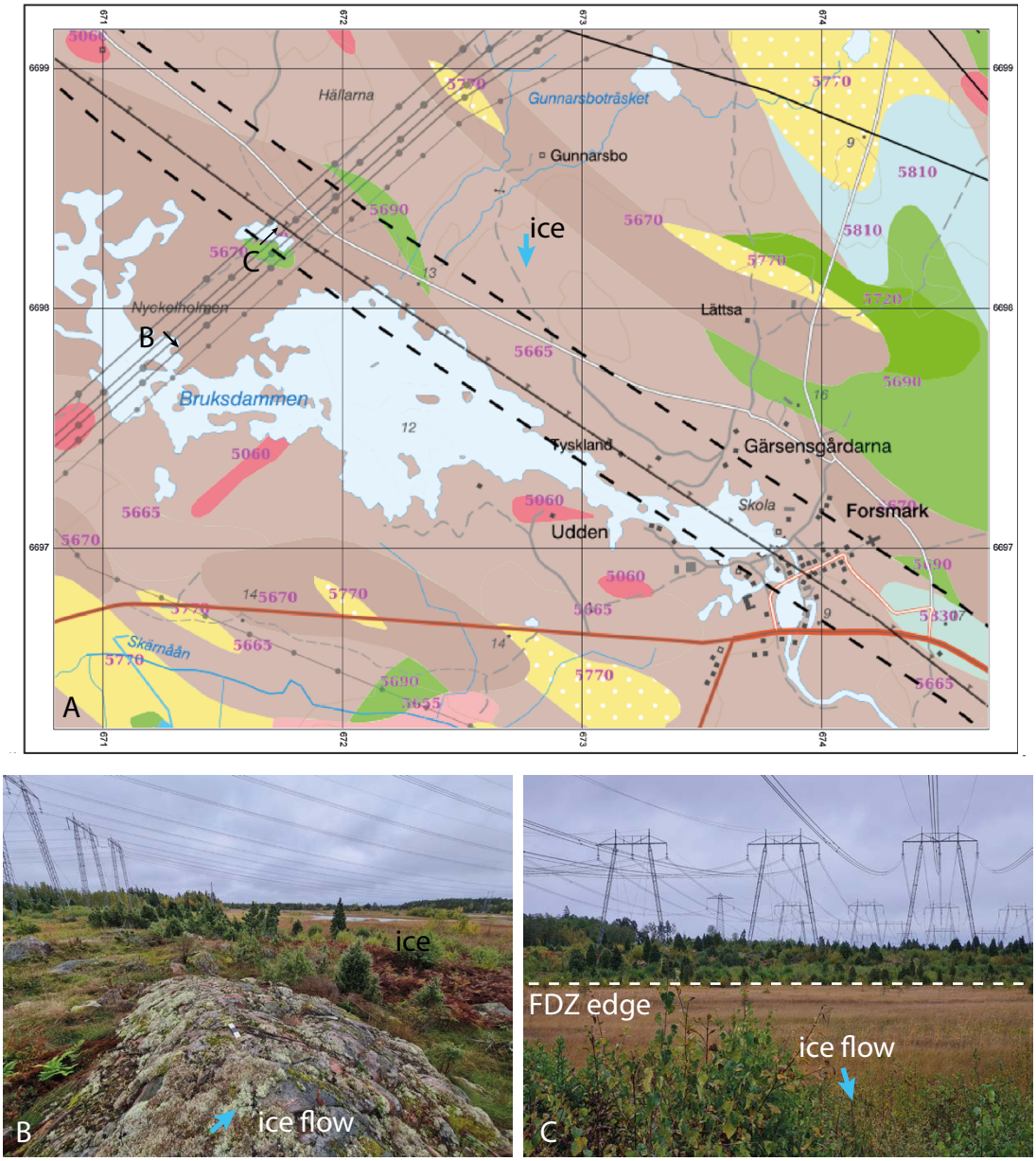

Figure 5-1. *The topographic expression of the Forsmark Deformation Zone at Bruksdammen, Forsmark. A. SGU geology map extract with the line of the FDZ show. Blue arrows show former ice-flow direction. B. Looking south-east from Nyckelholmen across part of the shallow, lake-filled depression along the southern edge of the deformation zone. C. Looking north-east across a swamp towards the break of slope in amphibolite (green on the geology map) along the northern edge of the deformation zone. Former ice flow from the north across the FDZ has excavated a shallow, linear depression.*

Future headward erosion. Past headward erosion has operated in submerged trenches on the edge of the Åland Deep at average rates of up to 1.5 km /100 ka. The steepening of trench thalwegs within the rim of the Åland Deep was a response to glacial overdeepening of the basin; headward erosion within the Öregrund archipelago has been limited. The ENE-WSW deformation zones which continue from the Öregrund archipelago to Forsmark and beyond offer potential for headward extension in future glacial cycles. Forsmark lies about 15 km WNW of the Öregrund archipelago. Hence, future headward erosion, at average past rates, would require around 1 Ma to reach Forsmark. However, future headward erosion is potentially obstructed by the broad rock thresholds that cross deformation zones.

6 Conclusions

The relatively large depths of topographic depressions in the Öregrund archipelago compared to Forsmark can be attributed mainly to differential glacial erosion of former Proterozoic sandstone and Early Palaeozoic limestone. Overdeepening was a response to the relatively low rock hardness and high fracture intensities of the sedimentary rocks compared to the Precambrian gneisses. Overdeepening in basement rocks is generally to lesser depths and occurred along regional deformation zones in the Öregrund archipelago and more generally in major fracture zones across the basement surface in Uppland. Fracture zones represent corridors with small *in situ* joint block sizes that were differentially eroded beneath the Fennoscandian ice sheet. The processes of joint block removal in rock trenches remain uncertain but likely involved interactions between subglacial traction and pressurised meltwater.

Depths and rates of Pleistocene glacial erosion in the Öregrund archipelago are estimated using the sub-Cambrian unconformity as a reference surface and by assuming the onset of ice sheet erosion at 1.2 Ma. Estimates for past downwearing of basement fault blocks are 1.8–2.0 m/100 ka and compare to rates of downwearing on rock surfaces at Forsmark derived from cosmogenic nuclides of 1.6–3.5 m/100 ka. The edges of fault blocks have retreated at rates of 42–125 m/100 ka. Rock trenches have been extended headward from the Åland Deep at 0.4–1.2 km/100 ka and deepened at average rates of 0.8–4.2 m/100 ka. Headward erosion has yet to reach the Öregrund archipelago. Future glacial erosion over the coming 1 Ma at Forsmark can be expected to proceed at similar rates. Selective linear glacial erosion of major deformation zones including the Singö deformation zone can be expected in future glaciations, but the trenches formed will remain narrow, shallow and aligned along the deformation zones. Should glacial cycles develop in the future in a similar way as over the past 1 Ma, past rates of headward erosion beneath the Fennoscandian Ice Sheet on the western rim of the Åland basin indicate that headward erosion of rock trenches from the Öregrund archipelago would require around 1 Ma to reach Forsmark. Recent modelling suggests, however, that glacial cycles over the coming 400–500 ka will be short; the timescale for headward erosion under this scenario would then be more than 1 Ma.

References

SKB's (Svensk Kärnbränslehantering AB) publications can be found at www.skb.com/publications.

Ahlbom K, Tirén S, 1991. Overview of geologic and geohydrologic conditions at the Finnsjön site and its surroundings. SKB TR 91-08, Svensk Kärnbränslehantering AB.

Ahlbom K, Andersson P, Ekman L, Gustafsson E, Smellie J, Tullborg E-L, 1986. Preliminary investigations of fracture zones in the Brändan area, Finnsjön study site. SKB TR 86-05, Svensk Kärnbränslehantering AB.

Ahlin S, 1987. Phanerozoic faults in the Västergötland basin area, SW Sweden. GFF 109, 221–227.

Alley R B, Cuffey K M, Zoet L K, 2019. Glacial erosion: status and outlook. Annals of Glaciology 60, 1–13.

Amantov A, Hagenfeldt S, Soderberg P, 1995. The Mesoproterozoic to Lower Palaeozoic sedimentary bedrock sequence In the northern Baltic proper, Aland Sea, Gulf of Finland and Lake Ladoga. In Mojski J E (ed). Proceedings of the Third Marine Geological Conference "The Baltic", Sopot, 1993. Warszawa: PIG.

Anderson R S, 2014. Evolution of lumpy glacial landscapes. Geology 42**,** 679–682.

André M-F, 2002. Rates of Postglacial rock weathering on glacially scoured outcrops (Abisko–Riksgränsen area, 68°N). Geografiska Annaler 84A, 139–150.

Aydin A, Basu A, 2005. The Schmidt hammer in rock material characterization. Engineering Geology 81, 1–14.

Banwart S, Gustafsson E, Laaksoharju M, Nilsson A-C, Tullborg E-L, Wallin B, 1994. Large-scale intrusion of shallow water into a vertical fracture zone in crystalline bedrock: Initial hydrochemical perturbation during tunnel construction at the Äspö Hard Rock Laboratory, southeastern Sweden. Water Resources Research 30, 1747–1763.

Beaud F, Venditti J G, Flowers G E, Koppes M, 2018. Excavation of subglacial bedrock channels by seasonal meltwater flow. Earth Surface Processes and Landforms 43, 1960–1972.

Beckholmen M, Tirén S A, 2010a. Rock-block configuration in Uppland and the Ålands-hav basin, the regional surroundings of the SKB site in Forsmark, Sea and land areas, eastern Sweden. Report 2010:41, Swedish Radiation Safety Authority.

Beckholmen M, Tirén S A, 2010b. Displacement along extensive deformation zones at the two SKB sites: Forsmark and Laxemar. Report. 2010:43, Swedish Radiation Safety Authority.

Bergman L, 1982. Clastic dykes in the Åland islands, SW Finland and their origin. Geological Survey of Finland Bulletin 317, 7–33.

Bergman S, Bergman T, Johansson R, Stephens M, Isaksson H, 1998. Förstudie Östhammar: delprojekt jordarter, bergarter och deformationszoner: kompletterande arbeten 1998. SKB R-98-57, Svensk Kärnbränslehantering AB. (In Swedish.)

Bingen B, Nordgulen Ø, Viola G, 2008. A four-phase model for the Sveconorwegian orogeny, SW Scandinavia. Norwegian Journal of Geology 88, 43–72.

Bishop P, Hoey T B, Jansen J D, Artza I L, 2005. Knickpoint recession rate and catchment area: the case of uplifted rivers in Eastern Scotland. Earth Surface Processes and Landforms 30, 767–778.

Boulton G S, Caban P E, Van Gijssel K, 1995. Groundwater flow beneath ice sheets: Part I – Large scale patterns. Quaternary Science Reviews 14, 545–562.

Boulton G S, Hagdorn M, Maillot P B, Zatsepin S, 2007. Drainage beneath ice sheets: groundwater–channel coupling, and the origin of esker systems from former ice sheets. Quaternary Science Reviews 28, 621–638.

Brocklehurst S H, Whipple K X, 2002. Glacial erosion and relief production in the Eastern Sierra Nevada, California. Geomorphology 42, 1–24.

Brojerdi F S, Zhang F, Juhlin C, Malehmir A, Lehtimäki T, Mattsson H, Curtis P, 2014. High resolution seismic imaging at the planned tunnel entrance to the Forsmark repository for spent nuclear fuel, central Sweden. Near Surface Geophysics 12, 709–720.

Burke M J, Brennand T A, Perkins A J, 2012. Evolution of the subglacial hydrologic system beneath the rapidly decaying Cordilleran Ice Sheet caused by ice-dammed lake drainage: implications for meltwater-induced ice acceleration. Quaternary Science Reviews 50, 125–140.

Carlsson A, Olsson T, 1977. Water leakage in the Forsmark tunnel, Uppland, Sweden. Uppsala: SGU. (Sveriges geologiska undersökning C 734)

Carlsson A, Christiansson R, 2007. Construction experiences from underground works at Forsmark. Compilation report. SKB R-07-10, Svensk Kärnbränslehantering AB.

Carlsten S, Petersson J, Stephens M, Mattsson H, Gustafsson J, 2004. Forsmark site investigation. Geological single-hole interpretation of KFM02A and HFM04-05 (DS2). SKB P-04-117, Svensk Kärnbränslehantering AB.

Claesson Liljedahl L, Munier R, Sandström B, Drake H, Tullborg E-L, 2011. Assessment of fractures classified as non-mineralised in the Sicada database. SKB R-11-02, Svensk Kärnbränslehantering AB.

Darcel C, Davy P, Bour O, de Dreuzy J R, 2006. Discrete fracture network for the Forsmark site. SKB R-06-79, Svensk Kärnbränslehantering AB.

Davy P, Le Goc R, Darcel C, Bour O, de Dreuzy J R, Munier R, 2010. A likely universal model of fracture scaling and its consequence for crustal hydromechanics. Journal of Geophysical Research: Solid Earth 115. doi:10.1029/2009JB007043

De Geer E H, 1948. The dislocated Scandinavian baselevel plain and the Mälar valley in the light of a close orographic analysis. Geologiska Föreningen i Stockholm Förhandlingar 70, 385–422.

Drake H, Heim C, Roberts N M W, Zack T, Tillberg M, Broman C, Ivarsson M, Whitehouse M J, Åström M E, 2017. Isotopic evidence for microbial production and consumption of methane in the upper continental crust throughout the Phanerozoic eon. Earth and Planetary Science Letters 470, 108–118.

Drake H, Ivarsson M, Tillberg M, Whitehouse M, Kooijman E, 2018. Ancient microbial activity in deep hydraulically conductive fracture zones within the Forsmark target area for geological nuclear waste disposal, Sweden. Geosciences 8, 211.

Dürst Stucki M, Schlunegger F, Christener F, Otto J-C, Götz J, 2012. Deepening of inner gorges through subglacial meltwater – An example from the UNESCO Entlebuch area, Switzerland. Geomorphology 139–140, 506–517.

Elmouttie M K, Poropat G V, 2012. A method to estimate in situ block size distribution. Rock Mechanics and Rock Engineering 45, 401–407.

Elvhage C, Lidmar-Bergström K, 1987. Some working hypotheses on the geomorphology of Sweden in the light of a new relief map. Geografiska Annaler Series A, Physical Geography 69, 343–358.

Embleton C, 1982. Fjorde, Fjärde, und Föhrden. In Schwartz M (ed). Beaches and coastal geology. Boston, MA: Springer, 426–427.

Ericson K, Migon P, Olvmo M, 2005. Fractures and drainage in the granite mountainous area: A study from Sierra Nevada, USA. Geomorphology 64, 97–116.

Ericsson L O, Ronge B S, 1988. Fracture mapping on outcrops in crystalline bedrock: a case study within the sub-Cambrian peneplain, southern Sweden. In Cundall P A, Starfield A M, Sterling R L (eds). Key questions in rock mechanics: Proceedings of the 29th U.S. Symposium on Rock Mechanics (USRMS), 1988. American Rock Mechanics Association.

Fagherazzi S, Baticci L, Brandon C M, Rulli M C, 2021. Bedrock erosion in subglacial channels. PloS ONE 16, e0253768. doi:10.1371/journal.pone.0253768

Flint R F, 1971. Glacial and Quaternary geology. New York: Wiley.

Flodén T, 1977. Tectonic lineaments in the Baltic from Gävle to Simrishamn. KBS Teknisk rapport 59, Kärnbränslesäkerhet.

Follin S (ed), 2019. Multidisciplinary description of the access area of the planned spent nuclear fuel repository in Forsmark prior to construction. SKB R-17-13, Svensk Kärnbränslehantering AB.

Follin S, Levén J, Hartley L, Jackson P, Joyce S, Roberts D, Swift B, 2007. Hydrogeological characterisation and modelling of deformation zones and fracture domains, Forsmark modelling stage 2.2. SKB R-07-48, Svensk Kärnbränslehantering AB.

Follin S, Hartley L, Rhén I, Jackson P, Joyce S, Roberts D, Swift B, 2013. A methodology to constrain the parameters of a hydrogeological discrete fracture network model for sparsely fractured crystalline rock, exemplified by data from the proposed high-level nuclear waste repository site at Forsmark, Sweden. Hydrogeology Journal 22, 313–331.

Fu P, Harbor J, 2011. Glacial erosion. Encyclopedia of snow, ice and glaciers. In Singh V P, Singh P, Haritashya U K (eds). Dordrecht: Springer Netherlands, 332–341.

Gabrielsen R H, Nystuen J P, Jarsve E M, Lundmark A M, 2015. The Sub-Cambrian Peneplain in southern Norway: its geological significance and its implications for post-Caledonian faulting, uplift and denudation. Journal of the Geological Society 172, 777–791.

Gao C, 2011. Buried bedrock valleys and glacial and subglacial meltwater erosion in southern Ontario, Canada. Canadian Journal of Earth Sciences 48, 801–818.

Gegg L, Buechi M W, Ebert A, Deplazes G, Madritsch H, Anselmetti F S, 2020. Brecciation of glacially overridden palaeokarst (Lower Aare Valley, northern Switzerland): result of subglacial water-pressure peaks? Boreas 49, 813–827.

Glamheden R, Mærsk Hansen L, Fredriksson A, Bergkvist L, Markstrom I, Elfstrom M, 2007. Mechanical modelling of the Singö Deformation Zone. SKB R-07-06, Svensk Kärnbränslehantering AB.

Glamheden R, Lanaro F, Karlsson J, Lindberg U, Wrafter J, Hakami H, Johansson M, 2008. Rock mechanics Forsmark: Modelling stage 2.3. Complementary analysis and verification of the rock mechanics model. SKB R-08-66, Svensk Kärnbränslehantering AB.

Goodfellow B W, Stroeven A P, Martel S J, Heyman J, Rossi M, Caffee M W, 2019. Exploring alternative models for the formation of conspicuously flat basement surfaces in southern Sweden. SKB TR-19-22, Svensk Kärnbränslehantering AB.

Gorbatschev R, 1962. The Precambrian sandstone of the Gotska Sandön boring core. Bulletin of the Geological Institutions of the University of Uppsala 39, 1–30.

Grigull S, Peterson G, Nyberg J, Öhrling C, 2019. Phanerozoic faulting of Precambrian basement in Uppland. SKB R-19-22, Svensk Kärnbränslehantering AB.

Gudmundsson A, Kusumoto S, Simmenes T H, Philipp S L, Larsen B, Lotveit I F, 2012. Effects of overpressure variations on fracture apertures and fluid transport. Tectonophysics 581, 220–230.

Hagenfeldt S E, 1995. Erratics and Proterozoic – Lower Palaeozoic submarine sequences between Åland and mainland Sweden. Uppsala: Geological Survey of Sweden. (SGU series Ca 84)

Hagenfeldt S E, Söderberg P, 1994. Lower Cambrian sandstone erratics and geophysical indications of sedimentary rock in the Stockholm area, Sweden. GFF 116, 185–190.

Hall A M, Migoń P, 2010. The first stages of landscape modification by ice sheets: evidence from central Europe. Geomorphology 123, 349–363.

Hall A M, Sarala P, Ebert K, 2015. Late Cenozoic deep weathering patterns on the Fennoscandian shield in northern Finland: a window on ice sheet bed conditions at the onset of Northern Hemisphere glaciation. Geomorphology 246, 472–488.

Hall A M, van Boeckel M, 2020. Origin of the Baltic Sea basin by Pleistocene glacial erosion. GFF 142, 237–252.

Hall A M, Ebert K, Goodfellow B W, Hättestrand C, Heyman J, Krabbendam M, Moon S, Stroeven A P, 2019a. Past and future impact of glacial erosion in Forsmark and Uppland. SKB TR-19-07, Svensk Kärnbränslehantering AB.

Hall A M, Krabbendam M, van Boeckel M, Hättestrand C, Ebert K, Heyman J, 2019b. The sub-Cambrian unconformity in Västergötland, Sweden. Reference surface for Pleistocene glacial erosion of basement. SKB TR-19-21, Svensk Kärnbränslehantering AB.

Hall A M, Krabbendam M, van Boeckel M, Goodfellow B W, Hättestrand C, Heyman J, Palamakumbura R N, Stroeven A P, Näslund J-O, 2020. Glacial ripping: geomorphological evidence from Sweden for a new process of glacial erosion. Geografiska Annaler: Series A, Physical Geography 102, 333–353.

Hall A M, Putkinen N, Hietala S, Lindsberg E, Holma M, 2021. Ultra-slow cratonic denudation in Finland since 1.5 Ga indicated by tiered unconformities and impact structures. Precambrian Research 352, 106000.

Henriksen H, Braathen A, 2006. Effects of fracture lineaments and in-situ rock stresses on groundwater flow in hard rocks: a case study from Sunnfjord, western Norway. Hydrogeology Journal 14, 444–461.

Heyman J, Goodfellow B W, Stroeven A P, Hall A M, Caffee M W, Hättestrand C, Ebert K, Näslund J-O, Hippe K, Martel S J, Moon S, Perron J T, Stuart A J, 2019. Erosion of low-relief basement by the Fennoscandian ice sheet based on bedrock ^{10}Be and ^{26}Al. Proceedings of INQUA, Dublin, 2019.

Hiester J, Sergienko O V, Hulbe C L, 2016. Topographically mediated ice stream subglacial drainage networks. Journal of Geophysical Research: Earth Surface 121, 497–510.

Holmlund P, Jakobsson M, Mannerfelt E S, O'Regan M, Wagner A, Weidner E, 2022. Geophysical surveys on sub marine land-and rock slides and on alpine glaciers. Report 2022:08, Swedish Radiation Safety Authority.

Hooke R L, Jennings C E, 2006. On the formation of the tunnel valleys of the southern Laurentide ice sheet. Quaternary Science Reviews 25, 1364–1372.

Hooyer T S, Cohen D, Iverson N R, 2012. Control of glacial quarrying by bedrock joints. Geomorphology 153–154, 91–101.

Hudson J A, Cosgrove J W, Kemppainen K, Johansson E, 2011. Faults in crystalline rock and the estimation of their mechanical properties at the Olkiluoto site, western Finland. Engineering Geology 117, 246–258.

Hökmark H, Lönnqvist M, 2014. Reply to comment by Christopher Talbot on "Approach to estimating the maximum depth for glacially induced hydraulic jacking in fractured crystalline rock at Forsmark, Sweden". Journal of Geophysical Research: Earth Surface 119, 955–959.

Iverson N R, 2012. A theory of glacial quarrying for landscape evolution models. Geology 40, 679–682.

Jacobsson L, 2004. Forsmark site investigation. Borehole KFM01A. Uniaxial compression test of intact rock. SKB P-04-223, Svensk Kärnbränslehantering AB .

Jakobsson M, Stranne C, O'Regan M, Greenwood S L, Gustafsson B, Humborg C, Weidner E, 2019. Bathymetric properties of the Baltic Sea. Ocean Science 15, 905–924.

Jansen J D, Codilean A T, Stroeven A P, Fabel D, Hättestrand C, Kleman J, Harbor J M, Heyman J, Kubik P W, Xu S, 2014. Inner gorges cut by subglacial meltwater during Fennoscandian ice sheet decay. Nature Communications 5, 3815. doi:10.1038/ncomms4815

Jern M, 2004. Determination of the *in situ* block size distribution in fractured rock, an approach for comparing in-situ rock with rock sieve analysis. Rock Mechanics and Rock Engineering 37, 391–401.

Jirner E, Johansson P-O, McConnachie D, Djurberg H, McCleaf P, Hummel A, Ahlgren S, Rohde L, Mikko H, 2016. Jordlagermodellering i 3D – exempel från Uppsalaåsen med hydrogeologisk tillämpning. SGU-rapport 2016:19, Geological Survey of Sweden. (In Swedish.)

Johansson M, Olvmo M, Söderström M, 1999. Application of digital elevation and geological data in studies of morphotectonics and relief–a case study of the sub-Cambrian peneplain in southwestern Sweden. Zeitschrift für Geomorphologie 43, 505–520.

Johansson M, Migon P, Olvmo M, 2001a. Development of joint-controlled rock basins in Bohus granite, SW Sweden. Geomorphology 40, 145–161.

Johansson M, Olvmo M, Lidmar-Bergström K, 2001b. Inherited landforms and glacial impact of different palaeosurfaces in southwest Sweden. Geografiska Annaler Series A, Physical Geography 83**,** 67–89.

Johansson P, 2003. Eskers and bedrock gorges (tunnel valleys) in the Pakasaivo area, western Finnish Lapland. Bulletin-Geological Society of Finland 75, 5–15.

Johansson P, 2005. Meltwater canyon lakes (saivos) in western Finnish Lapland. In Ojala A E K (ed). Quaternary studies in the northern and Arctic regions of Finland. Espoo: Geological Survey of Finland, 33–39.

Johnson M D, Öhrling C, Bergström A, Dreyer Isaksson O, Pizarro Rajala E, 2022. Geomorphology and sedimentology of features formed at the outlet during the final drainage of the Baltic Ice Lake. Boreas 51, 20–40.

Kim Y-S, Peacock D C P, Sanderson D J, 2004. Fault damage zones. Journal of Structural Geology 26, 503–517.

Kirkham J D, Hogan K A, Larter R D, Arnold N S, Nitsche F O, Kuhn G, Gohl K, Anderson J B, Dowdeswell J A, 2020. Morphometry of bedrock meltwater channels on Antarctic inner continental shelves: Implications for channel development and subglacial hydrology. Geomorphology 370, 107369. doi:10.1016/j.geomorph.2020.107369

Kleman J, Stroeven A P, Lundqvist J, 2008. Patterns of Quaternary ice sheet erosion and deposition in Fennoscandia and a theoretical framework for explanation. Geomorphology 97, 73–90.

Kohonen J, Rämö O T, 2005. Sedimentary rocks, diabases, and late cratonic evolution. In Lehtinen M J, Nurmi P A, Rämö O T (eds). Precambrian geology of Finland: Key to the evolution of the Fennoscandian shield. Amsterdam: Elsevier, 563–603.

Krabbendam M, Bradwell T, 2014. Quaternary evolution of glaciated gneiss terrains: pre-glacial weathering vs. glacial erosion. Quaternary Science Reviews 95, 20–42.

Krabbendam M, Glasser N F, 2011. Glacial erosion and bedrock properties in NW Scotland: abrasion and plucking, hardness and joint spacing. Geomorphology 130, 374–383.

Krabbendam M, Eyles N, Putkinen N, Bradwell T, Arbelaez-Moreno L, 2016. Streamlined hard beds formed by palaeo-ice streams: A review. Sedimentary Geology 338, 24–50.

Krabbendam M, Palamakumbura R, Arnhardt C, Hall A, 2021. Rock fracturing by subglacial hydraulic jacking in basement rocks, eastern Sweden: the role of beam failure. GFF 143, 390–405.

Krabbendam M, Dioguardi F, Arnhardt C, Roberson S, Hall A M, 2022a. Drag forces at the ice-sheet bed and resistance of hard-rock obstacles: the physics of glacial ripping. Journal of Glaciology. doi:10.1017/jog.2022.49

Krabbendam M, Hall A M, Palamakumbura R M, Finlayson A, 2022b. Glaciotectonic disintegration of roches moutonnées during glacial ripping in east Sweden. Geografiska Annaler: Series A, Physical Geography 104, 35–56.

Krall L, Sandström B, Tullborg E-L, Evins L Z, 2015. Natural uranium in Forsmark, Sweden: The solid phase. Applied Geochemistry 59, 178–188.

La Pointe P R, Olofsson I, Hermanson J, 2005. Statistical model of fractures and deformations zones for Forsmark. Preliminary site description Forsmark area – version 1.2. SKB R-05-26, Svensk Kärnbränslehantering AB.

Lanaro F, Fredriksson A, 2005. Rock Mechanics Model – Summary of the primary data. Preliminary site description Forsmark area – version 1.2. SKB R-05-83, Svensk Kärnbränslehantering AB.

Larson S-Å, Tullborg E-L, 1998. Why Baltic Shield zircons yield late Paleozoic, lower-intercept ages on U-Pb concordia. Geology 26, 919–922.

Leith K, Moore J R, Amann F, Loew S, 2014. Subglacial extensional fracture development and implications for Alpine Valley evolution. Journal of Geophysical Research: Earth Surface 119, 62–81.

Lelandais T, Mourgues R, Ravier É, Pochat S, Strzerzynski P, Bourgeois O, 2016. Experimental modeling of pressurized subglacial water flow: Implications for tunnel valley formation. Journal of Geophysical Research: Earth Surface 121, 2022–2041.

Lidmar-Bergström K, 1988. Denudation surfaces of a shield area in south Sweden. Geografiska Annaler Series A, Physical Geography, 337–350.

Lidmar-Bergström K, 1994. Morphology of the bedrock surface. In Fredén C (ed). National Atlas of Sweden. Stockholm: Almqvist and Wiksell International, 44–54.

Lidmar-Bergström K, 1995. Relief and saprolites through time on the Baltic Shield. Geomorphology 12, 45–61.

Lidmar-Bergström K, Olvmo M, Bonow J M, 2017. The South Swedish Dome: a key structure for identification of peneplains and conclusions on Phanerozoic tectonics of an ancient shield. GFF 139, 244–259.

Liivamägi S, Somelar P, Mahaney W C, Kirs J, Vircava I, Kirsimäe K, 2014. Late Neoproterozoic Baltic paleosol: Intense weathering at high latitude? Geology 42, 323–326.

Lord N S, Lunt D, Thorne M, 2019. Modelling changes in climate over the next 1 million years. SKB TR-19-09, Svensk Kärnbränslehantering AB.

MacGregor K R, Anderson R S, Anderson S P, Waddington E D, 2000. Numerical simulations of glacial-valley longtitudinal profile evolution. Geology 28, 1031–1034.

Malehmir A, Dahlin P, Lundberg E, Juhlin C, Sjöström H, Högdahl K, 2011. Reflection seismic investigations in the Dannemora area, central Sweden: Insights into the geometry of polyphase deformation zones and magnetite-skarn deposits. Journal of Geophysical Research: Solid Earth 116. doi:10.1029/2011JB008643

Margold M, Stokes C R, Clark C D, 2015. Ice streams in the Laurentide Ice Sheet: Identification, characteristics and comparison to modern ice sheets. Earth-Science Reviews 143, 117–146.

Marrett R, Ortega O J, Kelsey C M, 1999. Extent of power-law scaling for natural fractures in rock. Geology 27, 799–802.

Martinsson A, 1974. The Cambrian of Norden. In Holland C H (ed). Lower Palaeozoic rocks of the world. London: Wiley, Vol 2, 185–283.

McCaffrey K J W, Holdsworth R E, Pless J, Franklin B S G, Hardman K, 2020. Basement reservoir plumbing: fracture aperture, length and topology analysis of the Lewisian Complex, NW Scotland. Journal of the Geological Society 177, 1281–1293.

Milnes A G, Gee D G, 1992. Bedrock stability in southeastern Sweden. Evidence from fracturing in the Ordovician limestones of northern Öland. SKB TR 92-23, Svensk Kärnbränslehantering AB.

Min K-B, Stephansson O, 2011. The DFN-DEM approach applied to investigate the effects of stress on mechanical and hydraulic rock mass properties at Forsmark, Sweden. Tunnel and Underground Space 21, 117–127.

Moon S, Perron J T, Martel S J, Goodfellow B W, Mas Ivars D, Hall A, Heyman J, Munier R, Näslund J O, Simeonov A, Stroeven A P, 2020. Present-day stress field influences bedrock fracture openness deep into the subsurface. Geophysical Research Letters 47, e2020GL090581. doi:10.1029/2020gl090581

Munier R, 1993. Four-dimensional analysis of fracture arrays at the Äspö hard rock laboratory, SE Sweden. Engineering Geology 33, 159–175.

Munier R, Talbot C J, 1993. Segmentation, fragmentation and jostling of cratonic basement in and near Äspö, southeast Sweden. Tectonics 12, 713–727.

Munier R, Stenberg L, Stanfors R, Milnes A G, Hermanson J, Triumf C-A, 2003. Geological Site Descriptive Model. A strategy for the model development during site investigations. SKB R-03-07, Svensk Kärnbränslehantering AB.

Nielsen A T, Schovsbo N H, 2015. The regressive Early-Mid Cambrian 'Hawke Bay Event' in Baltoscandia: epeirogenic uplift in concert with eustasy. Earth-Science Reviews 151, 288–350.

Nordgulen Ö, Saintot A, 2008. Forsmark site investigation. The character and kinematics of deformation zones (ductile shear zones, fracture zones and fault zones) at Forsmark – report from phase 3. SKB P-07-111, Svensk Kärnbränslehantering AB .

Näslund J-O, Rodhe L, Fastook J L, Holmlund P, 2003. New ways of studying ice sheet flow directions and glacial erosion by computer modelling--examples from Fennoscandia. Quaternary Science Reviews 22, 245–258.

Olson J E, 2003. Sublinear scaling of fracture aperture versus length: an exception or the rule? Journal of Geophysical Research: Solid Earth 108. doi:10.1029/2001JB000419

Olvmo M, 1985. Meltwater canyons of the "Kursu" and the "Skura" type. Geografiska Annaler Series A, Physical Geography 67, 133–137.

Olvmo M, 1992. Glaciofluvial canyons and their relation to the Late Weichselian deglaciation in Fennoscandia. Zeitschrift für Geomorphologie, 343–363.

Olvmo M, 2010. Review of denudation processes and quantification of weathering and erosion rates at a 0.1 to 1 Ma time scale. SKB TR-09-18, Svensk Kärnbränslehantering AB.

Olvmo M, Johansson M, 2002. The significance of rock structure, lithology and pre-glacial deep weathering for the shape of intermediate-scale glacial erosional landforms. Earth Surface Processes and Landforms 27, 251–268.

Oskin M, Burbank D W, 2005. Alpine landscape evolution dominated by cirque retreat. Geology 33, 933–936.

Page L, Hermansson T, Söderlund P, Stephens M, 2007. Forsmark Site Investigation: $^{40}Ar/^{39}Ar$ and (U-Th)/He geochronology: Phase 2. SKB P-06-211, Svensk Kärnbränslehantering AB.

Pair D L, 1997. Thin film, channelized drainage, or sheetfloods beneath a portion of the Laurentide Ice Sheet: an examination of glacial erosion forms, northern New York State, USA. Sedimentary Geology 111, 199–215.

Palmqvist K, 1990. Groundwater in crystalline bedrock. SKB TR 90-41, Svensk Kärnbränslehantering AB.

Patton H, Hubbard A, Andreassen K, Winsborrow M, Stroeven A P, 2016a. The build-up, configuration, and dynamical sensitivity of the Eurasian ice-sheet complex to Late Weichselian climatic and oceanic forcing. Quaternary Science Reviews 153, 97–121.

Patton H, Swift D A, Clark C D, Livingstone S J, Cook S J, 2016b. Distribution and characteristics of overdeepenings beneath the Greenland and Antarctic ice sheets: Implications for overdeepening origin and evolution. Quaternary Science Reviews 148, 128–145.

Patton H, Hubbard A, Andreassen K, Auriac A, Whitehouse P L, Stroeven A P, Shackleton C, Winsborrow M, Heyman J, Hall A M, 2017. Deglaciation of the Eurasian ice sheet complex. Quaternary Science Reviews 169, 148–172.

Paulamäki S, Kuivamäki A, 2006. Depositional history and tectonic regimes within and in the margins of the Fennoscandian Shield during the last 1300 million years. Posiva Working Report 2006-43, Posiva Oy, Finland.

Peacock D, Dimmen V, Rotevatn A, Sanderson D, 2017. A broader classification of damage zones. Journal of Structural Geology 102, 179–192.

Persson C, 1985. Beskrivning till jordartskartan Östhammar NO. Uppsala: Geological Survey of Sweden. (SGU series Ae 73) (In Swedish.)

Peters L E, Anandakrishnan S, Alley R B, Smith A M, 2007. Extensive storage of basal meltwater in the onset region of a major West Antarctic ice stream. Geology 35, 251–254.

Petrone J, Sohlenius G, Ising J, 2020. Baseline Forsmark – Depth and stratigraphy of regolith. SKB R-17-07, Svensk Kärnbränslehantering AB.

Price R J, 1963. A glacial meltwater drainage system in Peeblesshire, Scotland. Scottish Geographical Magazine 79, 133–141.

Questiaux J-M, Couples G D, Ruby N, 2010. Fractured reservoirs with fracture corridors. Geophysical Prospecting 58, 279–295.

Quiquet A, Colleoni F, Masina S, 2016. Long-term safety of a planned geological repository for spent nuclear fuel in Forsmark, Sweden and Olkiluoto, Finland. Phase 2: impact of ice sheet dynamics, climate forcing and multi-variate sensitivity analysis on maximum ice sheet thickness. SKB TR-16-02, Svensk Kärnbränslehantering AB.

Reeves D M, Parashar R, Zhang Y, Rahman R, 2012. Hydrogeologic characterization of fractured rock masses intended for disposal of radioactive waste. INTECH Open Access Publisher. doi:10.5772/33168

Rippin D M, 2013. Bed roughness beneath the Greenland ice sheet. Journal of Glaciology 59, 724–732.

Rudberg S, 1970. The sub-Cambrian peneplain in Sweden and its slope gradient. Zeitschrift für Geomorphologie 9, 157–167.

Röthlisberger H, Iken A, 1981. Plucking as an effect of water-pressure variations at the glacier bed. Annals of Glaciology 2, 57–62.

Sahlin T, Malaga-Starzec K, Stigh J, Schouenborg B, 2000. Physical properties and durability of fresh and impregnated Limestone and Sandstone from central Sweden used for thin stone flooring and cladding. In Fassina V (ed). Proceedings of the 9th International Congress on Deterioration and Conservation of Stone. Amsterdam: Elsevier Science, 181–186.

Saintot A, Stephens M B, Viola G, Nordgulen Ø, 2011. Brittle tectonic evolution and paleostress field reconstruction in the southwestern part of the Fennoscandian Shield, Forsmark, Sweden. Tectonics 30. doi:10.1029/2010TC002781

Sanderson D J, Nixon C W, 2015. The use of topology in fracture network characterization. Journal of Structural Geology 72, 55–66.

Sanderson D J, Nixon C W, 2018. Topology, connectivity and percolation in fracture networks. Journal of Structural Geology 115, 167–177.

Sanderson D J, Peacock D C P, 2019. Line sampling of fracture swarms and corridors. Journal of Structural Geology 122, 27–37.

Sanderson D J, Peacock D C P, Nixon C W, Rotevatn A, 2019. Graph theory and the analysis of fracture networks. Journal of Structural Geology 125, 155–165.

Sandström B, Tullborg E-L, 2009. Episodic fluid migration in the Fennoscandian Shield recorded by stable isotopes, rare earth elements and fluid inclusions in fracture minerals at Forsmark, Sweden. Chemical Geology 266, 126–142.

Sandström B, Page L, Tullborg E-L, 2006a. Forsmark site investigation. $^{40}Ar/^{39}Ar$ (adularia) and Rb-Sr (adularia, prehnite, calcite) ages of fracture minerals. SKB P-06-213, Svensk Kärnbränslehantering AB.

Sandström B, Tullborg E-L, Torres T D, Ortiz J E, 2006b. The occurrence and potential origin of asphaltite in bedrock fractures, Forsmark, central Sweden. GFF 128, 233–242.

Sandström B, Tullborg E-L, Smellie J, MacKenzie A B, Suksi J, 2008a. Fracture mineralogy of the Forsmark site. SDM-Site Forsmark. SKB R-08-102, Svensk Kärnbränslehantering AB.

Sandström B, Tullborg E-L, Page L, 2008b. Forsmark site investigation. Fracture mineralogy and $^{40}Ar/^{39}Ar$ ages of adularia in fracture filling and K-feldspar in breccia. Data from drill cores KFM01C, KFM01D, KFM02B, KFM04A, KFM06A, KFM06B, KFM07A, KFM08A, KFM08B, KFM08C, KFM08D, KFM09A, KFM09B, KFM10A and KFM11A. SKB P-08-14, Svensk Kärnbränslehantering AB.

Sandström B, Tullborg E-L, Larson S Å, Page L, 2009. Brittle tectonothermal evolution in the Forsmark area, central Fennoscandian Shield, recorded by paragenesis, orientation and $^{40}Ar/^{39}Ar$ geochronology of fracture minerals. Tectonophysics 478, 158–174.

Sandström B, Annersten H, Tullborg E-L, 2010. Fracture-related hydrothermal alteration of metagranitic rock and associated changes in mineralogy, geochemistry and degree of oxidation: a case study at Forsmark, central Sweden. International Journal of Earth Sciences 99, 1–25.

Schumm S A, 1993. River response to baselevel change: implications for sequence stratigraphy. The Journal of Geology, 279–294.

Seidl M, Dietrich W, Schmidt K, de Ploey J, 1992. The problem of channel erosion into bedrock. Functional geomorphology 23, 101–124.

Shackleton C, 2019. Subglacial hydrology of the Fennoscandian and Barents Sea ice sheets. PhD thesis. The Arctic University of Norway.

Shackleton C, Patton H, Hubbard A, Winsborrow M, Kingslake J, Esteves M, Andreassen K, Greenwood S L, 2018. Subglacial water storage and drainage beneath the Fennoscandian and Barents Sea ice sheets. Quaternary Science Reviews 201, 13–28.

Shakesby R A, Matthews J A, Karlén W, Los S O, 2011. The Schmidt hammer as a Holocene calibrated-age dating technique: testing the form of the R-value-age relationship and defining the predicted-age errors. The Holocene 21, 615–628.

Shaw J, Gilbert R G, Sharpe D R, Lesemann J-E, Young R R, 2020. The origins of s-forms: Form similarity, process analogy, and links to high-energy, subglacial meltwater flows. Earth-Science Reviews 200, 102994. doi:10.1016/j.earscirev.2019.102994

Sissons J B, 1961. Some aspects of glacial drainage channels in Britain. Part II. Scottish Geographical Magazine 76, 15–36.

Sjöström H, Persson K S, 2001. Deformation zones in Eastern Bergslagen (Uppland-Sörmland). Uppsala University.

SKB, 2005. Preliminary site description. Forsmark area – version 1.2. SKB R-05-18, Svensk Kärnbränslehantering AB.

SKB, 2008. Site description of Forsmark at completion of the site investigation phase. SDM-site Forsmark. SKB TR-08-05, Svensk Kärnbränslehantering AB.

SKB, 2013. Site description of the SFR area at Forsmark at completion of the site investigation phase. SDM-PSU Forsmark. SKB TR-11-04, Svensk Kärnbränslehantering AB.

SKB, 2020. Post-closure safety for the final repository for spent nuclear fuel at Forsmark. Climate and climate-related issues, PSAR version. SKB TR-20-12, Svensk Kärnbränslehantering AB.

Stanfors R, Rhén I, Tullborg E-L, Wikberg P, 1999. Overview of geological and hydrogeological conditions of the Äspö hard rock laboratory site. Applied Geochemistry 14, 819–834.

Stephens M B, 2010. Forsmark site investigation. Bedrock geology – overview and excursion guide. SKB R-10-04, Svensk Kärnbränslehantering AB.

Stephens M B, Fox A, La Pointe P, Simeonov A, Isaksson H, Hermanson J, Öhman J, 2007. Geology Forsmark. Site descriptive modelling Forsmark stage 2.2. SKB R-07-45, Svensk Kärnbränslehantering AB.

Stephens M B, Follin S, Petersson J, Isaksson H, Juhlin C, Simeonov A, 2015. Review of the deterministic modelling of deformation zones and fracture domains at the site proposed for a spent nuclear fuel repository, Sweden, and consequences of structural anisotropy. Tectonophysics 653, 68–94.

Stålhös G, 1972. Beskrivning till Berggrundskartbladen: Uppsala SV och SO. Solid rocks of the Uppsala region (map-sheets Uppsala SW and SE). Uppsala: Geological Survey of Sweden. (SGU series Af 105/106) (In Swedish.)

Stålhös G, 1991. Beskrivning till berggrundskartorna Östhammar NV, NO, SV, SO med sammanfattande översikt av basiska gångar, metamorfos och tektonik i östra Mellansverige. Uppsala: Geological Survey of Sweden. (SGU series Af 161, 166, 169, 172) (In Swedish.)

Stölen L-K, Curtis P, Rodhe L, Jirner E, Antal-Lundin I, 2019. Three-dimensional geological mapping and modelling at the geological survey of Sweden. In MacCormack K E, Berg R C, Kessler H, Russell H A J, Thorleifson L H (eds). Synopsis of current three-dimensional geological mapping and modelling in geological survey organizations. AER/AGS Special Report 112, Alberta Energy Regulator / Alberta Geological Survey, 243–248.

Sturkell E, Lindström M, 2004. The target peneplain of the Lockne impact. Meteoritics & Planetary Science 39, 1721–1731.

Sugden D E, John B S, 1976. Glaciers and landscape: a geomorphological approach. London: Edward Arnold.

Sundblad K, Ahl M, Schöberg H, 1993. Age and geochemistry of granites associated with Momineralizations in western Bergslagen, Sweden. Precambrian Research 64, 31–-335.

Sutherland D G, 1993. Glen Valtos. In Gordon J E, Sutherland D G (eds.). Quaternary of Scotland. London: Chapman & Hall, 425–429.

Söderberg P, 1993. Seismic stratigraphy, tectonics and gas migration in the Åland Sea, northern Baltic proper. Stockholm: Almqvist & Wiksell International. (Stockholm Contributions in Geology 43)

Söderberg P, Hagenfeldt S E, 1995. Upper Proterozoic and Ordovician submarine outliers in the archipelago northeast of Stockholm, Sweden. GFF 117, 153–161.

Söderlund P, Hermansson T, Page L M, Stephens M B, 2009. Biotite and muscovite ^{40}Ar–^{39}Ar geochronological constraints on the post-Svecofennian tectonothermal evolution, Forsmark site, central Sweden. International Journal of Earth Sciences 98, 1835–1851.

Talbot C J, 2014. Comment on "Approach to estimating the maximum depth for glacially induced hydraulic jacking in fractured crystalline rock at Forsmark, Sweden" by M. Lönnqvist and H. Hökmark. Journal of Geophysical Research: Earth Surface 119, 951–954.

Thorslund P, Jaanusson V, 1960. The Cambrian, Ordovician, and Silurian in Västergötland, Närke, Dalarna, and Jämtland, central Sweden: Guide to excursions Nos A 23 and C 18. Stockholm: Geological Survey of Sweden.

Tirén S A, 1991. Geological setting and deformation history of a low-angle fracture zone at Finnsjön, Sweden. Journal of Hydrology 126, 17–43.

Tirén S A, Beckholmen M, 1989. Block faulting in southeastern Sweden interpreted from digital terrain models. GFF 111, 171–179.

Tirén S A, Beckholmen M, 1990. Rock block configuration in southern Sweden and crustal deformation. Geologiska Föreningen i Stockholm Förhandlingar 112, 361–364.

Tirén S A, Wänstedt S, Sträng T, 2001. Moredalen — a canyon in the Fennoscandian Shield and its implication on site selection for radioactive waste disposal in south-eastern Sweden. Engineering Geology 61, 99–118.

Tullborg E-L, Larson S Å, 1982. Fissure fillings from Finnsjön and Studsvik, Sweden. Identification, chemistry and dating. SKBF/KBS TR 82-20, Svensk Kärnbränsleförsörjning AB.

Tullborg E-L, Drake H, Sandström B, 2008. Palaeohydrogeology: A methodology based on fracture mineral studies. Applied Geochemistry 23, 1881–1897.

Vahlund F, Andersson J, Löfgren M, 2006. Data report for the safety assessment SR-Can. SKB TR-06-25, Svensk Kärnbränslehantering AB.

van Boeckel M, van Boeckel T, Hall A M, 2022. Late erosion pulse triggered by rapid melt in the cold-based interior of the last Fennoscandian Ice Sheet, an example from Rogen. Earth Surface Processes and Landforms doi:10.1002/esp.5464

Wang H, Latham J-P, Poole A B, 1991. Predictions of block size distribution for quarrying. Quarterly Journal of Engineering Geology and Hydrogeology 24, 91–99.

Werth E, 1908. Fjorde, Fjärde und Föhrden. Zeitschrift für Geomorphologie 3, 346–358.

Wichmann V, Strauhal T, Fey C, Perzlmaier S, 2019. Derivation of space-resolved normal joint spacing and in situ block size distribution data from terrestrial LIDAR point clouds in a rugged Alpine relief (Kühtai, Austria). Bulletin of Engineering Geology and the Environment 78, 4465–4478.

Wickström L M, Stephens M B, 2020. Tonian–Cryogenian rifting and Cambrian–Early Devonian platformal to foreland basin development outside the Caledonide orogen. Geological Society, London, Memoirs 50, 451–477.

Wiman E, 1942. Studies of the morpho-tectonics of the Mälar depression, Sweden. Bulletin of the Geological Institute of the University of Uppsala 29, 287–303.

Winterhalter B, Flodén T, Ignatius H, Axberg S, Niemistö L, 1981. Geology of the Baltic Sea. Elsevier Oceanography Series 30. doi:10.1016/S0422-9894(08)70138-7

Zernitz E R, 1932. Drainage patterns and their significance. The Journal of Geology 40, 498–521.

Arkitektkopia AB, Bromma, 2023

SKB is responsible for managing spent nuclear fuel and radioactive waste produced by the Swedish nuclear power plants such that man and the environment are protected in the near and distant future.

skb.se